CIVIL ENGINEERING STUDIES
Hydraulic Engineering Series No. 76

UILU-ENG-2005-2001

ISSN: 0442-1744

Sedimentation Management in Combined Sewer Overflow Storage Reservoirs Using Water Jets

By
Octavio E. Sequeiros[1]
Yarko Niño[2]
Marcelo H. García[3]

1. Research Assistant
2. Co-Principal Investigator
3. Principal Investigator

Sponsored by:

Metropolitan Water Reclamation District of Greater Chicago (MWRDGC)

U.S. Army Corps of Engineers (Chicago District)

HYDROSYSTEMS LABORATORY

DEPARTMENT OF CIVIL AND ENVIRONMENTAL ENGINEERING

UNIVERSITY OF ILLINOIS AT URBANA-CHAMPAIGN

URBANA, ILLINOIS

January 2005

EXECUTIVE SUMMARY

The proposed McCook Reservoir will store combined sewer overflows (CSOs) from the Tunnel and Reservoir Plan (TARP) system until they can be pumped back to the Stickney Water Reclamation Plant (WRP) for treatment. Based upon various assumptions, it has been estimated that about 2100 to 6000 dry tons of solids could accumulate in the reservoir after a large storm event. These sediments could form a layer on the reservoir floor having an estimated thickness of 10 to 50 centimeters and water content between 90 to 98 percent.

Several methods have been proposed for the washdown and cleaning of solids in McCook Reservoir. One such method consists in using water jets, in conjunction with a slopped reservoir bottom, to move the sediments to a collection sump while keeping a certain volume of CSOs in the reservoir to act as an odor cap.

The Metropolitan Water Reclamation District of Greater Chicago (MWRDGC) commissioned the Hydrosystems Laboratory of the University of Illinois at Urbana-Champaign to conduct research aimed at determining whether the use of water jets would be feasible for cleaning the reservoir bottom.

A one-year long study was undertaken to determine the feasibility of using multiple water jets for sediment management in McCook Reservoir. The study included:

1) Laboratory experiments to characterize the behavior (i.e. erosion and deposition) of CSOs solids from O'Hare CUP Reservoir.
2) Laboratory experiments with single and multiple water jets.
3) Numerical modeling of different water jet configurations (i.e. flow discharge, jet diameter and spacing between jets).

It was observed experimentally that single and/or multiple wall jets could be used to effectively clean a fixed bed covered by fine sediment. The amount of erosion induced by the wall jets was found to depend on jet velocity and diameter, density of the eroding fluid, and the properties of the sediment being eroded, in particular the effective or characteristic sediment diameter related to the critical shear stress for erosion.

A design criterion for jet arrays was developed as part of the study. The main design parameters are the jet diameter and discharge, and the spacing between jets. If only the momentum of the jets were used to clean the bottom of McCook, it was estimated that an array consisting of six (6) lines of jets, with a total of 336 jets, would be necessary to clean the surface area of Stage1 in McCook. Each individual jet was estimated to clean a bottom length of about 50 meters.

Further analysis, relative to the cost effectiveness of possible jet configurations, has shown that the most effective jet system would be one mounted along the side wall and

near the bottom, and operated in such a way that the cleaning of the reservoir bottom would take place in three stages, depending on the water level inside the reservoir.

With the water jet array along the wall, working as a manifold, the proposed operational strategy would be as follows:

1) With a full reservoir and a significant deposit of solids on the bottom, the jets would be operated with low velocity with the goal of resuspending a thin layer of sediment which would then flow by gravity (as a density current) towards a trench. This would prevent consolidation of the solids and it would remove the finer fractions of bed material. Since the flow discharge needed to generate the density currents will be very small, this bodes well with the fact that for a full reservoir the head difference between the reservoir and the river (canal) would also be small. Jet flows needed to induce density currents could be repeated every 12 hours or so for as long as the reservoir remains full.

2) With water depth of about 2 or 3 meters, during drainage of the reservoir, the jet manifold would be operated at full discharge capacity so as to resuspend as much sediment as possible. This should be done only in the final stages during reservoir drainage.

3) Once the reservoir is almost empty, the jets would be operated to create an "overland" erosive flow that would clean any remaining solids along the surface of the reservoir bottom. This mode of operation needs to be studied in more detail to determine the flow characteristics (discharge, depth) needed to make it effective.

This study clearly indicates that a jet system would be most effective for the cleaning of McCook Reservoir. However it is strongly recommended that before conducting the final design, a study is conducted at prototype scale to optimize the design of the jet system and its operation.

Another design parameter that needs to be studied more thoroughly, relates to the slope to be given to the bottom of the reservoir. This will have an effect on the erosion capabilities of the jets and the density currents, and will directly affect the design of the dewatering trench and sump systems. Numerical modeling would be the most effective tool to optimize the spacing of the jets; in conjunction with the bottom slope.

Further studies could also show that the most cost effective method for cleaning the reservoir is a combination of staggered jet manifolds, a smaller one consisting of closely spaced, small-diameter jets to create density currents and "overland" flows, as needed, and a second one having larger diameter jets that are more distantly spaced to induce momentum-driven erosion of bottom solids. Both jet manifolds could be mounted parallel to each other and, if needed, they could be operated simultaneously provided that there is enough flow discharge (i.e. head difference between the river and the reservoir) available.

Finally a word of caution is necessary. One of the main assumptions made in this study is that the solids entering McCook Reservoir will be deposited throughout Stage 1 as a layer of uniform thickness. Therefore, it is strongly recommended that the dynamics of the solids inside the reservoir during a storm event, in particular their depositional patterns, be studied in more detail. This would have most definitely an impact on the final design as well as the cost of the jet system since one could determine beforehand at what locations the jets will be really needed to clean the reservoir bottom. If the jet system is designed and built without understanding the mechanics of sediment deposition in McCook Reservoir, there is a risk of building an oversized and expensive jet system that would not be very effective for sediment management.

ACKNOWLEDGMENTS

We would like to acknowledge Jorge Abad and Mariano Cantero for their help with the numerical modelling of jets and turbidity currents, Silvina Mangini for her help with the characterization of the O'Hare sediments, and Andy Waratuke with the experiments.

The financial support of the Metropolitan Water Reclamation District of Greater Chicago (MWRDGC) and the U.S. Army Corps of Engineers, Chicago District, is gratefully acknowledged.

TABLE OF CONTENTS

LIST OF FIGURES

LIST OF TABLES

1. BACKGROUND

The proposed McCook Reservoir will store combined sewer overflows (CSOs) from the District's Tunnel and Reservoir Plan (TARP) system until they can be pumped back to the Stickney Water Reclamation Plant (WRP) for treatment. The McCook Reservoir will have an approximate storage capacity of 7.0 billion gallons equally divided between two stages. The stages are separated by a weir structure. A relatively small inlet stage is also part of the design. The total floor area of the reservoir is approximately 80 acres, and the maximum liquid depth will be approximately 250 feet. Based upon various assumptions regarding the suspended solids content of the CSOs and the operation of the McCook Reservoir, it is estimated that anywhere from 2100 to 6000 dry tons of solids could accumulate in the reservoir after a large storm event or a series of smaller storm events. These solids could form a layer on the reservoir floor that has been estimated by various methods as varying from 0.1 to 0.5 meters deep and having a water content somewhere between 90 and 98 percent.

The initial design plan for the McCook Reservoir is based on a horizontal reservoir floor with mechanical cleaning using street sweepers, plows, or similar vehicles to move the collected sediment to a sump for pumping back to the Stickney WRP after the reservoir has been completely dewatered. However, concerns have been raised that this will not be a cost-effective solution to the sediment handling problem, and that it may also result in odor problems in the vicinity of the reservoir due to the decomposition of the exposed solids.

It has been proposed that other methods of sediment transport/management may be feasible for McCook Reservoir. One such method is the use of water jets, in conjunction with a sloped reservoir bottom, to move the sediments to a collection sump while some volume of CSOs still remain in the reservoir to act as a liquid odor cap. The jets might be activated in conjunction with pump-back of the main liquid volume, or operated in some independent manner. The water source for the jets could be river water, if available, or the stored liquid in the reservoir. This method of sediment management has the potential to reduce the manpower costs for reservoir cleaning and also to alleviate potential odor problems. This technology may also be applicable to the Thornton Reservoir.

The Metropolitan Water Reclamation District of Greater Chicago commissioned the Hydrosystems Laboratory of the University of Illinois at Urbana-Champaign to conduct research aimed at determining whether water jets would be feasible for this application, and if such technology is feasible, developing basic design concepts for their use.

This report summarizes the results obtained as part of the research project conducted for MWRD, including a conceptualization of the problem, the research plan, and final results of the experimental and numerical modeling studies conducted.

2. CONCEPTUALIZATION OF THE PROBLEM

Flow Configurations

The application of water jets for sedimentation management rests on the ability of the jetting system to resuspend bottom sediments and to create enough of a density difference with respect to the water in the reservoir so that a density current will develop along a sloping bottom, carrying the solids towards a drainage channel. This process is illustrated in Fig. 2.1.

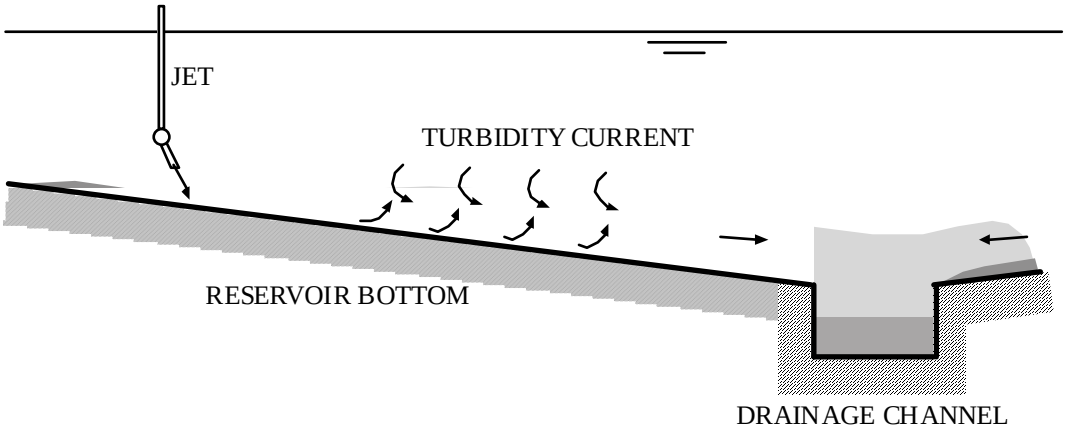

Figure 2-1 Water jet induces entrainment of sediment deposited on the reservoir bottom. Buoyancy effects create turbidity current that transports suspended sediment towards drainage channel.

Various arrays of multiple jets might be needed to mobilize the sediment deposited on the bottom of the reservoir. At least, two possible array configurations are considered herein, which will probably have to be combined for the final design of the system: a) parallel jets and b) longitudinal sequence of jets (Figs. 2.2 and 2.3). The first configuration provides spatial coverage to generate uniform sediment resuspension along the reservoir (parallel to the drainage channel). The second configuration provides a sustained entraining flow in the direction perpendicular to the drainage channel, in case self-accelerating turbidity currents conditions are not met within the reservoir. Self-accelerating currents are those driven purely by buoyancy effects and able to entrain sediment into suspension, generating a feedback mechanism that increases buoyancy and erosion capacity of the flow down the slope (Parker et al., 1986).

Each of the individual jets in any of the arrays described in Figs. 2.2 and 2.3 corresponds to what is known as a wall jet, i.e., the flow is affected by the no-slip and no-penetration conditions imposed by the bottom wall of the reservoir. Besides that, since the bottom shear stresses generated by the jets are supposed to entrain sediment into suspension, buoyancy effects tend to increase the initial momentum of the jet and far away from the source the flow conditions are not longer governed solely by the initial injection of fluid, but a sediment balance, leading to erosion or deposition along the sloping bottom, and

ambient water entrainment into the density current, ultimately determine its fate. Taking this behavior into account, it is convenient to define near- and far-field regions to analyze the flow in the vicinity of the jet discharge, or further away down the slope, once buoyancy forces and sediment transport processes take over as the driving mechanisms of the current, respectively.

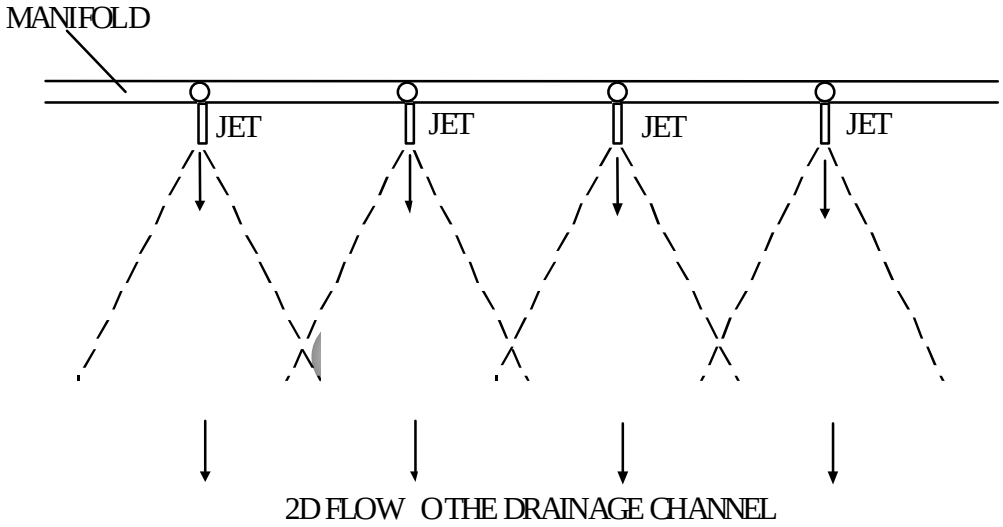

Figure 2-2 Array of parallel jets. Plan view. Jet interaction creates 2D density current moving along sloping bottom towards drainage channel.

The near field of an isolated jet comprises the region where the jet flow gets established as it is discharged into the ambient fluid. It includes the developing wall boundary layer and the expansion of the flow into the ambient fluid associated with the entrainment of ambient water, which causes a downslope decay of flow velocity and wall shear stress (Rajaratnam, 1976). Despite the decay of wall shear stress, erosion and entrainment into suspension of sediment deposited on the bed occurs as long as the bottom shear stress exceeds threshold or critical values (Hogg et al., 1997).

The far field of an isolated jet discharge is the region where buoyancy effects, generated by the sediment originally suspended in the near field, constitute the main driving force of the flow and the velocity and shear stress induced by the initial wall jet are mostly dissipated. Hence, the far field of a jet discharge corresponds to the region where a turbidity current develops along the sloping bed of the reservoir. The fate of such current (self-acceleration or extinction further downslope) depends on the ability of the buoyancy induced flow field to generate sediment entrainment rates in excess of deposition rates.

A further distinction is required in the case of parallel jets, when several jets of an array configuration such as that of Fig. 2.2 are operated simultaneously. Due to the lateral expansion of the jets, the flow fields generated by them eventually come to interact, as illustrated in Fig. 2.2. At a certain distance from the sources, which depends on the spacing between jets (the pitch, s), the initially 3D flow associated with each individual jet becomes 2D, that is, uniform in the transverse (along the reservoir) direction.

According to Wang et al. (2001) such distance, L_{2D}, is about 12 *s*. Thus in the case of parallel jets, the near- and far-field distinctions and the behavior of the flow in each region depend on how L_{2D} compares with the distance from the jet discharge at which the resulting turbidity current becomes fully established, L_t. Cantero (2002) did numerical simulations of turbidity currents generated by a plane jet discharging tangential to a sediment bed. An analysis of those simulations suggests that L_t is of the order of 100 times the thickness of the initial jet. Therefore, the characteristics of the flow in the near- and far-field regions depend on the design parameters of the jet system (pitch, size of the nozzles). A reasonable assumption, however, is to consider that the pitch will be large enough so $L_{2D} > L_t$, and the turbidity currents generated by individual jets will become fully established before interacting with flow fields generated by neighboring jets. In such case, it is convenient to define a near field identical to that of an isolated jet discharge, an intermediate field, comparable to the far field of an isolated jet discharge, and a far field consisting of a 2D turbidity current (uniform in the transverse direction) generated by the interacting currents of the parallel jet system.

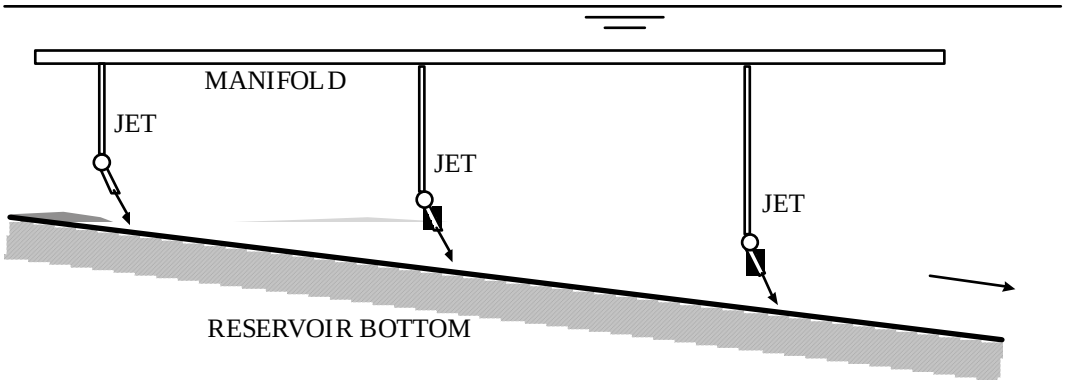

Figure 2-3 Longitudinal sequence of jets (side view). In case the turbidity currents are not self-accelerating, the sequence of jets induces entrainment of sediment into suspension along the bottom and the turbidity currents provide the downslope transport.

In the case of a longitudinal sequence of jets (Fig. 2.3), it is assumed that the spacing of the jets will be greater that L_t, and possibly comparable to L_{2D}. This suggests that the behavior of the downstream jets will be influenced by the presence of a near 2D turbidity current. Thus, the transition from the 3D near field to the 2D far field in the case of the downstream jets would be swifter than in the case of the jet at the upstream end of the sequence and the definition of an intermediate field in this case would not be justified.

Scouring and Sediment Transport Processes

i) Near field

Jenkins et al. (1981) and Dellaripa and Bailard (1986) have studied the use of jet arrays to manage sedimentation problems at Navy port facilities. The typical array configuration used, with 10 to 25 jet nozzles with a pitch of about 3 to 7 m and nozzle diameters of about 2 to 7 cm, cover spans of about 50 to 100 m with scour radius of about 15 to 30 m (Fig. 2.4). The scour radius is defined as the distance away from the jet, in the streamwise direction, that is scoured by the action of the induced flow field. The concept is that the bottom shear stress induced by a jet decays away from the source, therefore entrainment and scouring of bottom sediments will prevail only as long as the bottom shear stress exceeds the threshold scour stress of the sediment (Jenkins et al., 1981). The jet array is operated sequentially in time, using either one or several jet nozzles simultaneously at a time. Jenkins et al. used a 150 hp centrifugal pump, with a total discharge of about 120 l/s.

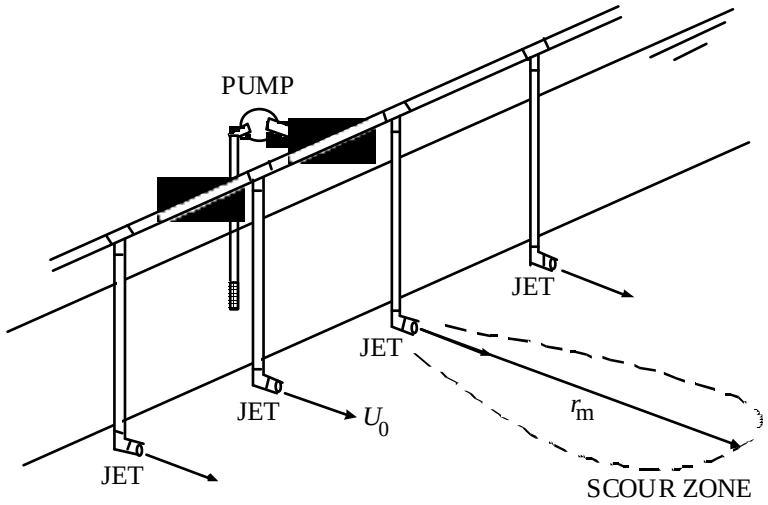

Figure 2-4 Jet array system used by Jenkins et al. (1981); r_m represents the scour radius.

A similar system might be used in McCook reservoir to provide the near field conditions for turbidity currents to develop, which would carry the suspended sediment down the slope and into the drainage channel. A network of jet arrays such as those of Fig. 2.4 would provide spatial coverage to maintain the reservoir free of sediment deposits. The network would be operated sequentially in time to optimize the cost of the cleaning process.

Consider an individual jet nozzle with a diameter d, located at a height h over the sediment bed, under a water column of total height H, having a discharge velocity U_0 at an angle θ with respect to the horizontal (Fig. 2.5). No density difference is assumed between the fluid discharged by the jet and the ambient fluid.

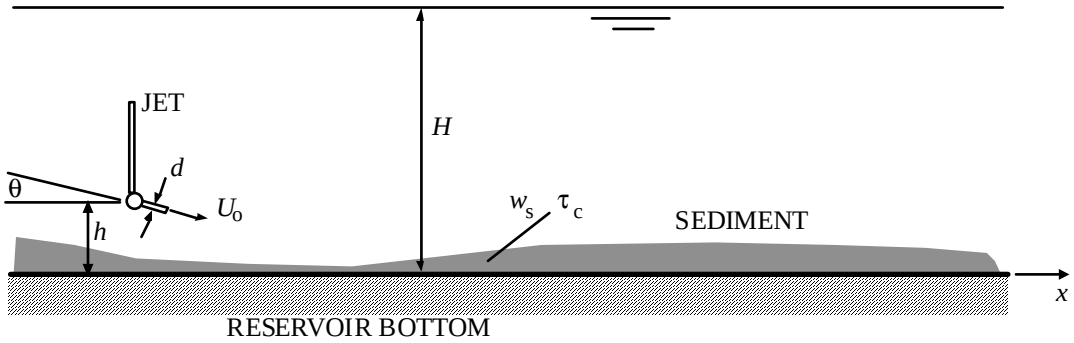

Figure 2-5 Circular jet impinging over sediment bed.

The shear stress exerted by a jet on a bottom surface, τ_b, is given by an expression such as:

$$\tau_b = f_1(U_0, d, h, \theta, H, \nu, \rho, x, y) \quad (2.1)$$

where ν and ρ denote kinematic viscosity and density of the jet fluid, respectively, and x and y denote longitudinal and transverse coordinates, respectively. Note that no dependence on gravity has been included, as there are no buoyancy effects involved and the flow is driven by inertia balanced by bottom friction. In dimensionless terms, Equation (2.1) reduces to:

$$\tau_b / (\rho\ U_0^2) = \phi_1(h/d, H/d, \theta, Re_0, x/d, y/d) \quad (2.2)$$

where $Re_0 = U_0\ d/\nu$ denotes the jet Reynolds number. In the case of a deep reservoir, the dependence on H/d can be neglected as this parameter approaches infinity. Dellaripa and Bailard (1986) suggest that the scouring area is maximized for small angles θ and low heights h (see Chapter 4.3). For $h = 0$, $\theta = 0$ and large H/d, Jenkins et al. (1981) proposed the following relationship for the decay of the bottom shear stress along the x axis, which completely agrees with the present dimensional analysis:

$$\tau_b / (\rho\ U_0^2) = 120\ Re_0^{-0.4}\ (x/d)^{-2.4} \quad (2.3)$$

The jet Reynolds number appears to be the dominant parameter that determines the bottom shear stress even in fully developed turbulent jets. In Appendix A, a theoretical analysis of the bottom shear stress induced by a wall jet, which supports the results obtained from this dimensional analysis, is presented. On the other hand, Wygnanski et al. (1992) suggest that the dependence on Re_0 indicated by (2.3) disappears for values of this parameter larger than about 10^4.

According to Jenkins et al. (1981) the design of a jet for sediment management purposes can be done with the help of (2.3) by setting U_0 and d in order to have, at a nominal distance $x = r_m$ (the scouring radius), a bottom shear stress, τ_b, that exceeds the threshold

or critical stress for the scour of the bottom sediments, τ_c. This can be analyzed as follows.

Consider a threshold shear velocity, u_{*c}, such that $\tau_c = \rho\, u_{*c}^2$, the scouring radius is then given by a relationship such as:

$$r_m = f_2(U_0, d, h, \theta, H, \nu, u_{*c}) \tag{2.4}$$

which in dimensionless terms can be written as:

$$r_m/d = \phi_2(h/d, H/d, \theta, Re_0, U_0/u_{*c}) \tag{2.5}$$

Similarly the lateral extension of the area scoured by the jet, y_m, is given by

$$y_m/d = \phi_3(h/d, H/d, \theta, Re_0, U_0/u_{*c}) \tag{2.6}$$

The dimensions of the scour pattern have been studied experimentally by Van Dorn et al. (1978). Dellaripa and Bailard (1986) argue, based on the data of Van Dorn et al., that the scouring area of the jet is self-similar such that the ratio y_m / r_m remains constant, taking a value of about 1/3.

Boundary conditions needed for the analysis of the far field behavior of the flow, or region where the subsequent turbidity current develops, corresponds to the relative density difference of the current at the onset, $\Delta\rho/\rho$, where $\Delta\rho = \rho_m - \rho$, and ρ_m denotes the density of the sediment-water mixture, and the corresponding mass flow rate per unit width, g_{si}. These variables are given by the following expressions:

$$\Delta\rho/\rho = f_3(U_0, d, h, \theta, \nu, w_s, u_{*c}, x, y) \tag{2.7}$$

$$g_{si} = f_4(U_0, d, h, \theta, \nu, \rho, w_s, u_{*c}, x, y) \tag{2.8}$$

where the settling velocity of the sediment particles, w_s, has been added as one of the independent variables, characterizing the suspension characteristics of the sediment. The fall velocity takes into account parameters such as sediment size, shape and density, cohesiveness and gravity effects, etc. In these relationships the total depth of the reservoir, H, has been taken out of the analysis assuming H/d is very large. Corresponding dimensionless relations are:

$$\Delta\rho/\rho = \phi_4(h/d, \theta, Re_0, U_0/w_s, U_0/u_{*c}, x/d, y/d) \tag{2.9}$$

$$g_{si}/(\rho\, U_0\, d) = \phi_5(h/d, \theta, Re_0, U_0/w_s, U_0/u_{*c}, x/d, y/d) \tag{2.10}$$

Note that the effect of gravity is included through the settling velocity. The erosion capacity of the jet-induced flow is dominated by inertia and friction. This changes in the far field, where buoyancy is the main driving force of the subsequent turbidity current.

ii) Far field

The far field is the region where the turbidity current generated by the jet-induced sediment suspension develops, carrying the suspended sediment down the slope towards the drainage channel of the reservoir. The main variable of this process corresponds to the mass transport rate of the turbidity current, g_{si}, as it determines the ultimate cleaning efficiency of the jet system. The following expression can be considered for the mass transport rate at the onset of the current:

$$g_{si} = f_5(U_0, d, h, \theta, \nu, \rho, g', w_s, u_{*c}, x, y) \tag{2.11}$$

where $g' = g\,\Delta\rho/\rho$, with g denoting gravitational acceleration, is the reduced gravity at the onset of the current which represents the main driving force of the flow in the far field. The resulting dimensionless relation is:

$$g_{si}/(\rho\, U_0\, d) = \phi_6(h/d, \theta, Re_0, Fr_{d0}, U_0/w_s, U_0/u_{*c}, x/d, y/d) \tag{2.12}$$

where Fr_{d0} denotes the densimetric Froude number defined as $Fr_{d0}^2 = U_0^2/(g'\, d)$. In Equation (2.12) the parameter U_0/w_s controls the characteristics of the sediment suspension, such as concentration distribution and deposition rate, while the parameter U_0/u_{*c} controls the erosive capacity of the turbidity current.

Instead of using the jet parameters in the relationship for g_{si} the velocity and height of the flow at the onset of the current, U_i and h_i, respectively, can be used to obtain:

$$g_{si}/(\rho\, U_i\, h_i) = \phi_7(Ri_i, U_i/w_s, U_i/u_{*c}, x/d, y/d) \tag{2.13}$$

where $Ri_i = g'\, h_i/U_i^2$ is the Richardson number at the onset of the current, which has been used instead of the densimetric Froude number of the flow (which is just the inverse of Ri_i) to be consistent with classical analyses of density currents (e.g., Ellison and Turner, 1959). In this relation the dependence on the kinematic viscosity was neglected, assuming fully developed turbulent flow (Ellison and Turner, 1959). Again, U_i/w_s controls the concentration distribution and deposition rate, while U_i/u_{*c} controls the erosive capacity of the turbidity current.

The transport capacity of the far field turbidity current at any point (x, y), g_s, will be given by an equation similar to (2.13), but based on local values of the flow velocity and Richardson number. These values are strongly dependent on the slope of the bottom surface over which the turbidity current develops. Therefore, the final destiny of the turbidity current (self acceleration or dilution) is strongly dictated by this slope.

The design of the jet system in McCook reservoir must provide the conditions for which g_s remains relatively constant or increases with x in the far field region of the flow. This ensures that the sediment scoured by the jets in the near field is evacuated from the system and, eventually, that the turbidity currents also contribute to eroding the sediment deposit to some extent.

Research Needs

From the analyses of previous sections it is concluded that a number of different flow situations and sediment characteristics must be studied in order to understand the phenomena involved and gather sufficient knowledge to design the sediment management system of McCook reservoir using water jets. These are:

1. Flow and sediment transport processes

- Flow and scour pattern of a jet impinging on a sediment deposit of limited thickness
- Flow field and bottom shear stress generated by parallel wall jets
- 2D eroding/depositing turbidity current
- 3D laterally expanding eroding/depositing turbidity current
- Interaction of jet and 2D turbidity current

2. Characterization of McCook sediments

- Settling velocity
- Critical shear stress for erosion
- Suspension dynamics

Although the information provided by Jenkins et al. (1981) and Dellaripa and Bailard (1986) regarding the design of jet array systems to manage sediment deposits in port facilities is useful for the McCook study, there are some aspects of such application that are different to the present one. In particular, the sediment deposit in McCook reservoir is going to be of a limited thickness (estimated by USACE, in the draft design documentation report, as about 0.1 to 0.5 m), which means that the scouring process will be limited by the solid bottom of the reservoir, changing the geometry of the scour zone and the scour radius in particular (Fig. 2.4), with respect to those given by the relationships proposed by Dellaripa and Bailard (1986).

Another aspect that needs to be investigated corresponds to the flow and sediment concentration conditions prevailing at the onset of the turbidity current, at the edge of the near field zone generated by the jet array. These constitute the boundary conditions that control the developing turbidity current in the far field zone of the jet arrays. It was found in some of the preliminary experiments conducted, however, that the turbidity currents that develop in a low-slope configuration such as the one that will probably prevail in McCook reservoir (slope lower than about 1%), are rather weak and in no case self-accelerating. This means that most of the cleaning of the bottom solids will be generated

by the jets themselves and that a configuration such as that shown in Fig. 2.3, to insure the continuous transport of the sediment towards the drainage channel, will be needed. This observation changes the emphasis of the study away from the far field turbidity currents and gives more relevance to the study of the near field flow and erosion processes. This was taken into account in the final version of the research program conducted, as is indicated below.

As concluded from the analysis of the previous section, the near field sediment transport problem depends, among other dimensionless parameters, on Re_0, U_0/w_s, and U_0/u_{*c}. A consequence of this result is that the only way to physically model the field situation meaningfully, i.e., without introducing major scale distortions, is by reproducing both the Reynolds number and the sediment of the prototype, and this results in the need to use a 1:1 model scale which is unpractical. Even though it can be argued that Re_0 would not be a relevant parameter in the prototype and therefore it may not necessarily be reproduced exactly in the laboratory experiments as long as it is large enough in those experiments, the need to reproduce the response of the sediment, which in McCook case it seems to be a complicated one given the origin of those sediments, imposes the use of prototype sediments in the experimental study and this leads, by dimensional considerations, to the need to reproduce also prototype flow velocities in the experiments.

The response of the sediments has been characterized in the previous section by essentially two parameters: the settling velocity, w_s, and the threshold or critical scour stress of the bottom sediments, τ_c. It has been observed in tests with solids form O'Hare reservoir, provided by MWRD, that they behave as cohesive sediment to some degree, and therefore both w_s and τ_c will probably depend on the degree of consolidation of the deposit. One of the main objectives of the present study is, therefore, to learn about the expected behavior of McCook sediments and its effect on the jetting management system.

These topics define specific objectives for the research project and the strategy used to approach their study is explained next.

Research Program

Given that the experimental research on the behavior of the jetting sediment management system requires model scales close to unity, which are not possible to obtain at a laboratory scale, an alternative approach is being used in the present study. This approach consists of combining experiments regarding flow and sediment transport induced by the jet array systems. The idea is to study at a laboratory scale the main aspects of the jetting system, eventually validate numerical models of some of the process involved using the experimental data, and then, apply them for the final design of the sediment cleaning system for McCook reservoir. Some pilot studies at prototype scale will be also needed (not included in the scope of the present study) to validate conclusions of this project and gather information for the final design of the jetting system. Based on this strategy, the following research program was conducted.

i) Characterization of McCook Sediments

The characterization of sediments representative of those to be deposited on the bottom of McCook reservoir was done by means of a number of different experiments performed upon CSO solids from O'Hare reservoir provided by MWRD. They concentrate on the following aspects:

S1 Settling velocity
S2 Critical shear stress for erosion
S3 Suspension dynamics

ii) Flow and Sediment Transport Process

Experimental studies

E1 Experimental study on flow and scour pattern by plane wall jet on bed of limited thickness
E2 Experimental study on scour pattern of plan jet on bed of limited thickness with CSO solids
E3 Experimental study on flow and scour pattern of single circular jet on bed of limited thickness
E4 Experimental study on flow and scour pattern of multiple circular jets on bed limited thickness

3. EXPERIMENTAL STUDY

3.1 Characterization of McCook sediments

a) Experimental methods

The characterization of sediments representative of those to be deposited on the bottom of McCook reservoir was approached by means of a number of different experiments. They concentrate on the following aspects:

S1 Settling velocity
S2 Critical shear stress for erosion and suspension dynamics

The experiments S1, to characterize settling velocity, were conducted with the help of a laser-diffraction instrument: LISST-ST. This instrument measures size distribution, concentration, and settling velocity distribution of suspended particles, among other parameters. The characterization of the settling velocity of McCook-type sediments (actually solids coming from O'Hare reservoir, provided by MWRD) was made considering dependence on both solids concentration and aggregate formation.

Experiments of series S2 also used the solids from O'Hare reservoir. They were conducted in an annular flume with an inner radius of 0.55 m, an outer radius of 0.75 m, and a total depth of 0.45 m, and with a rotating upper lid and an also rotating bottom plate (see Figure 3.1.a). The main advantage of using this type of flume for cohesive sediment research is that motion is transmitted to the fluid by means of wall friction, which prevents flocs to be broken up by pumps, thus preserving the aggregate structure of the suspended sediment during the experiments. The flow within the annular flume has, at least theoretically, a uniform shear stress distribution, which facilitates the analysis of the response of the sediment (entrainment from the bed, concentration distribution, change in the aggregate structure of the suspended sediment, etc.) to flow conditions. Numerical simulations and a series of experiments were conducted to relate flume operation conditions with shear stress in the water column. Measurements in experiments S2 include characterizing the flow field by means of an ADV that rotates with the upper lid of the flume (see Figure 3.1.a), measuring concentration distribution and suspended sediment properties by analyzing samples taken from the flume (see Figure 3.1.b), and direct observations of the behavior of the sediment suspensions.

The experiments S1 and S2 considered the effect of different degrees of consolidation of the bottom sediments in McCook reservoir, by starting from mechanically disaggregated samples and allowing them to consolidate for times ranging from 0 to a few days, which is the estimated residence time for the sediments within the reservoir.

Figure 3-1 Sampling taps in the annular flume.

b) Results

S1 Settling velocity experiments

A series of experiments was completed to characterize properties of solids from O'Hare reservoir, provided by MWRD. The LISST-ST laser-diffraction instrument was used for the analyses. Different test samples were prepared from the solids provided by MWRD. Solid concentrations used in those samples varied between 2 and 20 ml/l. Tests with and without disaggregated samples were made in order to estimate the size of aggregate formation. The mean size of particles belonging to the original samples (not disaggregated) is about 24.5 μm, and the typical settling velocity is 0.05 cm/s, while corresponding values for disaggregated samples were 10.8 μm and 0.008 cm/s, respectively. The results obtained indicate a negligible dependence of the settling velocity on sediment concentration and this applies to both the original and disaggregated samples. The mean size of the aggregates found in the original sediment samples (not disaggregated) was estimated indirectly, from particle size and concentration distributions measurements. The results indicate that the mean diameter of the aggregates is about 84 μm with a mean settling velocity of 0.5 cm/s. However this aggregates settling velocity could be not representative regarding it is one order of magnitude greater than previous measurements performed by MWRDGC. Based solely on the range of particles sizes found in this study, solids from O'Hare reservoir could be classified as cohesive.

The results from the sediment characterization analysis suggest that the type of solids to be deposited within McCook reservoir might be characterized as to be composed mainly by two fractions: a disperse fraction and flocs or aggregates of larger size and higher

settling velocity. The time scale associated with the formation of those aggregates, as well as their response to turbulence and flow shear stresses was investigated in series S2.

S2 Critical shear stress for erosion and suspension dynamics

Experiments of series S2 were conducted in an annular flume. Two different experiments were conducted: a deposition test and an erosion test, together with additional experiments to study the response of suspensions of solids from O'Hare reservoir under constant shear stress.

In the deposition test, a mixture of water and solids from O'Hare reservoir with an initial concentration of 1647 mg/l was introduced into the annular flume. At the beginning, the sediment suspension in the flume was well mixed to obtain a homogeneous distribution of sediment in the flume. After the mixing phase, the bottom shear stress in the flume was lowered stepwise from the maximum value given by the facility of 1.18 N/m^2 down to 0.06 N/m^2 in 20 hrs. The time steps were of 2 hrs for the highest shear stresses and of 3 hrs for the lower ones. Fig. 3.2.a shows the evolution of the concentration measured at half depth (0.2 m from the bottom) as the shear stress is reduced. The concentration at half depth can be shown theoretically to be representative of the depth-averaged concentration, at least for the range of shear stresses in the experiments conducted. It was found that some deposition occurs even for the highest shear stress. The concentration decreases almost linearly as the shear stress decreases. About 50% of the sediment is deposited for values of the shear stress of about 0.54 N/m^2. The concentration remains constant with a value of about 800 mg/l for values of the shear stress below this limit. The concentration of the sediment that remains in suspension for the lowest shear stress tested represents a 46% of the initial value. It means that only 54% of the initial sediment is deposited even for the lowest values of the shear stress tested. From these results, it is concluded that the solids from O'Hare reservoir do not behave exactly as cohesive sediment, since usually, under low shear stresses, cohesive sediment increases the deposition rate due to floc formation (a process that is precluded by turbulence at high shear stresses).

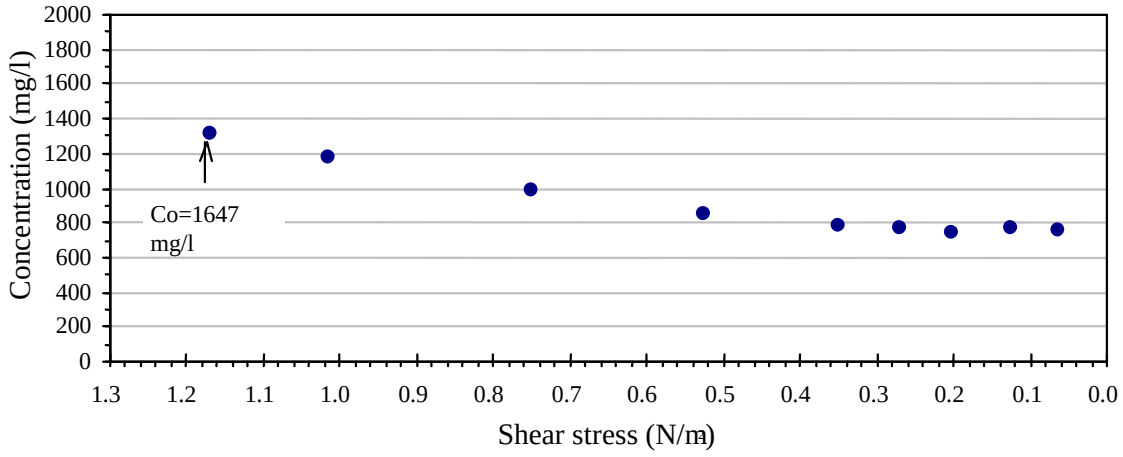

Figure 3-2 a Results of the deposition test: Concentration at half-depth as a function of the shear stress

In the erosion test, a sediment bed has to be developed on the bottom of the annular flume. This was accomplished by letting an initial homogeneous mixture of water and solids from O'Hare reservoir with a concentration of 2826 mg/l to settle under no stress conditions for a period of about 20 hrs. At the end of this period a bed was formed on the bottom of the flume and no relevant suspended solids concentration was observed in the water column. The initial concentration of 2826 mg/l represents the maximum homogeneous concentration that can be reached in the flume, only if all the sediment bed is entrained into suspension. The erosion test began with a minimum bottom shear stress of 0.06 N/m^2, which was increased stepwise, with time steps of 1.5 hrs, to a maximum value of 1.18 N/m^2. Samples were taken 15 minutes after the beginning of shear stress step and at the end of each step. Fig. 3.2.b shows the evolution of the concentration measured at half depth (0.2 m from the bottom) as the shear stress is increased, plotting the concentration at both the beginning and end of the shear stress step. The concentration increases as the shear stress increases. At the first shear stress step (0.06 N/m^2) the concentration reaches a value of about 60% of the original concentration (before settling). Only at the second shear stress step (0.13 N/m^2) an increment of the concentration during the 1.5 hrs of duration of the step is observed. At higher shear stresses no significant differences in the concentration at the beginning and end of the step are apparent. For values of the shear stress higher than 0.13 N/m^2 the concentration reaches a value close to 90% of the original concentration, which means that about 90% of the bed has been resuspended. The concentration remains invariant at 90% of the original value for values of the shear stress higher than 0.40 N/m^2.

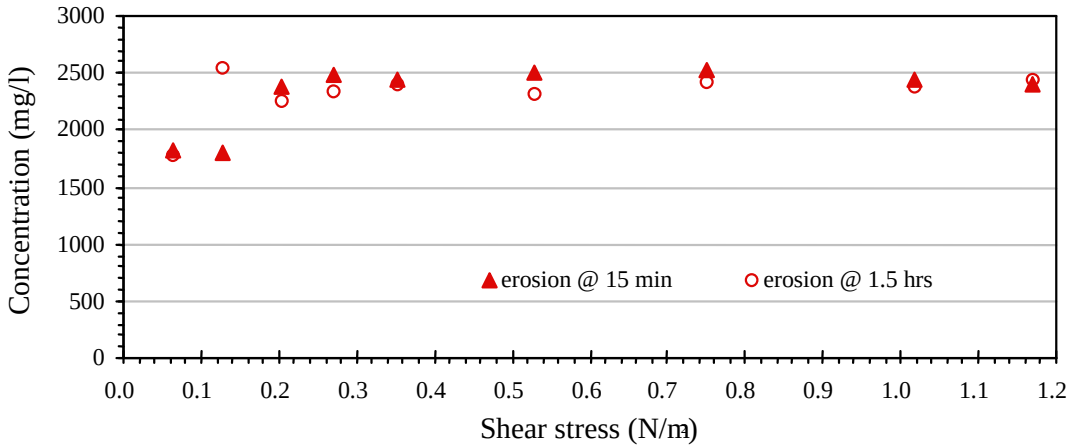

Figure 3-2 b Results of the erosion test: Concentration at half-depth, at the beginning and end of the shear stress step, as a function of shear stress.

Besides the deposition and erosion tests, other experiments were carried out. The goal of these was to study the behavior of suspension of solids from O'Hare reservoir under a constant shear stress in a lapse of time between 8 to 10 hrs. For each test, a sediment bed was developed. The same procedure to the one described in previous erosion test was carried out before beginning the tests. Two different initial homogeneous concentrations of solids were used: 2500mg/l and 7000 mg/l. The consolidation time was in these cases 18 hrs. The shear stress exerted over the bed created by deposition and consolidation was

0.27 N/m^2, a value for which about 90% of the sediment was resuspended in the erosion test previously reported (Fig. 3.2.b). Figs. 3.3 and 3.4 show the results obtained. A maximum of about 80 to 90% of the bed sediment gets resuspended, in both cases, in a time of about 20 min. The suspended sediment concentration reached during this initial entrainment process remains invariant afterwards, for the rest of the experiment. One last experiment was conducted with an initial homogeneous concentration of 7000 mg/l and a constant shear stress of 0.88 N/m^2. The response of the sediment suspension under this higher shear stress was similar to that in the previous tests. During the first 20 minutes most of the sediment bed gets entrained, defining a maximum concentration close to 90% of the initial homogeneous concentration (before settling), and only slightly higher than that obtained for the experiment with a lower shear stress (Fig. 3.5). The concentration remains constant during the rest of the experiment. The consolidation times expected in the McCook Reservoir are larger than 18 hours, because the water could be held in the reservoir for several days. It must be noted the consolidation times in experiments corresponding to the E2 series were approximately 2 days, and the shear stresses needed for erosion were found to be the same order of magnitude. However, as a general rule, the longer the consolidation time, the higher the shear stress needed to washdown the sediments. This reinforces the idea of generating density currents in a first operational stage to avoid excessive consolidation before the jet system is employed in its full capability. The discharge required to generate density currents should be significantly smaller than the one in the second operational stage. Besides, being the reservoir level probably high, the available head to create jets by gravity would be reduced. This last point is an advantage rather than a drawback because when the reservoir is full or nearly full it would not be convenient to resuspend sediment using high power jets.

These results reinforce the conclusion that the solids from O'Hare reservoir do not behave as cohesive sediment. Floc formation under rather low constant shear stress was not apparent, as the concentration remained invariant for as long as the shear stress was maintained. Similar values of the concentration were obtained at higher values of shear stress, which means that settling velocity is not sensitive to shear stress as it happens with cohesive sediment, for which higher shear stress means aggregate destruction and increasing settling velocities.

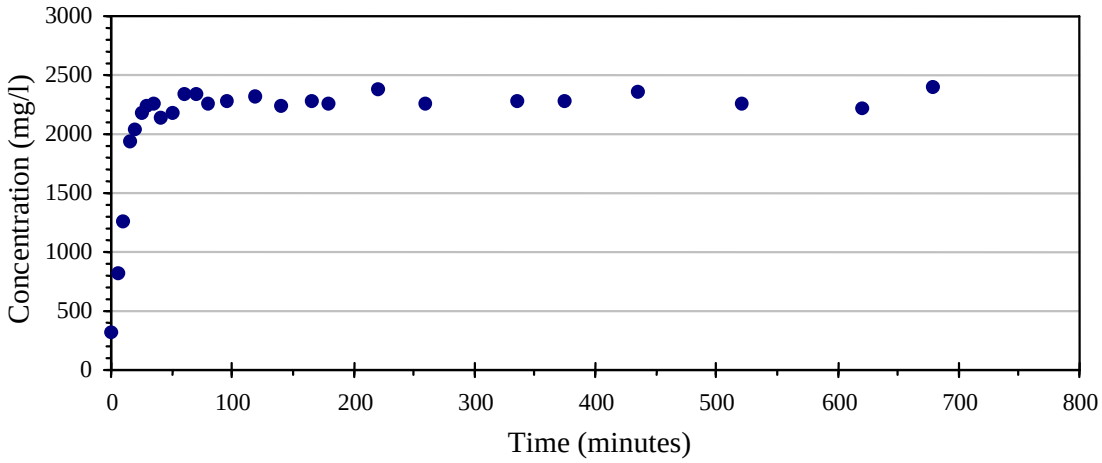

Figure 3-3 Time evolution of suspended sediment concentration. Constant shear stress value of 0.27 N/m^2; homogeneous initial sediment concentration before settling: 2500 mg/l.

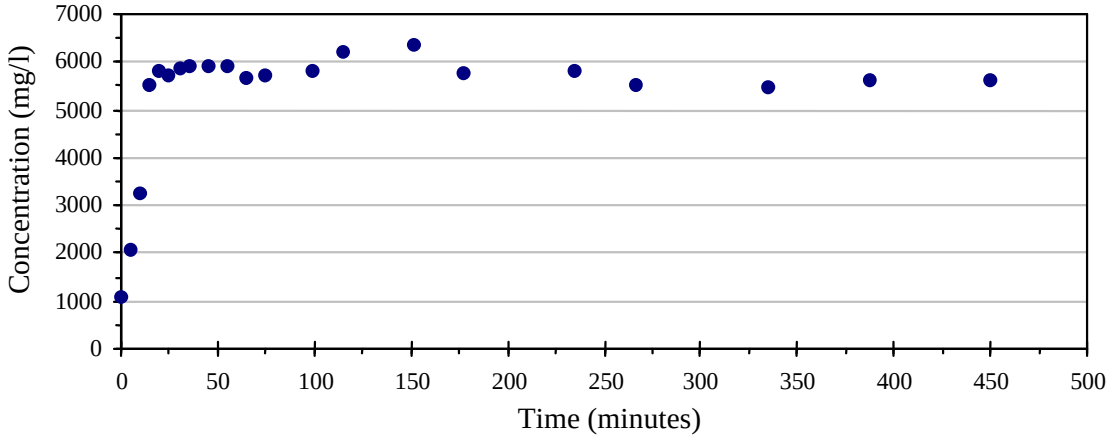

Figure 3-4 Time evolution of suspended sediment concentration. Constant shear stress value of 0.27 N/m^2; homogeneous initial sediment concentration before settling: 7000 mg/l.

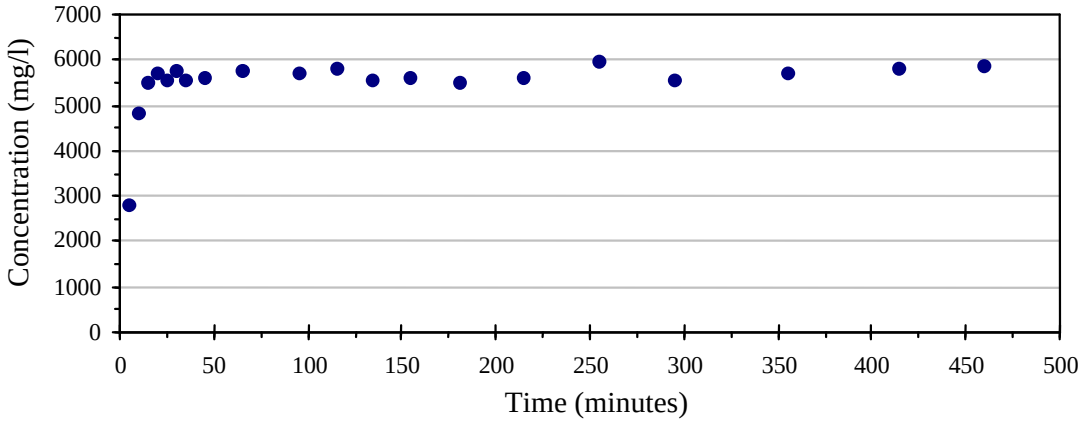

Figure 3-5 Time evolution of suspended sediment concentration. Constant shear stress value of 0.88 N/m^2; homogeneous initial sediment concentration before settling: 7000 mg/l.

c) Conclusions

The results from the sediment characterization analysis suggest that the type of solids to be deposited within McCook reservoir might be characterized as to be composed mainly by two fractions: a disperse fraction and flocs or aggregates of larger size and higher settling velocity. It is apparent from these results, that the process of formation of aggregates observed in the original O'Hare solid samples studied has time scales that are longer than 12 to 24 hours. Those aggregates do not respond sensibly to variations of shear stress values in the range expected to generate resuspension by the jet array system. In conclusion, cohesion effects are not relevant to the behavior of solids of O'Hare reservoir from the point of view of their management using a jet array system, and the same can be expected for solids to be deposited in McCook reservoir.

3.2 Flow and sediment transport processes induced by jets

Four series of experimental studies were conducted to study flow, erosion, and transport processes associated to different jet configurations, ranging from plane jets to single and multiple circular jets. In all cases a bed of limited thickness was created over a fixed bottom using different types of sediments, including the same solids from O'Hare reservoir tested in the previous set of experiments.

3.2.1 Series E1. Experimental study on flow and scour pattern by plane wall jet on a bed of limited thickness.

The magnitude of the erosion caused by a plane turbulent wall jet on fine but non-cohesive sediment laying on a fixed boundary was studied in laboratory experiments. The results show a clear link between the final profile of the scour front and the Froude number at the nozzle. The flow velocity structure induced by the jet was also studied as well as the evolution of the scour with time.

a) Experimental methods

The experimental study was carried out in a channel 5.0 m long, 0.30 m wide, and 0.4 m high. The channel was placed on a plate, located inside a water tank 7.3 m long, 2.7 m wide, and 2.3 m high. A pump conveyed the water from a secondary tank to feed a plane jet at the upstream end of the channel (Fig. 3.6.a). Inflow discharges were measured using a magnetic flowmeter McCrometer (Serial No. 96061675), having a capacity up to 20 l/s, located in the supply pipe. The adjustable bottom slope of the plate was set at 1.5%. The plane wall jet is a two-dimensional jet flowing out of a rectangular nozzle having a height b_0 and a width of 0.30 m (the whole channel width). The differences between two-dimensional jets (plane) and three-dimensional jets (circular) will be analyzed later.

A plane wall jet was discharged into the channel, parallel to the bottom plate. Two different situations were analyzed. Jets over a fixed bottom were studied first to confirm previous investigations regarding flow structure. Then, a movable bed 4.3 cm thick, formed with a fine granular quartz material provided by U.S. Silica Company (d_{50} = 45 μm, d_{95} = 196 μm) was set on the bottom of the channel, and another series of jets were run to study the bed erosion process. The jets were run parallel to the bottom (see Figures 3.11 and 3.12). Studies by Dellaripa and Bailard (1986) for circular jets showed that the jet scour pattern is also a function of the jet height from the bottom. This point will be expanded in the section corresponding to circular jets. During the experiments the flow field generated by the jet discharge was monitored by means of an array of 4 synchronized ADVs (Acoustic Doppler Velocimeters) located at different distances from the nozzle (see Figure 3.6.b). Erosion rates were registered by means of video recordings of the erosion process.

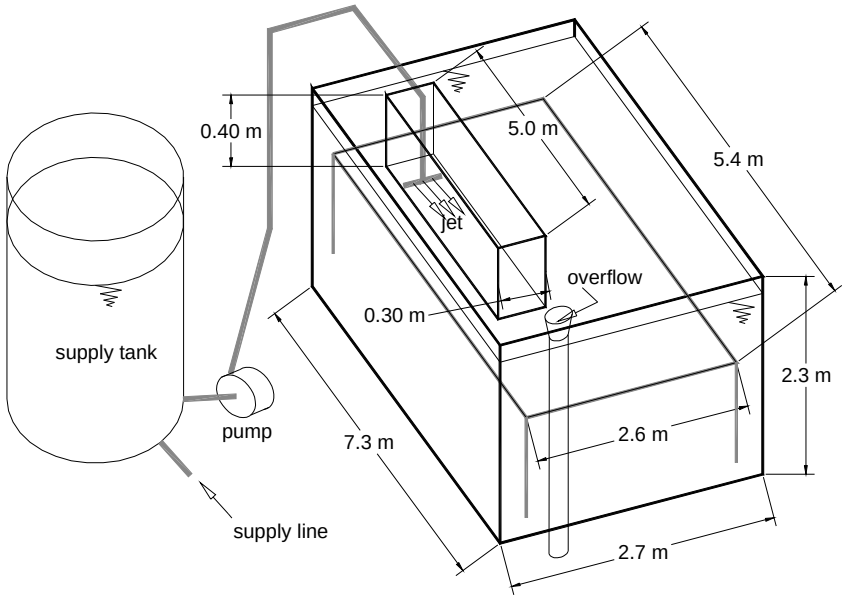

Figure 3-6 a Experimental set-up for plane wall jet experiments on non-cohesive sediment.

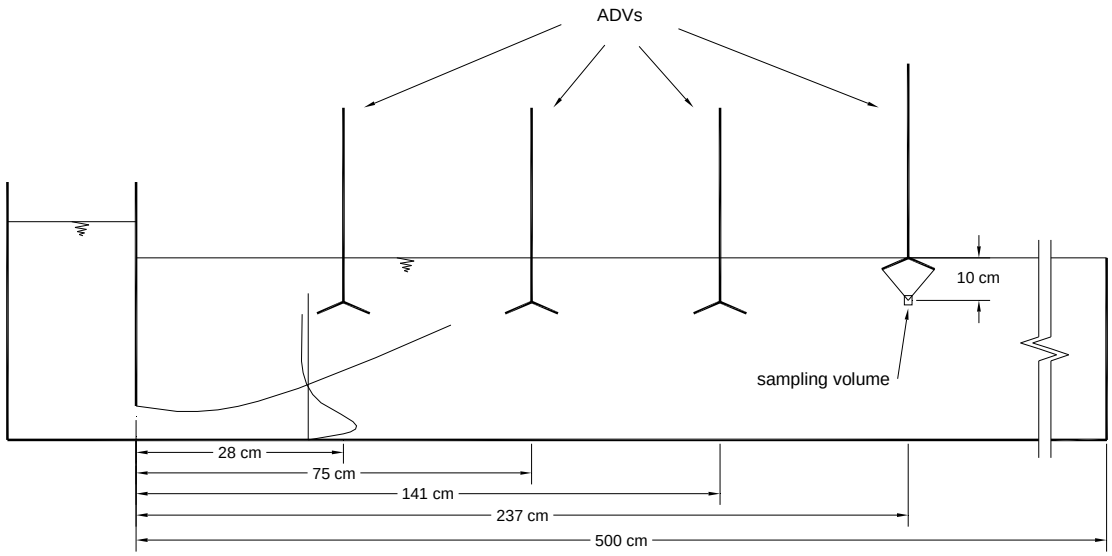

Figure 3-6 b Location of ADVs for plane wall jets experiments. Because of the distance between the instrument and the sampling volume, 10 cm for this ADV model, the first 10 cm of the vertical profiles from the free surface cannot be measured.

b) Results

b1) Flow measurements without a sediment bed

In order to confirm and better understand the flow generated by plane wall jets (Fig. 3.7), velocity measurements were performed using Acoustic Doppler Velocimeters (ADVs). Four 10 MHz Nortex NDVField ADVs (Fig. 3.8) were placed at different distances from

the nozzle and used to acquire the velocity profiles generated by plane wall jets having different nozzle Reynolds numbers. For the 10 MHz NDVField probes, this sampling volume is located 10 cm from the tip of the probe, thus data located closer than 10 cm to the water surface could not be measured (see Figure 3.6.b).

Six experiments were run, each one corresponding to a different discharge. Table 3.1 summarizes the basic parameters for all the runs.

The profiles matched with accuracy the empirical equation proposed by Verhoff (1963) for the two-dimensional turbulent wall jet over a smooth fixed boundary, with the exception of the recirculation region detected above the jet flow located near the nozzle (Fig. 3.9). This difference can be explained partially due to the conditions under which the experiments were run. Namely, a fluid of finite vertical extent contrasting with the practically semi-infinite fluid in previous studies by Myers et al. (1963), Verhoff (1963), and Wygnanski et al. (1992). These researchers experimented with deeply submerged jets (*H >> h)*. Due to water entrainment into the jet from the fluid above caused by mixing, when the ambient fluid height *H* is not infinite, negative velocities (velocities moving in the opposite direction of the jet) occur in the region above the jet to satisfy mass conservation.
As it was mentioned above, due to the model of ADV employed it was not possible to measure velocities at points located closer than 10 cm to the water surface. Thus, the upper 10 cm of the profile were not measured but extrapolated from the data. The profiles in Fig.3.9 and 3.10 show only the data measured with the ADVs. Predictions of Verhoff's equation are also shown. Maximum velocity and recirculation increases as the Reynolds number increases.

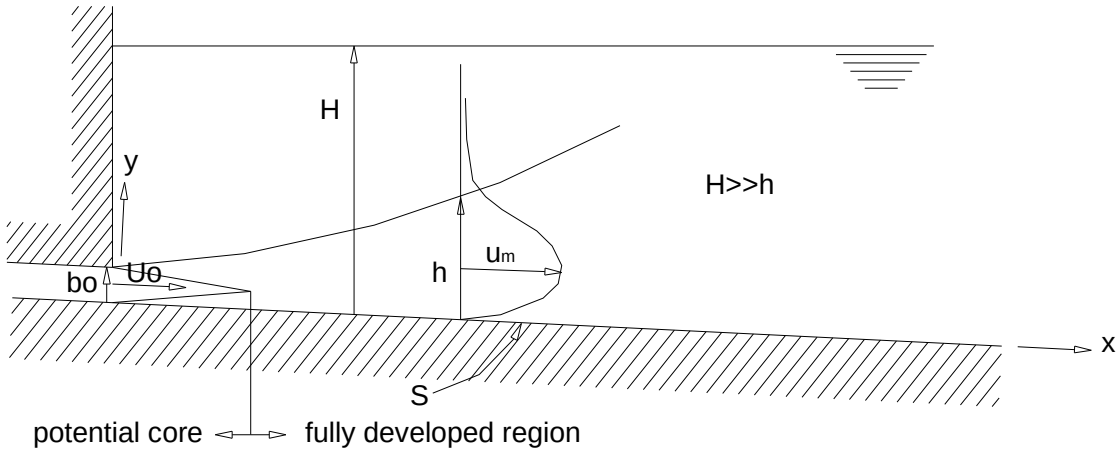

Figure 3-7 Plane wall jet over an almost semi-infinite fluid with solid bottom.

Figure 3-8 Acoustic Doppler velocimeter.

Table 3-1 Experimental conditions for the jet flow velocity characterization experiments.

Run	Slope [%]	Q [l/s]	b_0 [cm]	Re_0
1	4.5	4.9	1.35	16333
2	1.5	5.0	1.35	16667
3	1.5	6.0	1.35	20000
4	1.5	7.0	1.35	23333
5	1.5	7.7	1.35	25667
6	1.5	3.2	1.35	10667

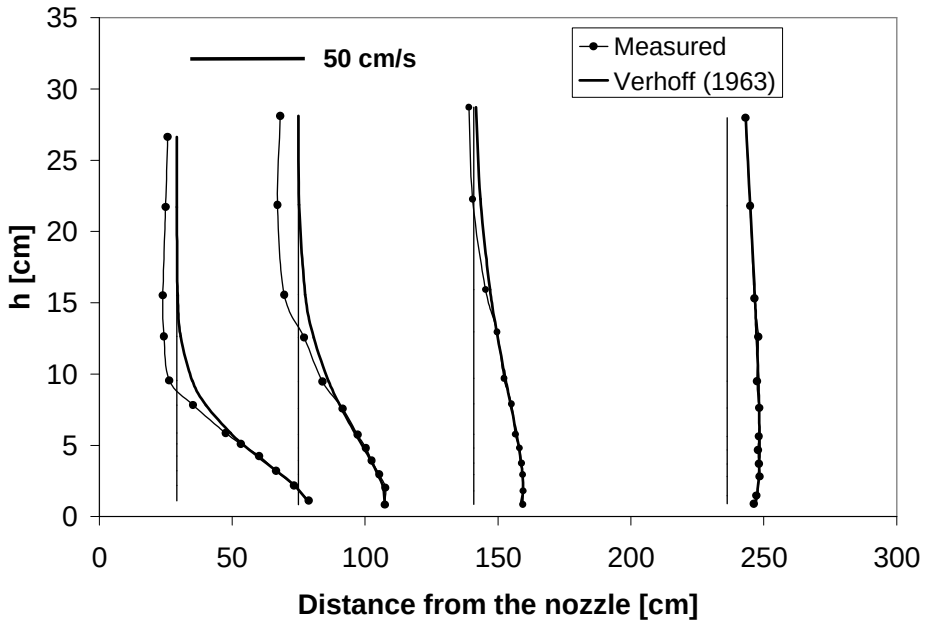

Figure 3-9 Velocity profiles measured for a Reynolds number at the nozzle Re_0 = 16333.

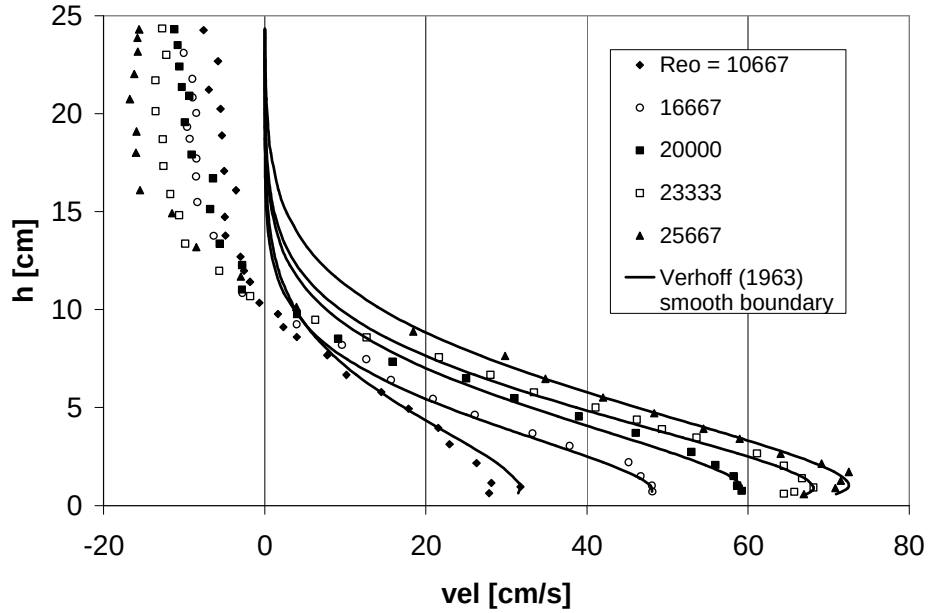

Figure 3-10 Velocity profiles for different initial Reynolds numbers at a point located 43 cm downstream from the nozzle.

b2) Plane wall jet erosion on non-cohesive sediment

General description of the erosive process

The experiments carried out to measure scour by plane wall jets on non-cohesive sediment laying on a fixed boundary were also monitored by 4 synchronized ADVs (10

MHz Nortex NDVField) and video recorded. The initial condition for these tests was set by a layer of sediment of constant thickness b_{so}, as depicted in Fig. 3.11. The sediment employed was Sil-Co-Sil 250 (Table 3.2). When the jet is released, the sediment is eroded creating a scour hole that grows in size as a scour fronts advances downstream, and at the same time the jet is deflected by the front (Fig. 3.12). The erosion rate, or velocity of the scour front, decreases as the front moves away from the jet nozzle, because both the flow velocity and bed shear stress decay away from the source of momentum. Eventually, the sediment front reaches a position where the shear stress of the jet induced flow is not able to erode the bed anymore. This corresponds to the so-called asymptotic or steady state. It was observed that the angle of the scour front slope with respect to the bottom alternates between 35˚ and almost 90˚, and this defines the front advancement pattern. Starting from a 35˚ slope front, approximately the sediment repose angle, the bottom tip of the front is eroded quickly while the apex of the front remains more or less motionless, until a front angle near to 90˚ is obtained. After that, the apex is rapidly eroded, thus advancing downstream, until the front angle is again close to 35˚ and the procedure repeats all over again. This explains the observed intermittent variation of the scour front velocity, especially during the first minutes of the experiment, since, for practical reasons, the bottom tip of the front was tracked in order to define its velocity. The process is shown in Fig. 3.13, where images for increasing time are sorted from left to right and from top to bottom. The first picture was taken 5 minutes after the experiment started and the last one 45 minutes after the beginning. Four plane wall jet erosion experiments on granular non-cohesive sediment where conducted. Characteristics of the sediment used are summarized in Table 3.2.

The densimetric Froude number is a better parameter to use in the analysis than the Reynolds number when dealing with granular non-cohesive sediment, because it involves an effective or representative diameter of the sediment. When analyzing flow characteristics alone, the Reynolds number is well suited, but when sediment is involved the densimetric Froude number should be used. The densimetric Froude number and the Reynolds numbers, both at the nozzle, are defined as follows:

$$F_0 = \frac{U_0}{\sqrt{g\, d_{95}\, \dfrac{\Delta\rho}{\rho}}} \;\; ; \;\; Re_0 = \frac{U_0\, b_0}{\nu} \tag{3.1}$$

The densimetric Froude number, a measure of the ratio of the tractive force on a grain to its resistive force, was defined using not the median d_{50} as the effective diameter but d_{95}. Well-graded mixtures, as opposed to uniformly graded mixtures, are better defined by the d_{95} diameter because of the phenomenon known as “armoring”. Little and Mayer (1976), Raudkivi (1990), and Aderibigbe and Rajaratnam (1998) studied the armoring of different mixtures. The former reported that armoring occurs when the geometric standard deviation, σ_g, is larger than 1.3. The latter is defined as:

$$\sigma_g = \sqrt{\frac{d_{84}}{d_{16}}}$$

Thus, materials 1 and 2 (Sil-Co-Sil 106 and 250 respectively) can be classified as well-graded mixtures prone to armoring (Table 3.2). As it will be explained later in the sections of circular wall jets the proper selection of the effective diameter in the densimetric Froude number is important for a good collapse of data when working with dimensionless variables.

Flow features change significantly after the jet is deflected by the scour front. In the region where the jet hits the front, strong vertical velocities where measured. Before the jet is deflected, the profiles match satisfactorily the empirical equation proposed by Verhoff (1963). Downstream, the front the profiles become more uniform resembling the logarithmic profiles found in gravity driven flows. Fig. 3.14 illustrates this fact.

Table 3-2 Sediment characteristics.

	d_{50} [μm]	d_{95} [μm]	d_{84} [μm]	d_{16} [μm]	σ_g
Material 1: Sil-Co-Sil 106	19	86	56	5	3.28
Material 2: Sil-Co-Sil 250	45	196	118	7	4.26
Material 3: Silica Sand 60-80	250	360	325	196	1.29

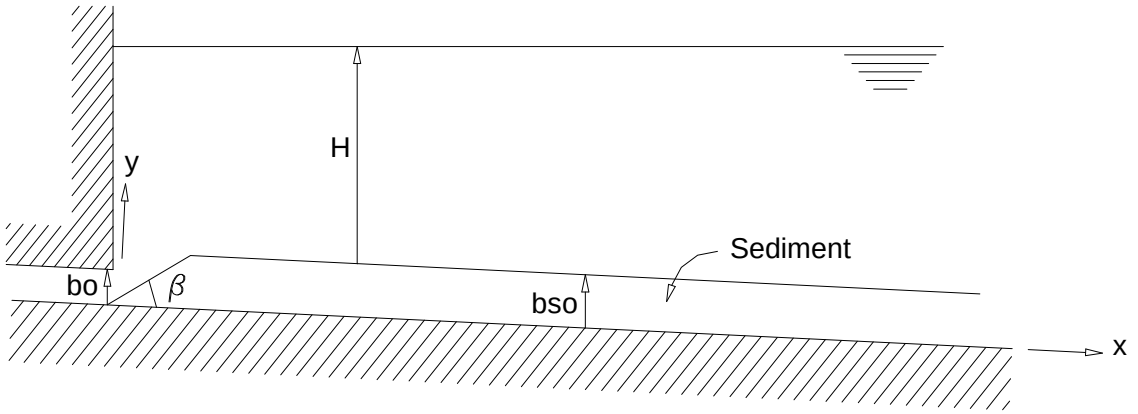

Figure 3-11 Initial condition for plane wall jet erosion experiments.

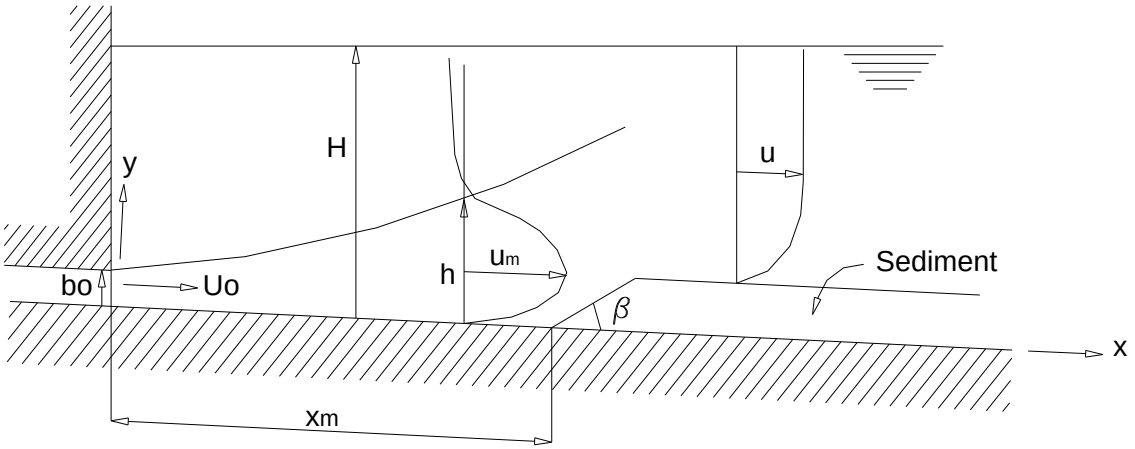

Figure 3-12 Definition of variables for plane wall jet erosion experiments.

Table 3-3 Experimental conditions for erosion by plane wall jets on granular sediment

Test	Time [sec]	Slope [%]	Q [l/s]	b_0 [cm]	F_0	Re_0
1	2647	1.5	4.1	1.34	17.9	13567
2	2897	1.5	6.1	1.34	26.6	20167
3	9922	1.5	7.8	1.34	34.2	26000
4	9303	1.5	5.0	1.34	21.9	16667

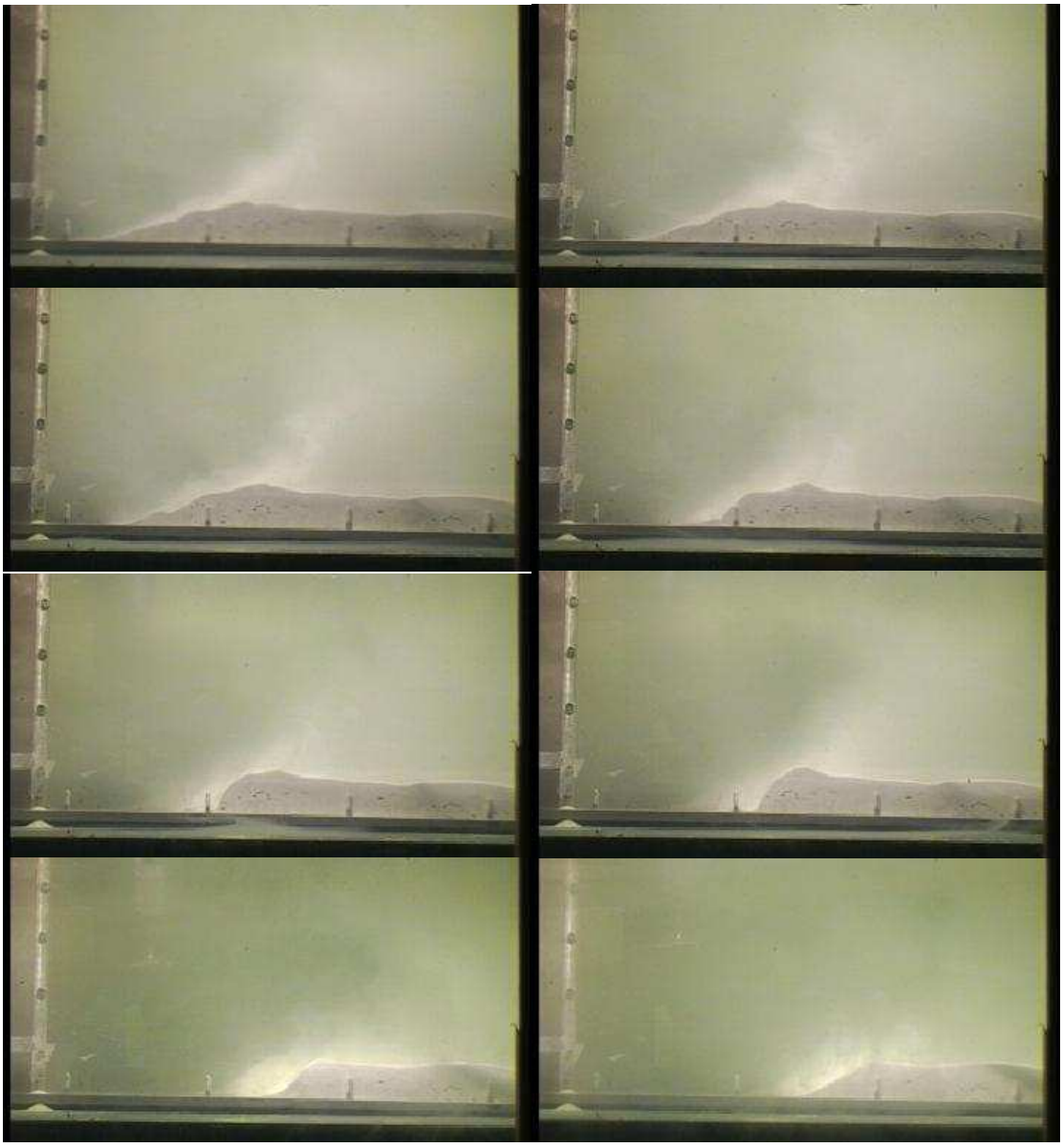

Figure 3-13 Plane wall jet erosion sequence for F_0 = 17.9. The times from the beginning of the test for each picture are: 367 sec, 427 sec, 487 sec, 607 sec, 847 sec, 967 sec, 1747 sec, and 2347 sec.

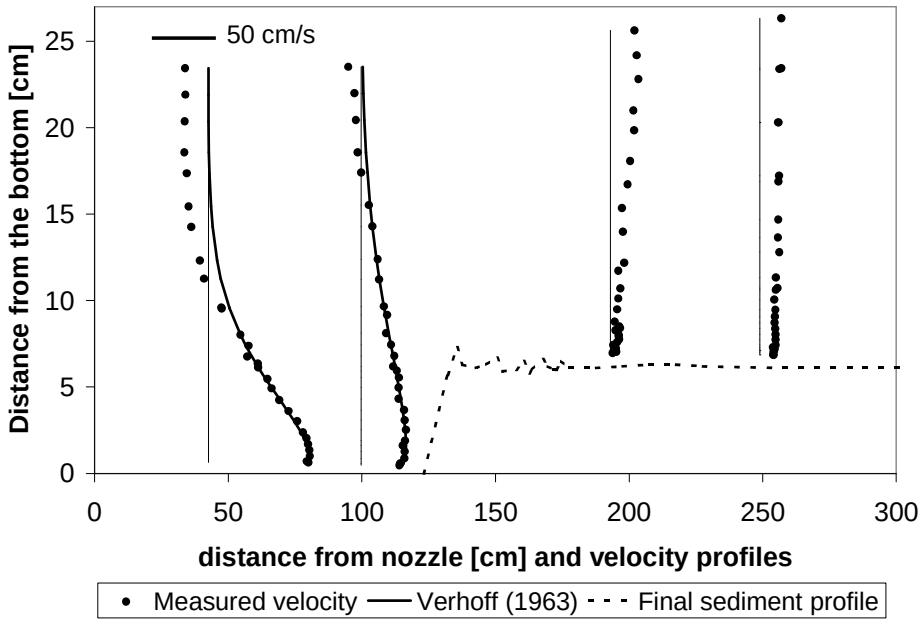

Figure 3-14 Velocity profiles close to the steady state for $F_0 = 17.9$.

Asymptotic values analysis

The maximum length of erosion at the steady state, denoted $x_{m\infty}$, is a function of:

$$x_{m\infty} = f_1(U_0, b_0, \rho, \mu, g\,\Delta\rho, d_{95}, b_{s0}, H) \tag{3.2}$$

where U_o is the velocity at the nozzle, b_o is the thickness of the nozzle, ρ and μ are the density and dynamic viscosity of the eroding fluid, $\Delta\rho$ is the difference between the mass density of the bed material and that of the fluid ρ, d_{95} is the representative size of the bed material in this situation, b_{so} is the initial thickness of the sediment layer, and H is the water depth. Applying dimensional analysis, it can be shown that:

$$\frac{x_{m\infty}}{b_0} = f_2\left(F_0, Re_0, \frac{b_{s0}}{b_0}, \frac{b_0}{d_{95}}, \frac{H}{b_0}\right) \tag{3.3}$$

As it was already explained, the effective diameter was chosen to be d_{95} instead of d_{50} because the sediment can be characterized as well graded and is prone to armoring.

Rajaratnam (1976) showed that the effect of the Reynolds number can be neglected if it is larger than a few thousands ($Re_0 > 3000$). Experiments conducted by Rajaratnam and Berry (1977) proved that the effect of b_0/d_{95} can be neglected even for values of this ratio that are smaller than those of our tests. Aderibigbe and Rajaratnam (1998) found that the effect of submergence, H/b_0, is not important when the mean velocity field in the flow is similar to that of a classical (infinitely submerged) wall jet (Rajaratnam 1976), and the flow depth, on average, is at least four times the sediment thickness. It was also found in

the experiments with sewer sediment, reported in the next section, that the ratio b_{s0}/b_0 has no influence on the steady state profiles as long as it is kept at least below 5. Under these conditions, Equation (3.3) can be reduced to

$$\frac{x_{m\infty}}{b_0} = f_3(F_0) \tag{3.4}$$

The asymptotic or steady state was not reached in any of these four plane wall jet experiments, so Equation (3.4) could not be estimated. However Fig. 3.15 shows the maximum scour values reached in the experiments, here assumed to be $x_{m\infty}$, as a function of the densimetric Froude number. It can be seen qualitatively that the scour length increases as F_0 increases.

The final longitudinal profiles were also measured and compared to the initial profiles. Fig. 3.16 shows the final bed longitudinal profiles obtained in each experiment, where negative values correspond to erosion and positive ones to sedimentation.

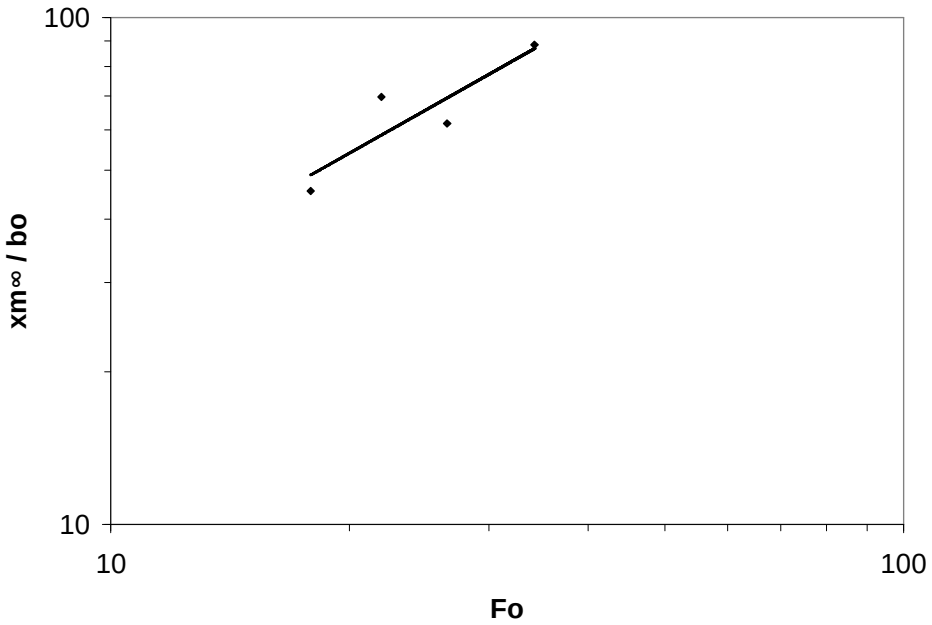

Figure 3-15 Maximum scour length, , as a function of the densimetric Froude number for plane wall jets.

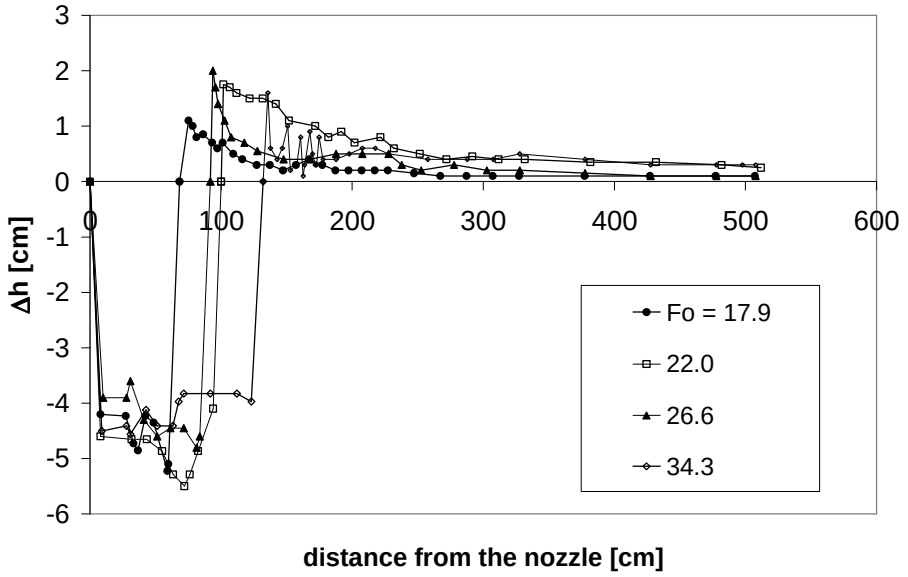

Figure 3-16 Final longitudinal profiles showing erosion and sedimentation zones for different densimetric Froude numbers.

Evolution of scour with time

The evolution of scour with time was obtained from the video recordings of this process. As can be seen in Fig. 3.17 the scour length, that is the position of the front, increases linearly with the logarithm of time. Eventually, after a long period of time that can take even days, an asymptotic or steady state is reached. Rajaratnam (1981) observed this phenomenon studying erosion by plane wall jets upon a semi-infinite layer of non-cohesive sediment. The asymptotic state was not reached in any of the four plane wall jet experiments, but the region of linear grow with the logarithm of time can be clearly noted. Small steps inside the general linear tendency can also be observed. This is because the front does not move as a solid body, but migrates downstream intermittently, advancing its apex and bottom tip at different stages, as was discussed previously.

The velocity of the scour front as a function time was also estimated. Fig. 3.18 shows a sharp decrease after the first 500 seconds for all the tests, but even if the velocity slows down, the front keeps moving and the asymptotic state is not easily reached.

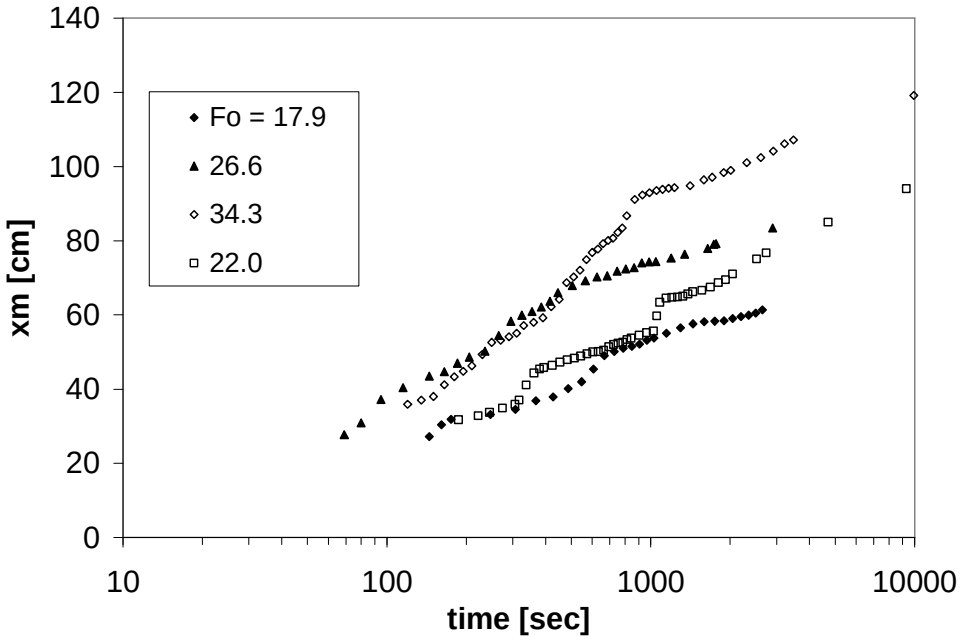

Figure 3-17 Scour front position as a function of time for different densimetric Froude numbers.

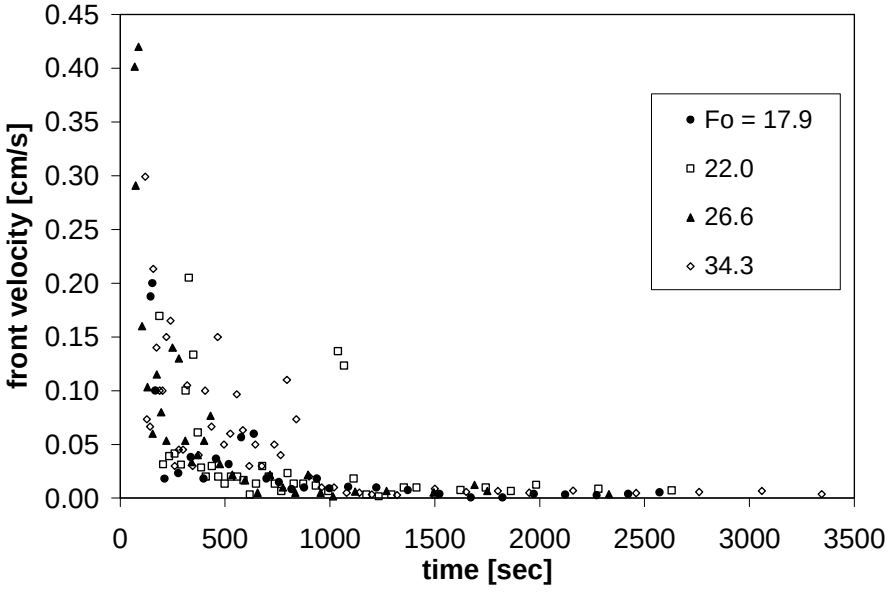

Figure 3-18 Scour front velocity as a function of time for different densimetric Froude numbers.

c) Conclusions

It has been shown experimentally that a wall plane jet can be used to effectively clean a bed created by fine granular sediment resting on a fixed boundary. The erosion induced by plane wall jets impinging on a granular non-cohesive layer of sediment was found to be a function of the densimetric Froude number. The variables involved in this parameter are the jet velocity at the nozzle, the acceleration of gravity, the effective diameter that characterizes the sediment, and the relative density difference between fluid and sediment. The sediment bed is eroded in the form of a scour hole with a depth equal to the bed thickness, whose longitudinal extension increases in time as the scour front advances in the downstream direction. The characteristics of the jet induced flow change significantly once the jet is deflected by the sediment front. Before the jet is deflected, flow velocity profiles match satisfactorily the empirical equation proposed by Verhoff (1963) for a plane wall jet. Downstream of the front the velocity profiles become more uniform resembling the logarithmic profiles found in gravity driven flows. The scour hole was found to grow initially with the logarithm of time and then tend slowly towards an asymptotic value, however, the asymptotic state was not reached in these tests. In any case it was found that the maximum extension of the scoured region increases as the densimetric Froude number of the jet increases.

3.2.2 Series E2. Experimental study on scour pattern by plane wall jet on a bed of CSO solids with limited thickness.

The magnitude of the erosion caused by a plane turbulent wall jet on a bed created by a layer of solids from O'Hare reservoir was studied with the help of laboratory experiments. Solids from O'Hare are believed to be representative of those to be found in McCook reservoir. The results from this study show a cleaning capacity of the plane jet that is similar to that observed in the experiments of Series E1, implying that the behavior of CSO solids is not very different from that observed for granular sediment. A connection is established between the final steady state profile of the eroded bed and the parameter $\lambda = \rho u_0^2$, closely associated with the bottom shear stress created by the flow. The erosion rate, or velocity of the scour front, decreases with time as the front moves away from the jet entrance, because both flow velocity and bed shear stress decay away from the source of momentum. Eventually an asymptotic front position is reached and the bottom shear stress is not longer able to erode the bed.

a) Experimental methods

The sewer solids studied were provided by MWRD. The samples were taken from O'Hare reservoir. Based on the experiments of Series S1 and S2, these solids are composed mainly by two fractions: a disperse fraction with a mean diameter of about 10.8 μm and a settling velocity of about 0.008 cm/s, and flocs or aggregates of larger size and higher settling velocity (84 μm and 0.5 cm/s, respectively). Despite this range of particle sizes, the solids do not behave exactly as cohesive, as the aggregates do not change their properties sensibly in response to variations of shear stress values in the range expected to generate resuspension by the jet array system. The experiments in the annular flume showed that the sediment was easily eroded by shear stress values as low as 0.06 N/m^2.

The bed erosion experiments were conducted in the tank showed in Fig. 3.19. It has a length of 1.18 m, a height of 0.3 m and a width of 0.15 m. In the same way as the experiments of Series E1 a two-dimensional plane wall jet taking up the whole channel width of 0.15 m was employed. The width is half the one used in the experiments of Series E1 and the length even much smaller. The small scale of experiments conducted with the CSO solids is due to several reasons. In the first place, the volume of solids available for the tests was rather low, and the volume needed for the experiments in the tank of Series E1 would have been very large, particularly because most of the bed material eroded by the jet system is lost as it is mixed with a large amount of water inside the tank when it leaves the channel partition created within. In the small tank the solids are only redistributed as the bed is eroded by the action of the jet system, therefore, the same volume of solids could be reused for different experiments. In the second place, manipulating a large amount of CSO solids is potentially hazardous for the health of the researchers and difficult because of the odors released by them. Even with the small scale tank the laboratory had to be ventilated, and no other activity could be carried out inside during the experiments.

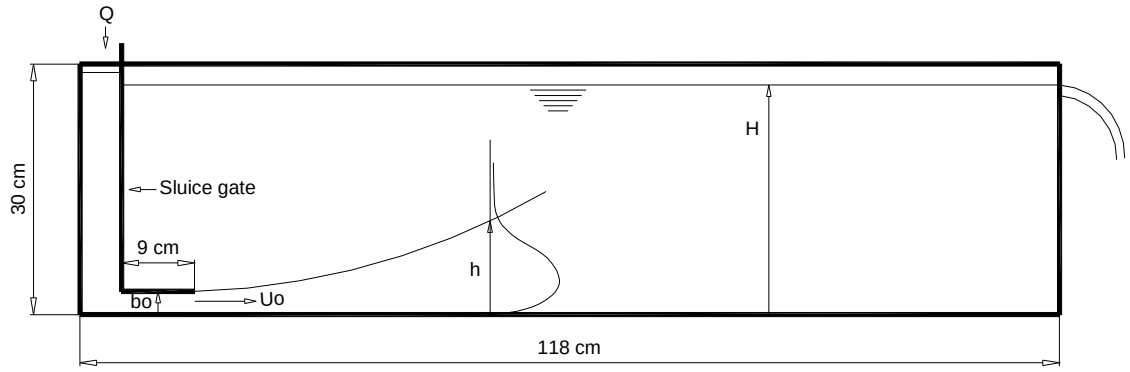

Figure 3-19 Experimental apparatus, Series E2.

b) Results

General description of the erosive process

A submerged turbulent plane wall jet was applied onto a layer of CSO solids placed on the tank bottom. For each experiment the solids were poured inside the tank and allowed to deposit for about 48 hours. The bed was meant to be as uniform as possible in order to characterize its thickness with a single value b_{s0}. The jet was discharged through a sluice gate with a 9 cm long horizontal diffuser, with the purpose of controlling the jet initial thickness, b_0, and to obtain an initial region of uniform velocity at the entrance (Fig. 3.19). A weir located in the end wall of the tank evacuates the jet inflow keeping the water volume in the tank constant. When the jet is released the sediment is eroded while the jet is deflected by the front (Fig. 3.20). The erosion rate, or velocity of the sediment front, decreases away of the nozzle because the flow velocity and shear stress decay away from the source of momentum. Eventually the scour reaches the so called asymptotic or steady state position. The process is shown in Figure 3.21, where images for increasing time are sorted from left to right and from top to bottom. The experiments were run until the scour front created by the jet reached an asymptotic state, beyond which its displacement could be neglected. The experiments were video recorded in order to study the time evolution of the scour front. Different values of b_{s0}, b_0 and the jet initial velocity, U_0, were chosen in order to study the influence of the b_{s0}/b_0 ratio and the Reynolds number, Re_0, on the final scour profile and front displacement. Experimental conditions are shown in Table 3.4, where Q denotes the jet flow discharge and $\lambda = \rho U_0^2$.

The erosion of the bed material by the jet induced flow within the tank was similar to that observed in the experiments of Series E1. The jet is able to clean the deposited solids creating a scour front that advances downstream until a final equilibrium state is reached.

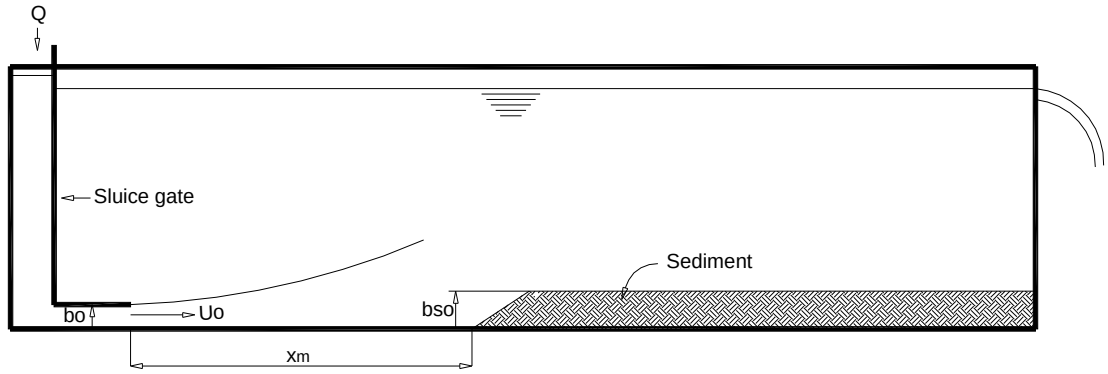

Figure 3-20 Sketch for plane wall jet experiments on sewer sediment.

Table 3-4 Summary of experimental conditions and results

Exp.	Q [l/s]	b_0 [cm]	U_0 [cm/s]	Re_0	b_s [cm]	b_s/b_0	λ [N/m^2]	T_{ime} [s]	$x_{m\infty}$ [cm]
4	0.25	1.6	10.6	1692	3.2	2.0	11.2	1010	13.0
5	0.22	1.6	9.2	1479	3.3	2.1	8.5	1020	10.7
6	0.43	1.6	18.1	2897	2.8	1.8	32.8	1470	25.9
7	0.29	1.6	12.0	1919	2.7	1.7	14.4	1210	16.6
8	0.85	1.6	35.4	5670	2.8	1.7	125.6	1100	71.1
9	0.27	1.6	11.2	1791	4.7	2.9	12.5	1290	15.2
10	0.32	1.6	13.3	2128	4.3	2.7	17.7	1234	18.9
11	0.38	1.2	21.1	2528	4.8	4.0	44.4	1273	30.5
12	0.74	1.8	27.4	4929	2.4	1.3	75.0	1223	50.8
13	0.93	1.7	36.3	6179	2.4	1.4	132.1	1710	69.9
14	1.02	1.7	39.8	6774	2.4	1.4	158.8	2005	77.5

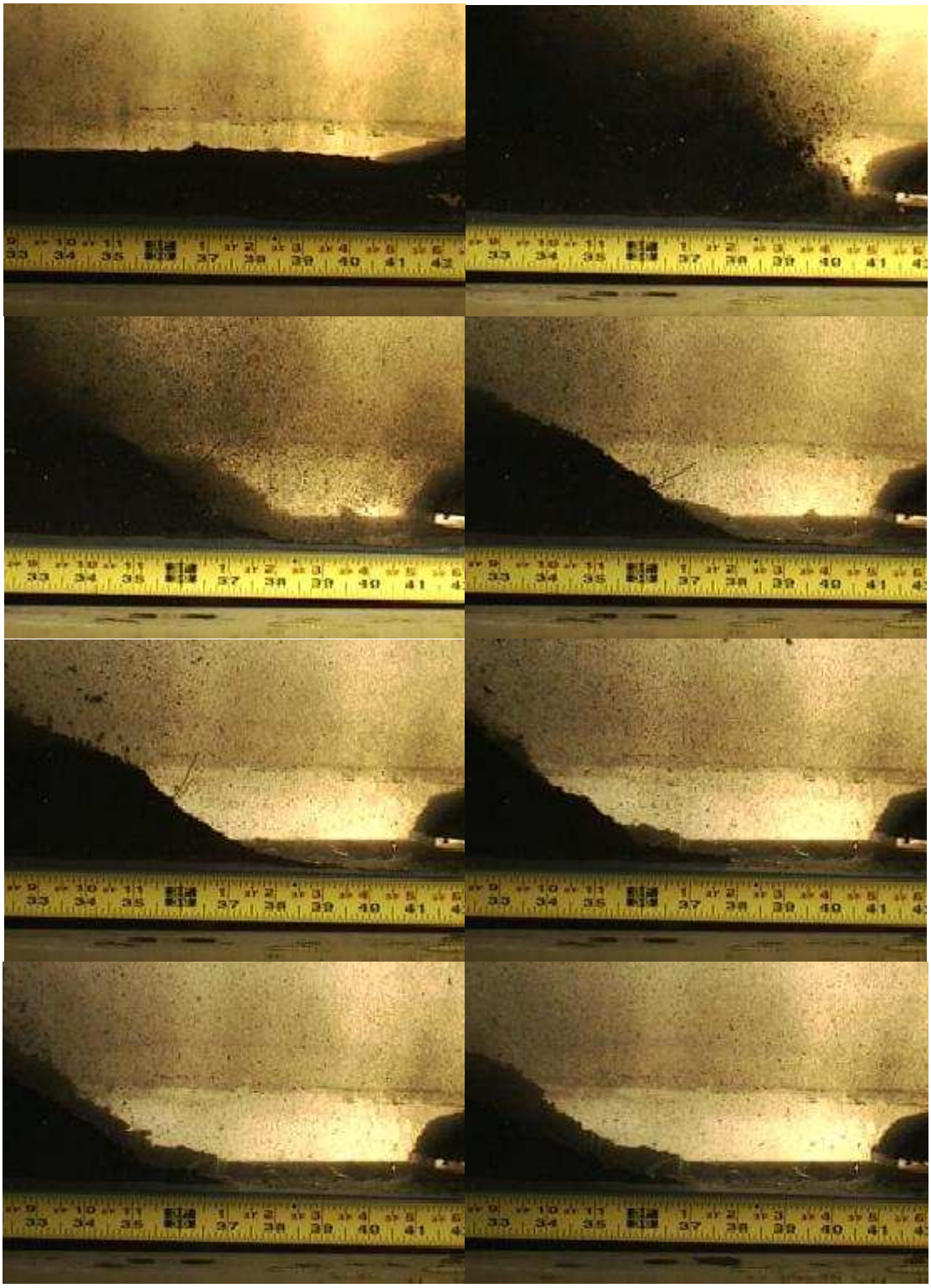

Figure 3-21 Time evolution of scour front for Experiment 9. From left to right and top to bottom, the times corresponding to the sequence shown are: 0 s, 104 s, 162 s, 272 s, 392 s, 515 s, 695 s and 1290 s (final condition), respectively.

Asymptotic values analysis

The maximum length of erosion caused by the jet, $x_{m\infty}$, can be expressed by the relationship:

$$x_{m\infty} = f_1(U_0, b_0, \rho, \mu, \tau_c, b_{s0}, H) \tag{3.5}$$

where U_0 is the velocity at the nozzle, b_0 is the thickness of the nozzle, ρ and μ are the density and dynamic viscosity of the eroding fluid, τ_c is the critical shear stress of the soil under which no significant erosion occurs, b_{s0} is the thickness or the sediment layer, and H is the water depth. Applying dimensional analysis it can be shown that:

$$\frac{x_{m\infty}}{b_0} = f_2\left(\frac{\rho U_0^2}{\tau_c}, \frac{U_0 b_0}{\nu}, \frac{b_{s0}}{b_0}, \frac{H}{b_0}\right) \tag{3.6}$$

According to Rajaratnam (1976), the effect of the Reynolds number can be neglected if it is greater than 3000. The values of Reynolds numbers used in this analysis ranged from 10^3 to 10^4; nevertheless it will be shown that the Reynolds number does not have a significant influence on the observed asymptotic scour profile. Aderibigbe and Rajaratnam (1998) found that the effect of submergence is not important when the mean velocity field in the flow is similar to that of a classical (infinitely submerged) wall jet and the flow depth, on average, is at least four times the sediment thickness. The tests also showed that the ratio b_{s0}/b_0 is not important in determining the final scour, at least in the range covered by the present study ($b_{s0}/b_0 < 4$). In this case we can write:

$$\frac{x_{m\infty}}{b_0} = f_3\left(\frac{\rho U_0^2}{\tau_c}\right) \tag{3.7}$$

Following Mazurek (2003) notation, we call $\lambda = \rho U_0^2$. This parameter is related to the bottom shear stress generated by the wall jet. The bottom shear stress τ_b is related to the velocity as $\tau_b = C_f \rho U_0^2/2$, where C_f represents the friction factor. Sigalla (1958), Schwarz and Cosart (1961), Myers et al. (1963), and Wygnanski et al. (1992) have studied the friction factor in wall jets, with different results. In general, it can be said that the friction factor decreases slowly in the direction of the flow and depends slightly on the Reynolds number. The critical value of the bottom shear stress corresponds to the critical value of λ, and working with the excess in stress that cause erosion we obtain:

$$\frac{x_{m\infty}}{b_0} = f_4\left(\frac{\lambda - \lambda_c}{\lambda_c}\right) \tag{3.8}$$

Fig. 3.22 shows the dependence of the final scour length on λ. The final scour length, $x_{m\infty}$, was averaged at three positions along the front. For the range of Reynolds numbers tested, the ratio b_{s0}/b_0 does not influence the final scour. The critical value of λ was

estimated as λ_c = 7 Pa by extrapolating the experimental data to the condition $x_{m\infty} = 0$. It should be noted that the extrapolation of λ_c is subject to error because of the difficulty in performing precise experiments for low velocities U_0. For lower velocities than the ones in the present tests the evolution of the front would become more uneven because it would be more difficult to obtain a uniform jet along the whole channel width for such small discharges. Furthermore, viscous effects might not be neglected for lower Reynolds numbers. Thus the determination of $x_{m\infty}$ would turn to be more imprecise. From Myers et al. (1963) and Wygnanski et al. (1992) we can estimate a value of the friction coefficient C_f = 0.011 for our range of Reynolds number. This gives a value of critical shear stress τ_c = 0.02 Pa, which results to be insignificant value compared to results for cohesive soil obtained by Mazurek et al. (2003), but has the same order of magnitude as the results obtained in the annular flume (Series S2). Recall that it was concluded that erosion of O'Hare solids was achieved with values of the shear stress of 0.06 Pa or lower. Jenkins et al. (1981) performing circular jet studies found that the critical shear stress for diatomaceous earth was 0.1 Pa. Apparently, the erodibility of McCook solids is higher than that of Jenkins et al.'s earth and much higher than that typical of cohesive sediments. This support the idea discussed in previous sections that O'Hare solids do not behave as cohesive sediment.

Relating the dimensionless final scour length with $(\lambda - \lambda_c)/\lambda_c$, as shown in Fig. 3.23, yields the power law that best fits the data as:

$$\frac{x_{m\infty}}{b_0} = 6.05 \left(\frac{\lambda - \lambda_c}{\lambda_c} \right)^{0.559} \tag{3.9}$$

Images of the asymptotic scour extent for some of the experiments conducted are shown in Fig. 3.24. Some fronts did not achieve a final uniform position but presented variations from one lateral wall to the other. In order to obtain a wall jet as uniform as possible a diffuser was incorporated before the sluice gate, nevertheless this pattern kept appearing and some fronts persisted in having different displacement velocities for different points in the front. Images of the final state in Experiments 6, 7, and 11 depict this phenomenon. As long as the discrepancies were not significant, the average of the final position of the front at three points was used to obtain the final nominal value for $x_{m\infty}$. Apart from the difficulties in obtaining a perfect uniform plane wall jet, these variations in front position can be explained because of the heterogeneity of the sediment. It was found that apart form the characteristic flocks and aggregates that compose the material, other elements such as pieces of papers and plastic, little stones, and strings were also found, making the sediment more heterogeneous. Sidewall effects could also be influencing the uneven evolution of the front, though for the present scale of experiments it should not have an important role compared to jet uniformity and sediment heterogeneity.

Evolution of scour with time

The displacement of the scour front in time was determined from the analysis of video recordings of the experiments, and position-time curves were assembled with these data.

As Rajaratnam (1981) has observed studying non-cohesive sediment, the scour length initially increases with the logarithm of time, then the rate of erosion slows down until the asymptotic state is reached. This same phenomenon was also observed in these experiments, even though the erosion pattern is different. Some typical curves of front position versus time can be seen in Fig. 3.25. The logarithmic fit is not valid after a certain time beyond which the curves tend to their asymptotic values. Thus, an arbitrary time t^* can be defined, beyond which the straight slope of the scour-log(time) curve decreases towards zero as the asymptotic or steady state is reached. It can be observed that the sewer sediment does not show the "step" effect characteristic of the granular material when the front is moving (see Figure 3.17). This could be partially explained because the sewer sediment lacks the interlocking among grains responsible in granular material for the angle of repose. Besides under the impact of a submerged jet, sewer sediment resembles more a viscous fluid than a granular material.

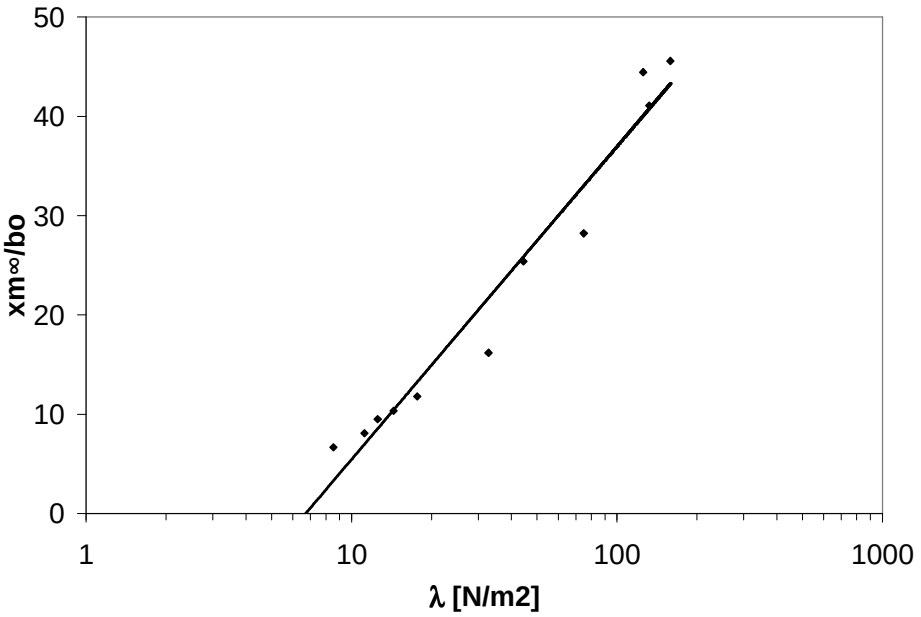

Figure 3-22 Dimensionless scour length as a function of λ. Determination of λ_c was done by extrapolating the data to the condition $x_{m\infty} = 0$.

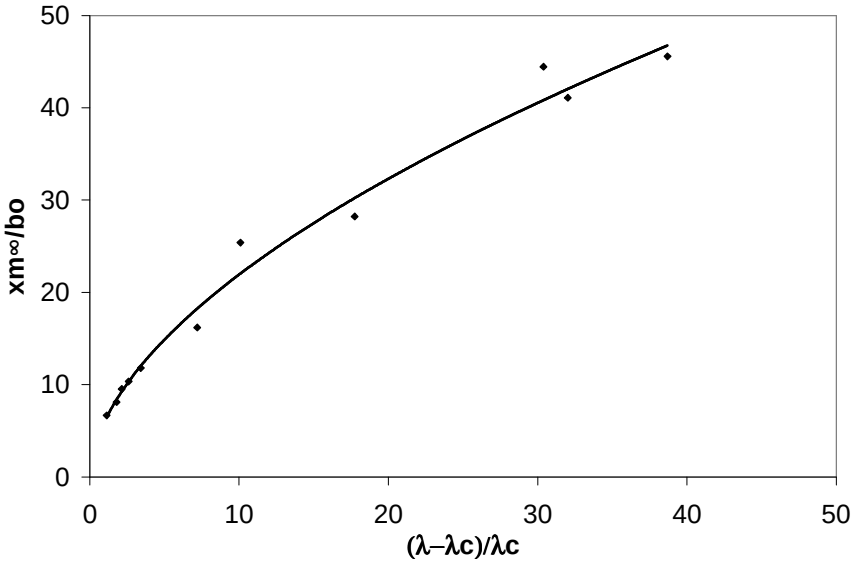

Figure 3-23 Asymptotic scour length as a function of $(\lambda - \lambda_c)/\lambda_c$ and power law best fit given by Equation (3.9).

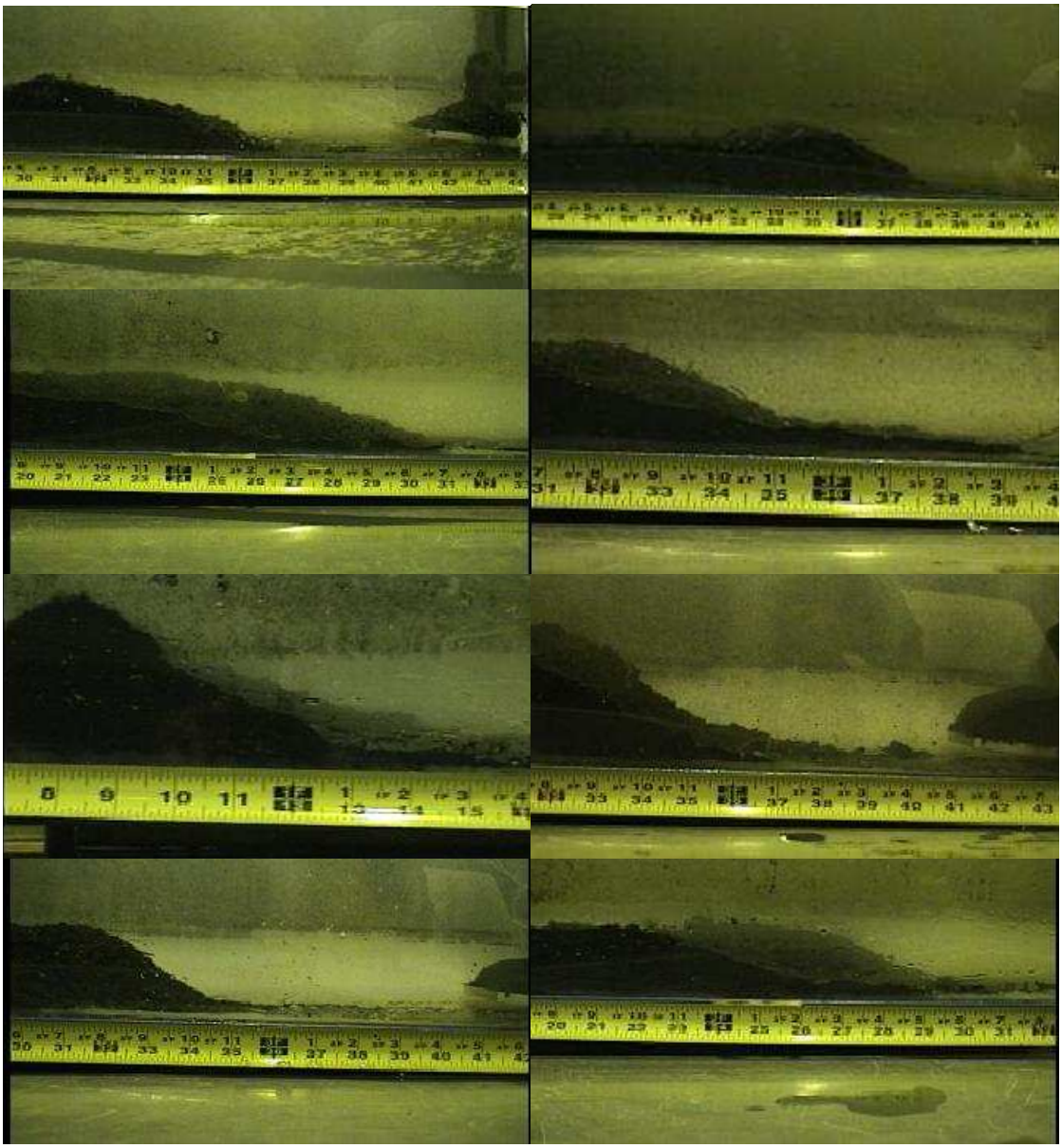

Figure 3-24 Images of final scour condition in Experiments (from left to right): 4, 5, 6, 7, 8, 9, 10, 11 (see Table 3.4 for experimental conditions).

The distance used to evaluate the front movement along time, x_m, was measured from the nozzle to the base of the front. Another variable could have been defined, for instance, the distance from the nozzle to the apex of the front, or an average or both. However, since the slope of the front tends to be the same once the jet has stopped and measuring to the front base is easy, the first option was chosen. As explained above, the value $x_{m\infty}$ is the average of x_m at three points across the front once the experiment is finished.

The evolution of the scour in time in Experiment 9 was shown in 3.21. Immediately after the jet starts, the suspension of sediment turns it very difficult to visualize the location of

the front, and only after the aggregates begin to be deposited or swept away it is possible to follow the front movement with better precision.

In order to collapse the data into one self-similar time evolution of the scour front, the length and time scales $x_{m\infty}$ and t^* (the equilibrium scour length and time at which the scour stops growing proportionally to the logarithmic of time) were used.

Fig. 3.26 depicts a plot of $x_m/x_{m\infty}$ versus t/t^* for the tests where t^* could be obtained. When t approaches t^*, x_m is approximately 0.95 $x_{m\infty}$; and x_m approaches $x_{m\infty}$ when t is approximately 4 times t^*.

The ratio b_{s0}/b_0 may play a role in the development of the front along time. For a given nozzle thickness the jet needs to move more sediment when the sediment thickness is larger, even if the final scour, that depends on the critical shear stress, is to be the same. Fig. 3.27 illustrates two pairs of experiments presenting similar nozzle velocities and Reynolds numbers but different ratios b_{s0}/b_0. It can be seen that this ratio does not affect much the final scour length even when the evolution of the front for the initial stages is slower for higher ratios of b_{s0}/b_0.

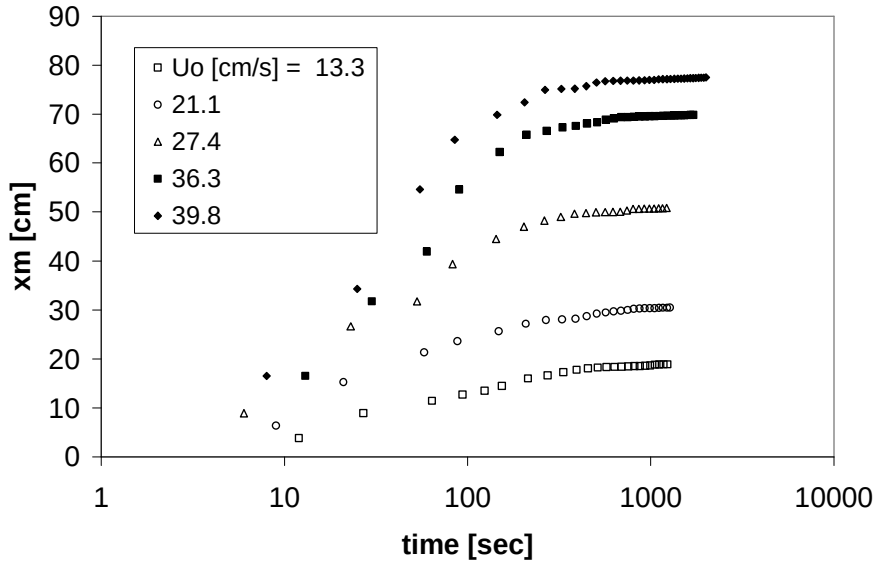

Figure 3-25 Typical evolution of the scour length with time in Experiments 10, 11, 12, 13, and 14 (see Table 3.4 for experimental conditions).

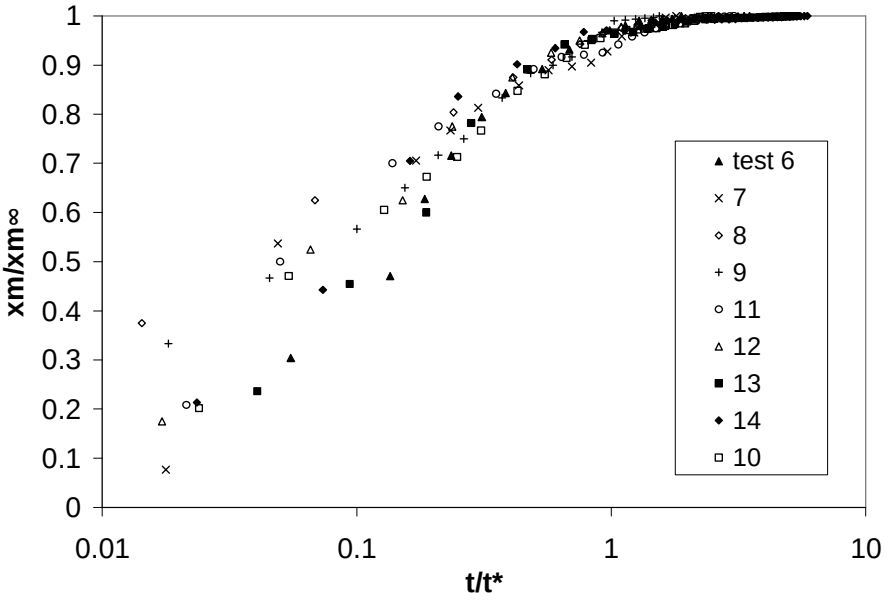

Figure 3-26 Dimensionless time evolution of the scour length with time for plane wall jets on sewer sediment.

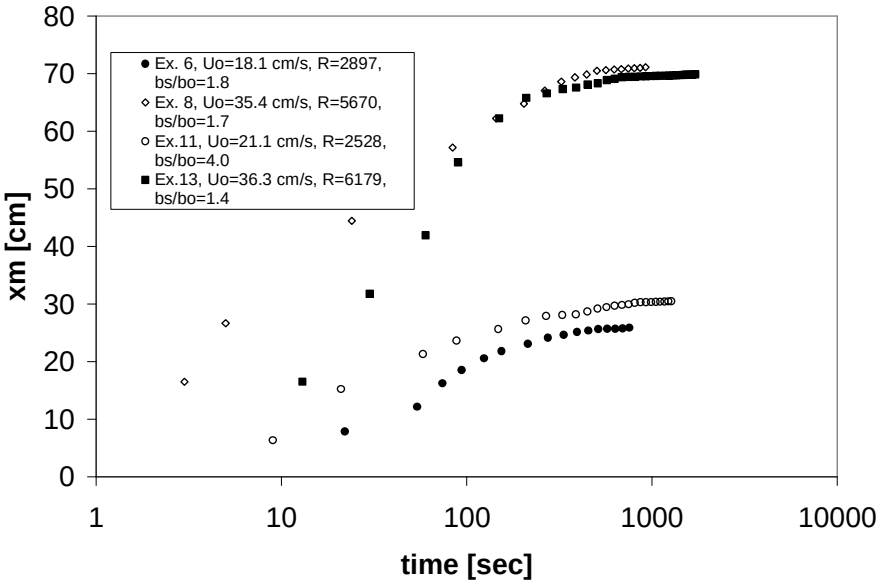

Figure 3-27 Dimensionless evolution of scour length with time for plane wall jet tests on sewer sediment.

c) Conclusions

The erosion caused by a plane turbulent wall jet applied onto a bed of sewer sediment of limited thickness appears to be a function of the jet properties: velocity and thickness, the properties of the eroding fluid, and the characteristics of the sediment: critical shear stress and bed thickness. The final scour seems to depend only on the factor $(\lambda-\lambda_c)/\lambda_c$, a variable closely related with the dimensionless excess shear stress, and not on the jet

Reynolds number or the bed to nozzle thickness ratio, b_{s0}/b_0. Nevertheless, these two last variables could play a role in the development of the scour front with time, at least for the range of Reynolds numbers covered in this study. A power law that relates the final scour length or asymptotic scour front position with the parameter $(\lambda-\lambda_c)/\lambda_c$ was fitted to the data. Initially the scour grows with the logarithm of time, after a certain time t^* the rate of scouring decreases and finally the asymptotic state is reached. By neglecting the effect of the Reynolds number we are assuming the effect of viscosity is not important on the turbulent jet flow (Rajaratnam, 1976). When plotting the asymptotic scour length as a function of $(\lambda - \lambda_c)/\lambda_c$ (Figure 3.23) the data collapse to a single curve. If the Reynolds number had significant influence the collapse would not be so clear, specially for low values of λ, and there would be several curves of $x_{m\infty}/b_0$ vs $(\lambda - \lambda_c)/\lambda_c$ corresponding to different Reynolds numbers. However, the Reynolds number being a ratio of inertia and viscous forces depends also on the jet velocity, and plotting $x_{m\infty}/b_0$ vs the Reynolds will also expose a tendency. Then, choosing the parameter λ and not the Reynolds number is equivalent to neglect the viscous effects.

The sewer solids used in the experiments presented singular characteristics that make them unclassifiable either as granular or cohesive material. The size of the particles and aggregates, and the flocks observed are typical of cohesive sediments, but the extremely low value of the critical shear stress obtained in the experiments distinguishes them from typical cohesive sediment.

3.2.3 Series E3 and E4. Experimental study on flow and scour pattern of single and multiple circular jets on bed of limited thickness.

The magnitude of the erosion caused by single and multiple submerged circular turbulent wall jets on a non-cohesive sediment bed of finite thickness laying on a fixed boundary was studied with the help of laboratory experiments. Different combinations of jet diameter, jet separation and ratio between the sediment thickness and the jet diameter were tested. The results show a connection between the steady state bed profile and the densimetric particle Froude number given by the velocity at the nozzle, and the submerged specific density and effective diameter of the sediment. Analysis of the evolution of scour with time is also presented.

a) Experimental methods

A linear array of submerged turbulent circular wall jets parallel to the bottom was applied upon a layer of sediment resting on a fixed boundary. The diameter of the jets and the distance between jets were two of the variables studied. Single jets tests were also carried out to compare the scour patterns of jets acting alone and as a group.

Two different non-cohesive sediments were used in the jet tests, Sil-Co-Sil 106 and Sil-Co-Sil 250. Both were fine granular quartz material provided by U.S. Silica Company having a specific gravity equal to 2.65. Characteristic diameters of the sediment can be seen in Table 3.5. The experiments were carried out over a plate 5.4 m long and 2.5 m wide, located inside a water tank 7.3 m long, 2.7 m wide, and 2.3 m high, the same used in experiments of Series E1. A pump conveyed the water from a secondary tank placed nearby to the jet array (Fig. 3.28). In most cases the discharge was measured using a magnetic flowmeter McCrometer (Serial No. 96061675) having a capacity up to 20 l/s, located in the supply pipe. In a few experiments the discharge was lower than 0.10 l/s and the flow was obtained by measuring the time required to fill a certain volume of water. A manifold with a diameter of 50.8 mm, having branches separated 0.13 m composed the jet system. The use of threaded joints allowed the creation of different arrays, by modifying jet diameter and spacing. The manifold thus formed comprised up to 13 jets (Fig. 3.29). The distribution of the flow along the ports of the manifold was computed following the procedure described by Roberson et al. (1988). The adjustable bottom slope of the plate was set at 1.5%.

An even layer of sediment of thickness b_{s0} set the initial condition. The water depth at the nozzle was 0.35 m. The experiments were run until the steady state or asymptotic condition for the bed scour was almost reached. Once the jets were stopped, measurements of final scour were taken using a digital camera. A 3-mm definition grid was placed at the bottom to improve the accuracy of the data collection process. Some experiments were also video recorded to study the evolution of the scour with time.

The thickness of the sediment layer was changed in different experiments to study the influence of the ratio between the sediment thickness and the jet diameter (b_{s0}/b_0). Different discharges were used in order to determine the scour patterns for different densimetric Froude numbers.

Table 3-5 Characteristic diameters of sediments used in the experimental study.

	d_{50} [μm]	d_{95} [μm]	d_{84} [μm]	d_{16} [μm]	σ_g
Material 1: Sil-Co-Sil 106	19	86	56	5	3.28
Material 2: Sil-Co-Sil 250	45	196	118	7	4.26
Material 3: Silica Sand 60-80	250	360	325	196	1.29

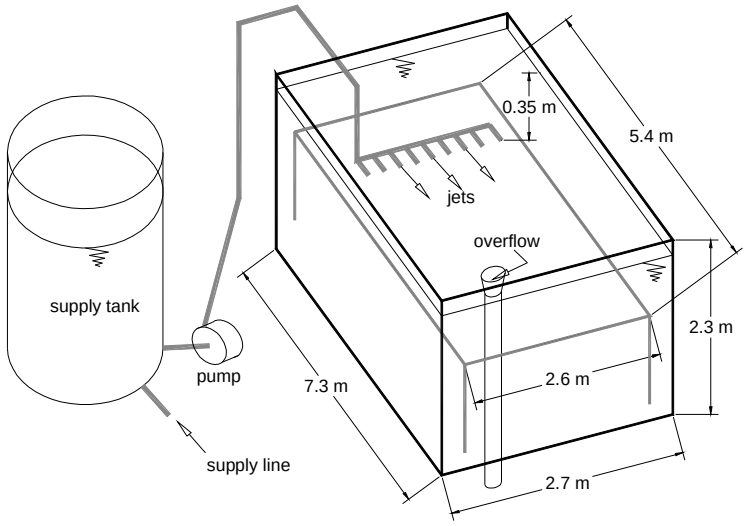

Figure 3-28 Set-up for circular wall jet experiments.

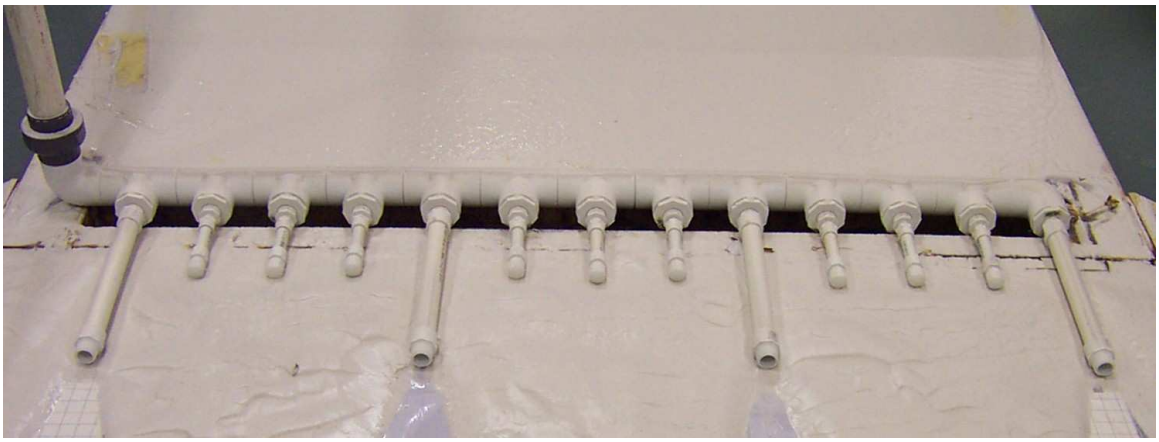

Figure 3-29 Manifold for circular wall jet experiments showing a configuration of 4 jets. The manifold allows up to 13 jets changing jet diameter, jet separation, and diffuser lengths. The jets having shorter diffuser lengths are not taking part of the test showed in the picture, they are closed.

b) Results

General description of the erosive process

The scour pattern created by a single jet was characterized by measuring certain parameters: the maximum scour length r_m; the maximum scour width y_m; the distance from the nozzle to the point where the maximum width occurs, r_y; the angle ϕ formed by the jet downstream the nozzle. Starting from the nozzle, there is a region in the pattern of erosion where the scour width grows linearly as a function of the distance from the nozzle times. This rate of increment in scour width is maintained up to a certain distance from the nozzle, r_ϕ. Beyond this point, due to lateral dissipation of momentum, the jet is no longer able to keep the linear rate of lateral erosion and the scour width grows at a lower rate until it reaches its maximum value y_m at r_y. Farther away, the scour width decreases until the scour hole is closed at a distance r_m. These parameters are defined in Figs. 3.30 and 3.31. Considering the boundary of the scour pattern to be an isoline of constant threshold bottom shear stress (Van Dorn et al., 1975), the scour will tend to the asymptotic state as long as it is given enough time to develop. When the asymptotic state is reached, the jet can no longer transport sediment because its momentum has been dissipated through friction, and the scour boundaries remain fixed. At this point r_m, y_m, r_ϕ, and r_y, become $r_{m\infty}$, $y_{m\infty}$, $r_{\phi\infty}$, and $r_{y\infty}$, respectively. The velocity decreases longitudinally away from the nozzle and laterally away from the centerline, and so does the erosive capacity quantified by the bottom shear stress.

In case of multiple jets, the distance between jet nozzles is denoted d_j. All other parameters used to characterize the scour in the case of a single jet remain the same for multiple jets, although it must be pointed out that, depending on the distance between nozzles and the densimetric Froude number of the jet, the scour created by different jets may or may not be in superposition. In the sketch of Fig. 3.31 the case in which superposition of the scour by individual jets is shown. In this case, some parameters characterizing the scour of individual jets are lost or cannot be directly measured. The maximum scour width of the middle jets cannot be measured, and that of the jets in the extremes can only be estimated as twice the distance from the corresponding centerline. The parameter $r_{\phi\infty}$ of the middle jets may or may not be measured in a particular experiment, depending again on d_j and the Froude number.

Once the jet is released, the solid particles next to the nozzle are swept away and in a few seconds the scour pattern can be perceived. The rate of erosion decreases significantly after some minutes but the scour keeps advancing and hours could pass before the asymptotic state is reached. Due to a general downstream movement of displaced material, be it in suspension or as a bed load, a ridge is formed around the scour especially at the downstream end of it. The parameter l_s denotes the projected magnitude of the side slope over a horizontal plane. It stretches from the ridge base to the ridge top. Its magnitude depends on the thickness of the sediment layer, the angle or repose of the sediment, and the location along the boundary. At the apex of the ridge the sediment grains are launched downstream with a certain angle. The finer particles are entrained into suspension and travel up to the end of the plate, the coarser particles roll and saltate

down the ridge. Some ripples were observed to form beyond the ridge moving downstream, but their height was rather small and less than 2 mm in all cases.

It was found that the ratio between the original sediment thickness and the jet diameter b_{s0}/b_0 does not affect the final scour length as long as it is kept below a certain value. In these series of experiments, the ratio varied from 0.2 to 4. It is believed that even larger values of the ratio would not influence the asymptotic scour length, although the time evolution of the scour hole could be affected by this parameter.

As it was already explained, the first two granular materials used in the tests had a finer particle size distribution than the third one (Table 3.5). This was manifested in a more significant suspended load conveyed and deposited farther downstream and the rapid generation of turbidity that hindered the observation and recording of the experiments after a certain time. On the other hand, in the experiments performed with the third material, medium size sand, scarce suspended load was observed and the water stayed clear enough to record the tests completely. Table 3.6 summarizes the conditions of the experiments conducted and their associated results.

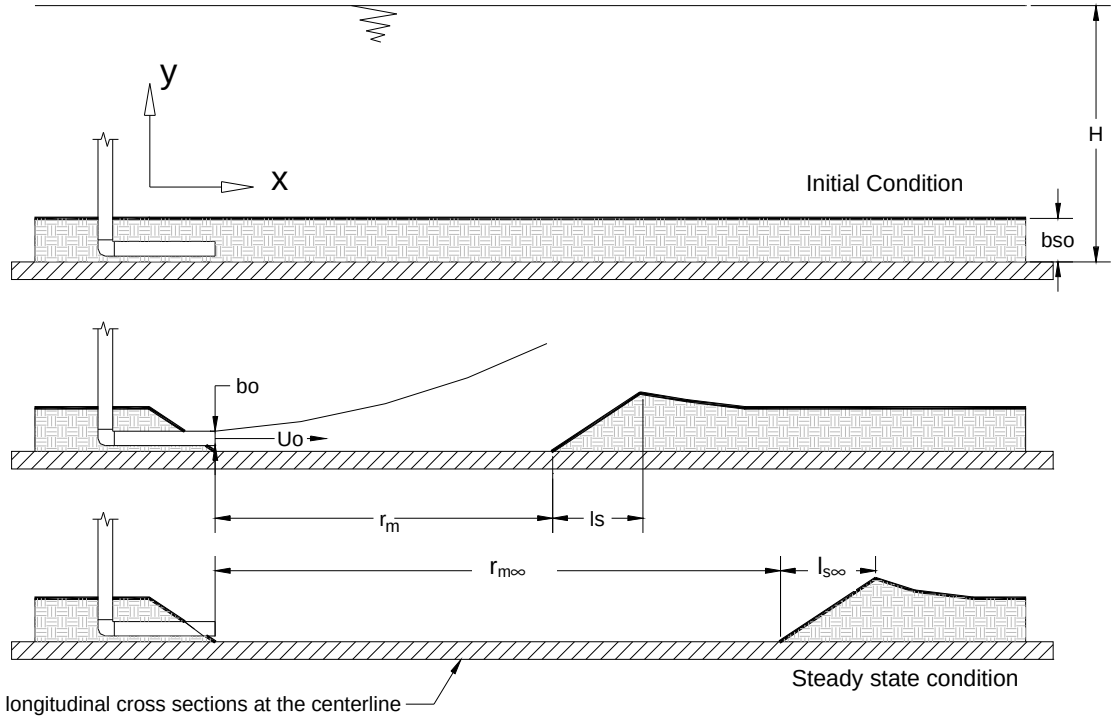

Figure 3-30 Definition of variables characterizing longitudinal scour profile for single and multiple circular wall jet experiments.

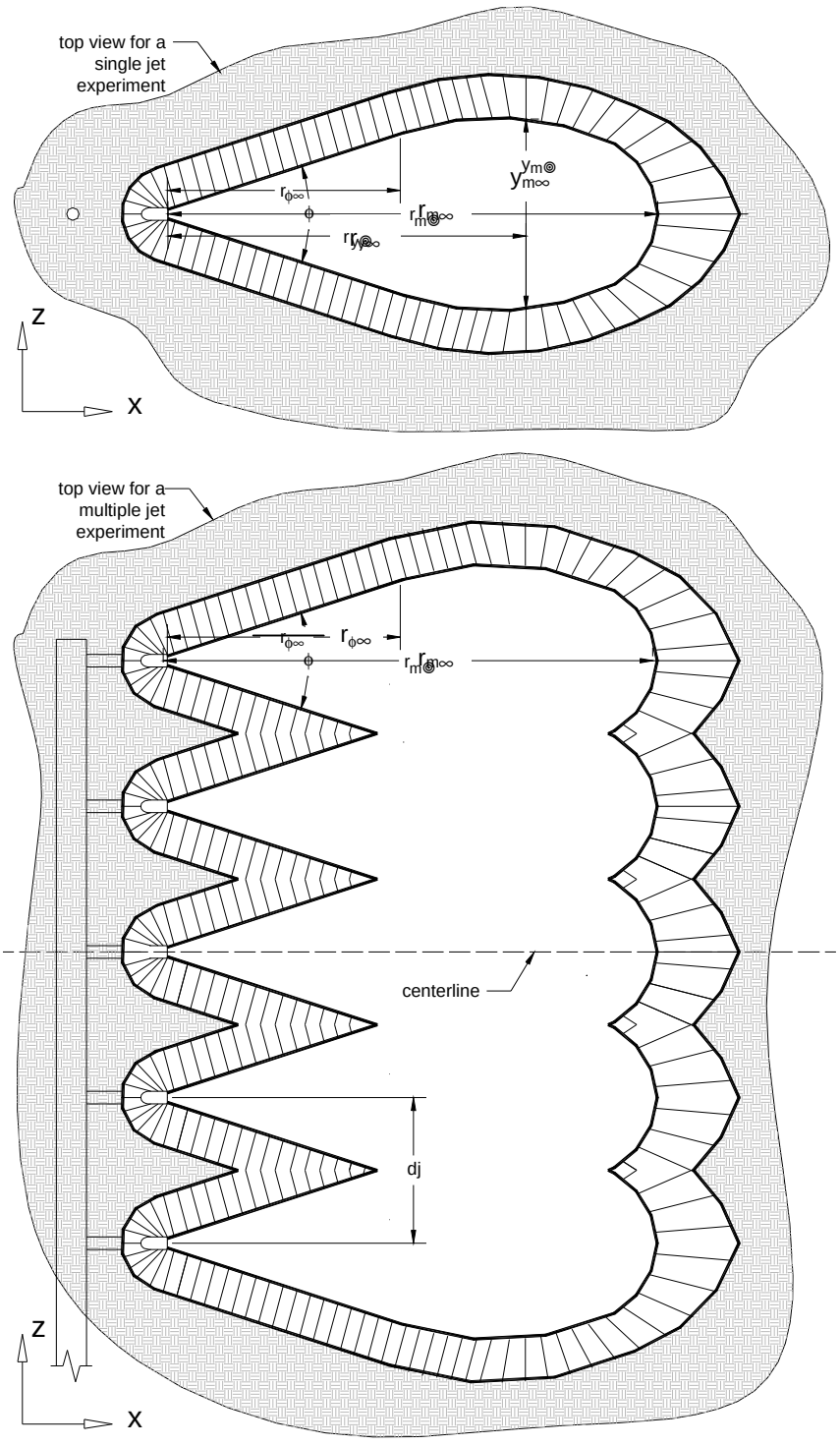

Figure 3-31 Definition of variables characterizing the scour hole of single and multiple circular wall jet experiments.

Table 3-6 Experimental conditions and results for circular wall jets experiments.

Jet [⊥]	running time	Discharge	bo	bso	bso/bo	Uo	rm∞	ym∞	ry∞	rϕ∞	ϕ	d95	Fo	rm∞/bo	ym∞/bo	ry∞/bo	rϕ∞/bo	dj	dj/bo	rm∞/ym∞
	[sec]	[l/s]	[mm]	[mm]		[m/s]	[cm]	[cm]	[cm]	[cm]	[deg.]	[mm]						[cm]		
1*	191	0.67	15	60	4	3.79	-	-	-	-	-	0.196	67.3	-	-	-	-	-	-	-
2	3600	0.55	15	60	4	3.11	95.0	-	-	-	32	0.196	55.3	63.3	-	-	-	-	-	-
3	4680	0.71	15	60	4	4.02	111.0	-	-	-	33	0.196	71.3	74.0	-	-	-	-	-	-
4	4130	1.15	15	60	4	6.51	122.0	-	-	-	-	0.196	115.5	81.3				-	-	-
5	3600	0.43	15	60	4	2.43	85.0	25.1	55.0	33.0	32	0.196	43.2	56.7	16.7	36.7	22.0	-	-	3.4
6	3680	0.03	15	60	4	0.20	1.5	1.3	-	-	-	0.196	3.5	1.0	0.9	-	-	-	-	1.2
7	4080	0.05	15	60	4	0.28	7.6	2.2	5.4	-	16	0.196	5.0	5.1	1.5	3.6		-	-	3.4
8	4430	0.07	15	60	4	0.40	15.6	3.8	7.9	5.1	20	0.196	7.2	10.4	2.5	5.3	3.4	-	-	4.1
9	5030	0.09	15	60	4	0.51	22.5	5.1	15.2	10.2	18	0.196	9.1	15.0	3.4	10.2	6.8	-	-	4.4
10	5100	0.12	15	60	4	0.68	27.9	5.7	17.8	14.0	24	0.196	12.1	18.6	3.8	11.9	9.3	-	-	4.9
11	4920	0.15	15	60	4	0.84	36.5	7.3	23.5	15.2	28	0.196	15.0	24.3	4.9	15.7	10.2	-	-	5.0
12	4940	0.17	15	60	4	0.98	42.9	8.6	27.3	16.5	31	0.196	17.3	28.6	5.7	18.2	11.0	-	-	5.0
13	5730	0.20	15	60	4	1.15	51.4	11.7	37.1	17.8	32	0.196	20.5	34.3	7.8	24.8	11.9	-	-	4.4
14	4850	0.24	15	60	4	1.38	56.5	13.3	39.7	19.8	30	0.196	24.5	37.7	8.9	26.5	13.2	-	-	4.2
15	5330	0.27	15	60	4	1.55	62.5	15.6	46.0	20.3	33	0.196	27.5	41.7	10.4	30.7	13.5	-	-	4.0
16	7230	0.30	15	60	4	1.71	67.9	18.7	50.2	35.0	30	0.196	30.4	45.3	12.5	33.4	23.3	-	-	3.6
17	6840	0.34	15	60	4	1.95	72.4	21.6	53.3	37.0	31	0.196	34.6	48.3	14.4	35.6	24.7	-	-	3.4
18	7380	0.38	15	60	4	2.18	75.9	22.9	54.6	40.0	32	0.196	38.6	50.6	15.2	36.4	26.7	-	-	3.3
19	7880	0.49	15	60	4	2.76	88.6	25.4	58.4	40.0	30	0.196	49.0	59.1	16.9	38.9	26.7	-	-	3.5
20	3780	0.53	15	60	4	2.98	95.3	27.9	68.6	41.0	30	0.196	52.9	63.5	18.6	45.7	27.3	-	-	3.4
21	4560	0.59	15	60	4	3.33	97.2	29.8	71.1	43.0	33	0.196	59.1	64.8	19.9	47.4	28.7	-	-	3.3
22_1	3600	0.18	15	20	1.3	1.01	41.9	10.8	29.8	12.7	29	0.196	17.9	27.9	7.2	19.9	8.5	52.0	34.7	3.9
22_2	3600	0.18	15	20	1.3	1.01	43.5	11.4	29.8	12.7	33	0.196	17.9	29.0	7.6	19.9	8.5	52.0	34.7	3.8
22_3	3600	0.18	15	20	1.3	1.01	45.7	11.4	31.8	11.4	25	0.196	17.9	30.5	7.6	21.2	7.6	52.0	34.7	4.0
22_4	3600	0.18	15	20	1.3	1.01	47.6	10.5	31.8	14.0	28	0.196	17.9	31.8	7.0	21.2	9.3	52.0	34.7	4.5
23_1	4080	0.19	15	20	1.3	1.06	47.9	12.7	31.1	17.8	32	0.196	18.8	32.0	8.5	20.7	11.9	52.0	34.7	3.8
23_2	4080	0.19	15	20	1.3	1.06	48.3	13.0	32.4	15.7	31	0.196	18.8	32.2	8.7	21.6	10.5	52.0	34.7	3.7
23_3	4080	0.19	15	20	1.3	1.06	49.2	12.7	32.1	16.5	31	0.196	18.8	32.8	8.5	21.4	11.0	52.0	34.7	3.9
23_4	4080	0.19	15	20	1.3	1.06	52.7	12.4	33.0	21.6	24	0.196	18.8	35.1	8.3	22.0	14.4	52.0	34.7	4.3
24_1	3660	0.25	15	20	1.3	1.41	56.2	16.5	34.9	22.9	30	0.196	25.0	37.5	11.0	23.3	15.2	52.0	34.7	3.4
24_2	3660	0.25	15	20	1.3	1.41	56.8	16.5	36.2	22.4	31	0.196	25.0	37.9	11.0	24.1	14.9	52.0	34.7	3.4
24_3	3660	0.25	15	20	1.3	1.41	54.3	16.2	34.6	22.9	28	0.196	25.0	36.2	10.8	23.1	15.2	52.0	34.7	3.4
25_1	4140	0.37	15	25	1.7	2.10	72.4	23.8	47.6	26.7	39	0.196	37.2	48.3	15.9	31.8	17.8	52.0	34.7	3.0
25_2	4140	0.37	15	25	1.7	2.10	74.3	24.1	48.9	27.9	38	0.196	37.3	49.5	16.1	32.6	18.6	52.0	34.7	3.1
25_3	5400	0.37	15	25	1.7	2.10	71.1	25.4	44.5	27.9	38	0.196	37.3	47.4	16.9	29.6	18.6	52.0	34.7	2.8
25_4	5400	0.37	15	25	1.7	2.10	80.6	25.7	49.5	25.4	39	0.196	37.3	53.8	17.1	33.0	16.9	52.0	34.7	3.1
26_1	2760	0.74	15	25	1.7	4.18	110.5	35.6	67.3	48.3	33	0.196	74.2	73.7	23.7	44.9	32.2	52.0	34.7	3.1
26_2	4440	0.74	15	25	1.7	4.19	123.2	43.2	85.1	40.6	32	0.196	74.4	82.1	28.8	56.7	27.1	52.0	34.7	2.9
26_3	3840	0.74	15	25	1.7	4.19	128.3	45.7	82.6	48.3	33	0.196	74.4	85.5	30.5	55.0	32.2	52.0	34.7	2.8
26_4	4080	0.74	15	25	1.7	4.19	135.9	40.6	95.3	50.8	33	0.196	74.4	90.6	27.1	63.5	33.9	52.0	34.7	3.3
27	6600	0.67	24	22	0.9	1.47	99.1	33.0	72.4	40.6	33	0.196	26.2	41.3	13.8	30.2	16.9	-	-	3.0
28	6720	0.67	24	22	0.9	1.47	114.3	30.5	77.5	48.3	-	0.196	26.2	47.6	12.7	32.3	20.1	-	-	3.8
29	7740	0.56	24	22	0.9	1.23	99.1	20.3	68.6	50.8	29	0.196	21.8	41.3	8.5	28.6	21.2	-	-	4.9
30	4860	0.43	24	22	0.9	0.96	74.9	15.2	49.5	35.6	26	0.196	17.1	31.2	6.4	20.6	14.8	-	-	4.9
31_1	3660	0.97	24	22	0.9	2.15	127.0	35.6	88.9	45.7	35	0.196	38.3	52.9	14.8	37.0	19.1	52.0	21.7	3.6
31_2	3660	0.99	24	22	0.9	2.19	129.5	34.3	86.4	53.3	33	0.196	38.8	54.0	14.3	36.0	22.2	52.0	21.7	3.8
31_3	3660	0.99	24	22	0.9	2.19	134.6	33.0	87.6	48.3	30	0.196	38.9	56.1	13.8	36.5	20.1	52.0	21.7	4.1
31_4	3660	0.99	24	22	0.9	2.19	137.2	38.1	88.9	55.9	31	0.196	38.9	57.2	15.9	37.0	23.3	52.0	21.7	3.6
32_1	3660	1.97	24	22	0.9	4.36	215.9	-	-	91.4	37	0.196	77.4	90.0	-	-	38.1	52.0	21.7	-
32_2	3660	2.01	24	22	0.9	4.44	218.4	-	-	-	35	0.196	78.8	91.0	-	-	-	52.0	21.7	-
32_3	3660	2.01	24	22	0.9	4.45	241.3	-	-	-	35	0.196	79.0	100.5	-	-	-	52.0	21.7	-
32_4	3660	2.01	24	22	0.9	4.45	221.0	-	-	-	40	0.196	79.0	92.1	-		-	52.0	21.7	-
33_1	2760	2.74	24	15	0.6	6.06	325.1	-	167.6	109.2	39	0.086	162.3	135.5	-	69.9	45.5	39.0	16.3	-
33_2	2760	2.75	24	15	0.6	6.09	332.7	-	167.6	-	37	0.086	163.2	138.6	-	69.9	-	39.0	16.3	-
33_3	2760	2.75	24	15	0.6	6.09	327.7	-	167.6	106.7	40	0.086	163.2	136.5	-	69.9	44.5	39.0	16.3	-

[⊥] The number to the right of the underline is the position of the jet in the array for multiple jet tests.

[*] Discarded because nozzle vibrations resulted in non-symmetric pattern.

Table 3.6 (cont.)

Jet	running time	Discharge	bo	bso	bso/bo	Uo	rm∞	ym∞	ry∞	rϕ∞	ϕ	d95	Fo	rm∞/bo	ym∞/bo	ry∞/bo	rϕ∞/bo	dj	dj/bo	rm∞/ym∞
	[sec]	[l/s]	[mm]	[mm]		[m/s]	[cm]	[cm]	[cm]	[cm]	[deg.]	[mm]						[cm]		
34_1	2580	4.13	24	15	0.6	9.12	347.3	141.6	215.9	139.7	38	0.196	161.9	144.7	59.0	90.0	58.2	78.0	32.5	2.5
34_2	2580	4.13	24	15	0.6	9.12	367.3	146.7	218.4	132.1	39	0.196	161.9	153.1	61.1	91.0	55.0	78.0	32.5	2.5
35_1	2940	0.56	14	10	0.7	3.66	101.6	-	-	38.1	37	0.086	98.1	72.6	-	-	27.2	26	18.6	-
35_2	2940	0.57	14	10	0.7	3.69	132.1	-	-	-	33	0.086	98.9	94.3	-	-	-	26	18.6	-
35_3	2940	0.57	14	10	0.7	3.71	132.1	-	-	43.2	34	0.086	99.5	94.3	-	-	30.8	26	18.6	-
35_4	2940	0.57	14	10	0.7	3.73	134.6	-	-	43.2	33	0.086	99.9	96.2	-	-	30.8	26	18.6	-
35_5	2940	0.58	14	10	0.7	3.74	134.6	-	-	-	38	0.086	100.2	96.2	-	-	-	26	18.6	-
35_6	2940	0.58	14	10	0.7	3.74	137.2	-	-	-	36	0.086	100.2	98.0	-	-	-	26	18.6	-
35_7	2940	0.58	14	10	0.7	3.74	149.9	-	-	48.3	37	0.086	100.2	107.0	-	-	34.5	26	18.6	-
36_1	2400	0.84	14	12	0.9	5.49	154.9	-	-	40.6	43	0.086	147.0	110.7	-	-	29.0	26	18.6	-
36_2	2400	0.85	14	12	0.9	5.53	172.7	-	-	-	39	0.086	148.2	123.4	-	-	-	26	18.6	-
36_3	2400	0.86	14	12	0.9	5.56	177.8	-	-	-	34	0.086	149.1	127.0	-	-	-	26	18.6	-
36_4	2400	0.86	14	12	0.9	5.59	190.5	-	-	-	35	0.086	149.8	136.1	-	-	-	26	18.6	-
36_5	2400	0.86	14	12	0.9	5.61	226.1	-	-	-	38	0.086	150.2	161.5	-	-	-	26	18.6	-
36_6	2400	0.86	14	12	0.9	5.61	233.7	-	-	-	43	0.086	150.4	166.9	-	-	-	26	18.6	-
36_7	2400	0.86	14	12	0.9	5.61	238.8	-	-	63.5	38	0.086	150.4	170.5	-	-	45.4	26	18.6	-
37_1	3540	1.13	14	13	0.9	7.36	195.6	-	-	50.8	49	0.086	197.2	139.7	-	-	36.3	26	18.6	-
37_2	3540	1.14	14	13	0.9	7.42	203.2	-	-	-	49	0.086	198.8	145.1	-	-	-	26	18.6	-
37_3	3540	1.15	14	13	0.9	7.47	231.1	-	-	-	38	0.086	200.1	165.1	-	-	-	26	18.6	-
37_4	3540	1.15	14	13	0.9	7.50	266.7	-	-	-	41	0.086	201.1	190.5	-	-	-	26	18.6	-
37_5	3540	1.16	14	13	0.9	7.52	271.8	-	-	-	37	0.086	201.7	194.1	-	-	-	26	18.6	-
37_6	3540	1.16	14	13	0.9	7.53	274.3	-	-	-	42	0.086	201.8	195.9	-	-	-	26	18.6	-
37_7	3540	1.16	14	13	0.9	7.53	276.9	-	-	78.7	37	0.086	201.8	197.8	-	-	56.2	26	18.6	-
38_1	1920	1.32	14	7	0.5	8.57	231.1	60.7	124.5	66.0	37	0.086	229.7	165.1	-	-	47.2	26	18.6	3.8
38_2	1920	1.33	14	7	0.5	8.63	279.4	-	-	-	37	0.086	231.2	199.6	-	-	-	26	18.6	-
38_3	1920	1.33	14	7	0.5	8.67	297.2	-	-	-	38	0.086	232.3	212.3	-	-	-	26	18.6	-
38_4	1920	1.34	14	7	0.5	8.69	297.2	-	-	-	34	0.086	233.0	212.3	-	-	-	26	18.6	-
38_5	1920	1.34	14	7	0.5	8.70	299.7	-	-	-	34	0.086	233.2	214.1	-	-	-	26	18.6	-
38_6	1920	1.34	14	7	0.5	8.70	302.3	-	-	71.1	35	0.086	233.2	215.9	-	-	50.8	26	18.6	-
39	2460	1.30	14	7	0.5	8.44	261.6	99.1	160.0	83.8	50	0.086	226.3	186.9	70.8	114.3	59.9	-	-	2.6
40	1800	1.52	14	7	0.5	9.87	284.5	106.7	177.8	101.6	50	0.086	264.7	203.2	76.2	127.0	72.6	-	-	2.7
41	1860	1.73	14	3	0.2	11.24	309.9	114.3	198.1	111.8	46	0.086	301.2	221.3	81.6	141.5	79.8	-	-	2.7
42	1860	1.02	14	3	0.2	6.63	231.1	91.4	160.0	71.1	43	0.086	177.6	165.1	65.3	114.3	50.8	-	-	2.5
43	2040	0.63	14	3	0.2	4.09	165.1	55.9	109.2	45.7	37	0.086	109.7	117.9	39.9	78.0	32.7	-	-	3.0
44	1800	0.60	14	3	0.2	3.90	175.3	50.8	119.4	50.8	40	0.086	104.5	125.2	36.3	85.3	36.3	-	-	3.5
45	1800	0.80	14	3	0.2	5.20	193.0	61.0	132.1	63.5	37	0.086	139.3	137.9	43.5	94.3	45.4	-	-	3.2
46	1860	0.83	14	3	0.2	5.39	185.4	71.1	121.9	55.9	39	0.086	144.5	132.4	50.8	87.1	39.9	-	-	2.6
47	1860	1.01	14	13	0.9	6.56	182.9	66.0	121.9	63.5	42	0.196	116.5	130.6	47.2	87.1	45.4	-	-	2.8
48	1800	1.02	14	13	0.9	6.63	195.6	68.6	124.5	61.0	42	0.196	117.6	139.7	49.0	88.9	43.5	-	-	2.9
49	1980	1.52	14	13	0.9	9.87	261.6	91.4	160.0	88.9	42	0.196	175.3	186.9	65.3	114.3	63.5	-	-	2.9
50	1800	1.53	14	13	0.9	9.94	269.2	99.1	162.6	101.6	42	0.196	176.5	192.3	70.8	116.1	72.6	-	-	2.7
51_1	1860	1.57	14	13	0.9	10.18	279.4	104.1	175.3	104.1	44	0.196	180.7	199.6	74.4	125.2	74.4	52	37.1	2.7
51_2	1860	1.57	14	13	0.9	10.18	269.2	-	-	-	43	0.196	180.7	192.3	-	-	-	52	37.1	-
51_3	1860	1.57	14	13	0.9	10.18	276.9	-	-	-	44	0.196	180.7	197.8	-	-	-	52	37.1	-
52_1	1800	2.16	14	13	0.9	14.05	312.4	121.9	188.0	121.9	44	0.196	249.5	223.2	87.1	134.3	87.1	52	37.1	2.6
52_2	1800	2.16	14	13	0.9	14.06	320.0	-	-	-	44	0.196	249.6	228.6	-	-	-	52	37.1	-
52_3	1800	2.16	14	13	0.9	14.06	322.6	-	-	-	42	0.196	249.6	230.4	-	-	-	52	37.1	-
53	19980	0.55	14	8	0.6	3.57	114.1	40.5	85.9	40.6	32	0.360	46.8	81.5	28.9	61.4	29.0	-	-	2.8
54	19800	0.25	14	10	0.7	1.62	69.0	18.9	50.5	30.2	31	0.360	21.3	49.3	13.5	36.1	21.6	-	-	3.7
55	19920	0.65	14	10	0.7	4.22	141.2	45.2	94.8	55.9	38	0.360	55.3	100.9	32.3	67.7	39.9	-	-	-
56	20700	1.05	14	10	0.7	6.82	210.5	72.5	134.8	66.0	40	0.360	89.4	150.4	51.8	96.3	47.2	-	-	-
57_1	3720	0.75	14	10	0.7	4.88	137.2	48.3	101.6	45.7	39	0.360	63.9	98.0	34.5	72.6	32.7	26	18.6	2.8
57_2	3720	0.75	14	10	0.7	4.88	135.1	-	-	-	38	0.360	63.9	96.5	-	-	-	26	18.6	-
57_3	3720	0.75	14	10	0.7	4.88	130.0	43.2	96.5	45.7	38	0.360	63.9	92.9	30.8	68.9	32.7	26	18.6	3.0
58_1	2580	1.01	14	10	0.7	6.55	173.7	76.2	152.4	71.1	39	0.360	85.9	124.1	54.4	108.9	50.8	26	18.6	2.3
58_2	2580	1.01	14	10	0.7	6.56	176.8	-	-	-	38	0.360	85.9	126.3	-	-	-	26	18.6	-
58_3	2580	1.01	14	10	0.7	6.56	160.5	58.4	124.5	61.0	38	0.360	85.9	114.7	41.7	88.9	43.5	26	18.6	2.7

Asymptotic values analysis

The maximum length of erosion at the steady state denoted $r_{m\infty}$ is a function of:

$$r_{m\infty} = f_1(U_0, b_0, \rho, \mu, g\ \Delta\rho, d_{95}, b_{s0}, H) \tag{3.10}$$

where U_0 is the velocity at the nozzle, b_0 is the nozzle diameter, ρ and μ are the density and dynamic viscosity of the eroding fluid, $\Delta\rho$ is the difference between the density of the bed material and that of the fluid ρ, d_{95} is the representative size of the bed material, b_{s0} is the initial thickness or the sediment layer, and H is the water depth. Applying dimensional analysis, it can be shown that:

$$\frac{r_{m\infty}}{b_0} = f_2\left(\frac{U_0}{\sqrt{g\ d_{95}\frac{\Delta\rho}{\rho}}}, \frac{U_0\ b_0}{\nu}, \frac{b_{s0}}{b_0}, \frac{b_0}{d_{95}}, \frac{H}{b_0}\right) \tag{3.11}$$

where

$$F_0 = \frac{U_0}{\sqrt{g\ d_{95}\frac{\Delta\rho}{\rho}}}, Re_0 = \frac{U_0\ b_0}{\nu}$$

are the densimetric Froude number and the Reynolds number at the nozzle, respectively. The densimetric Froude number, a measure of the ratio of the tractive force on a grain to its resistive force, was defined using not the median d_{50} as the effective diameter but d_{95}. Aderibigbe and Rajaratnam (1998) showed that for well-graded mixtures the most significant grains are the coarser ones instead of the median value usually employed in uniform mixtures. Exposed to a certain flow, the smaller grains are more easily moved while the coarser grains remain in place. This is called hydraulic segregation because the top layer of the bed, also called the armor coat, will eventually become a region formed mainly by coarser grains with just a few smaller grains. This top layer has a better resistance to erosion and the degree of endurance is related to the bottom shear stress (Raudkivi, 1990). Thus the size of the original sediment mixture that best correlates to the scour length was found to be d_{95}, which is equivalent to the median size of the armor coat. According to Little and Mayer (1976) armoring occurs when the geometric standard deviation is beyond 1.3. Materials 1 and 2 employed were thus expected to armor and that was actually confirmed when analyzing the experimental data. The data collapse into dimensionless curves obtained using d_{95} was much better than that obtained using the median diameter. Material 3 was not expected to armor given its uniformity, and, in fact, no significant differences were found when choosing either d_{95} or d_{50} as the effective diameter in this case.

Rajaratnam (1976) showed that the effect of the Reynolds number on the scour created by wall jets on a semi-infinite layer of sediment can be neglected if it is larger than a few thousands ($Re_0 > 3000$). Besides, experiments conducted by Rajaratnam and Berry (1977) proved that the effect of b_0/d_{95} can also be neglected even for values of this ratio that are smaller than those of our tests. Similarly, Aderibigbe and Rajaratnam (1998) found that the effect of submergence, H/b_0, is not important when the mean velocity field in the flow is similar to that of a classical (infinitely submerged) wall jet (Rajaratnam 1976) and the flow depth, on average, is at least four times the sediment thickness. Finally, as mentioned before, it was found that the ratio b_{s0}/b_0 has no influence on the steady state profiles as long as it is kept at least below 5. This limit is taken from the range of b_{s0}/b_0 considered in the experiments, however there are no qualitative reasons to think this is actually the top limit. Larger ratios b_{s0}/b_0 should still present the same erosive pattern and final steady state though it could take more time to reach it. As long as the mechanics of jet erosion applies to the problem it is expected the same kind of front movement. In the event the sediment thickness b_{s0} is much larger than the jet diameter the whole setup would be different, resembling more a groundwater problem than a submerged jet scouring a finite layer of sediment. Under these conditions Equation (3.11) can be reduced to:

$$\frac{r_{m\infty}}{b_0} = f_3(F_0) \tag{3.12}$$

A similar analysis can be done to predict $y_{m\infty}$, $r_{y\infty}$, and $r_{\phi\infty}$. Fig. 3.32 shows the dimensionless maximum scour length versus the densimetric Froude number, sorted using the ratio d_j/b_0. Fig. 3.33 depicts the same data as Fig. 3.32 but sorted by the effective diameter d_{95}. The behavior of the maximum scour length $r_{m\infty}$ resembles the pattern found in experiments conducted by Van Dorn et al. (1975), even though the nozzle configuration was slightly different, allowing the jet to expand at a larger angle. They worked with a finer material, in the range ascribed to smoothly graded silt, with sizes ranging from 0.5 to 62 μm. Equation (3.13) fits the data for densimetric Froude numbers larger than 7. It must be noted that the exponent found was similar to that of Chiew and Lim (1996) for jets applied on a semi-infinite layer of sediment, as shown in Equation (3.14). However both equations cannot be used for direct quantitative comparison because Chiew and Lim, working with uniform sediment, expressed the densimetric Froude number as a function d_{50}, instead of d_{95}.

$$\frac{r_{m\infty}}{b_0} = 3.51\, F_0^{0.75} \tag{3.13}$$

$$\frac{r_{m\infty}}{b_0} = 4.41\, F_0^{0.75} \tag{3.14}$$

Figs. 3.34, 3.35, and 3.36 illustrate the behavior of $y_{m\infty}$, $r_{y\infty}$, and $r_{\phi\infty}$, respectively, measured in the present experiments. Equations (3.15), (3.16) and (3.17) present the respective relationships that best fit the data.

$$\frac{y_{m\infty}}{b_0} = 0.47\ F_0^{0.96} \tag{3.15}$$

$$\frac{r_{y\infty}}{b_0} = 2.41\ F_0^{0.74} \tag{3.16}$$

$$\frac{r_{\phi\infty}}{b_0} = 1.87\ F_0^{0.65} \tag{3.17}$$

Consistently with Dellaripa and Bailard (1986) tests, Fig. 3.37 reveals that the angle ϕ tends to be located in a band ranging from 30° to 45° for densimetric Froude numbers higher than 20, however a minor number of tests resulted in angles larger than 45°. The ratio between the maximum scour length, $r_{m\infty}$, and the maximum scour width, $y_{m\infty}$, was found to be approximately 2.5 as can be appreciated in Fig. 3.38. Fig. 3.39 depicts asymptotic longitudinal bed profiles at the centerline, measured downstream from the end of the scour hole, showing the ridge formed in this region for some experiments.

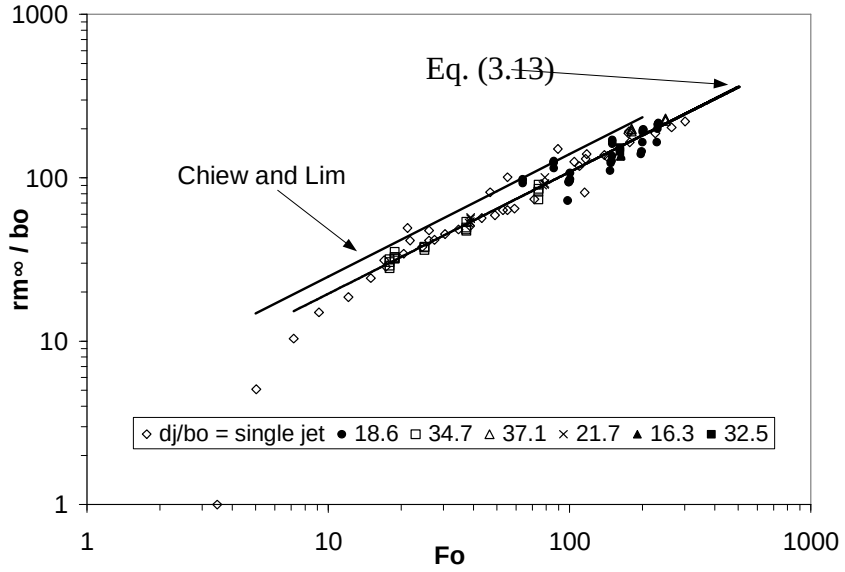

Figure 3-32 Asymptotic dimensionless value of maximum scour length as a function of the densimetric Froude number (symbols indicate different values of the jet spacing to jet diameter ratio, d_j/b_0).

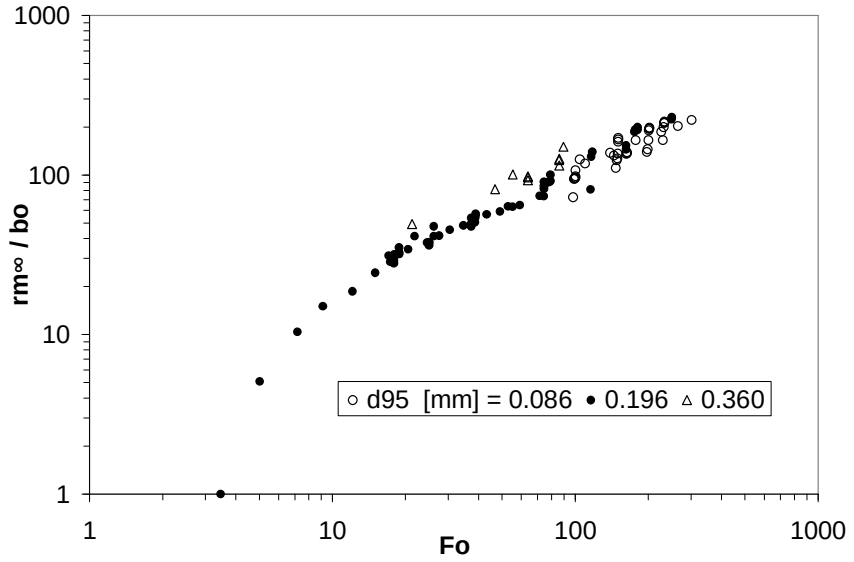

Figure 3-33 Asymptotic dimensionless value of maximum scour length as a function of the densimetric Froude number (symbols indicate different values of the effective diameter d_{95}).

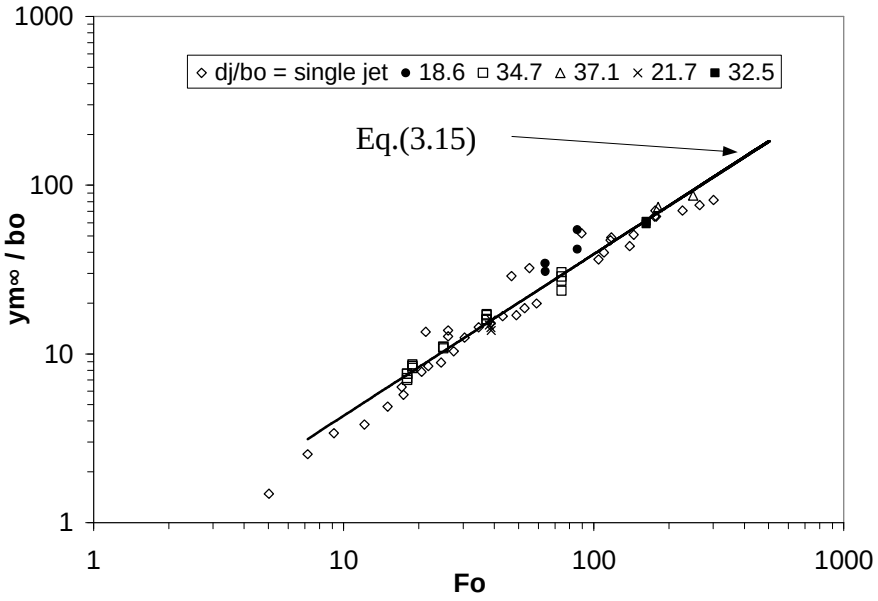

Figure 3-34 Asymptotic dimensionless value of maximum scour width as a function of the densimetric Froude number (symbols indicate different values of the different values of the jet spacing to jet diameter ratio, d_j/b_0).

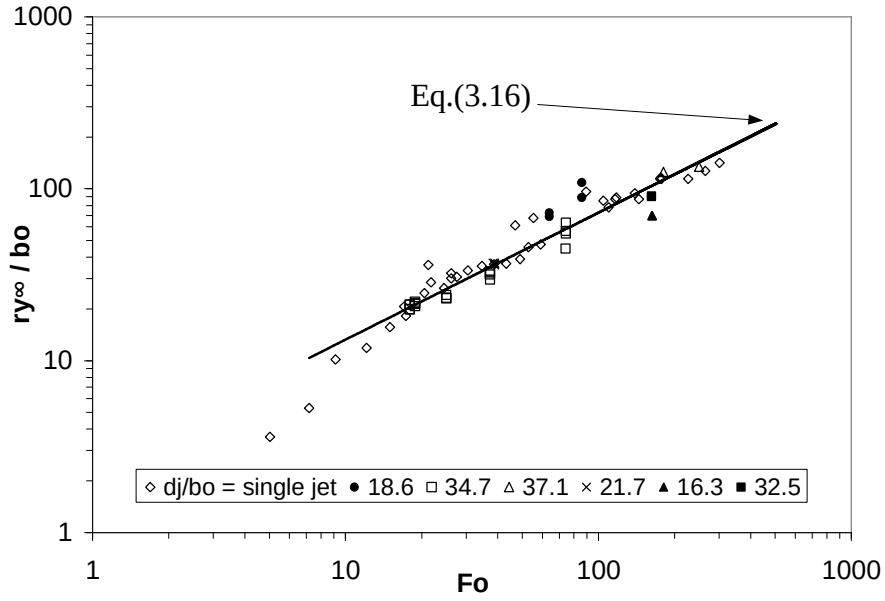

Figure 3-35 Asymptotic dimensionless value of the position of maximum scour width as a function of the densimetric Froude number (symbols indicate different values of the different values of the jet spacing to jet diameter ratio, d_j/b_0).

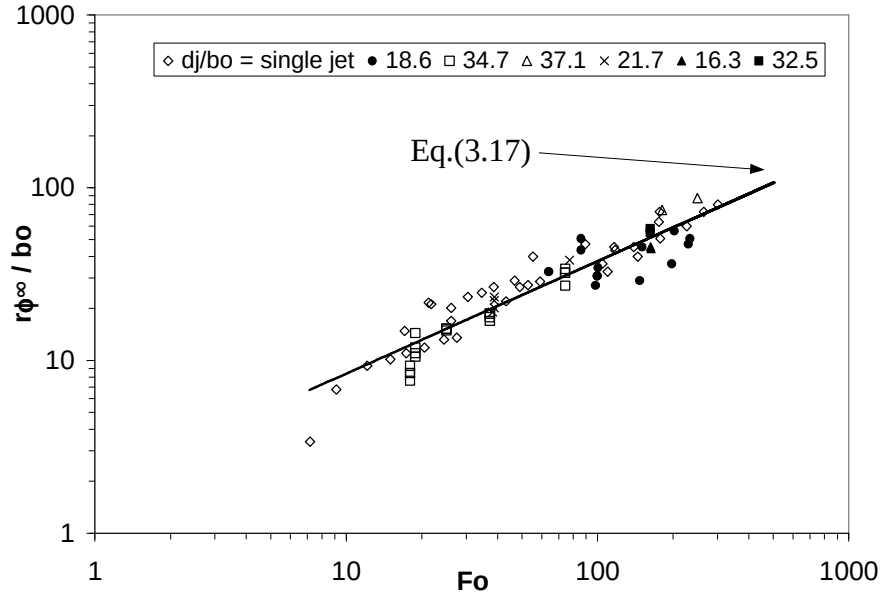

Figure 3-36 Asymptotic dimensionless value of $r_{\phi\infty}$ as a function of the densimetric Froude number (symbols indicate different values of the different values of the jet spacing to jet diameter ratio, d_j/b_0).

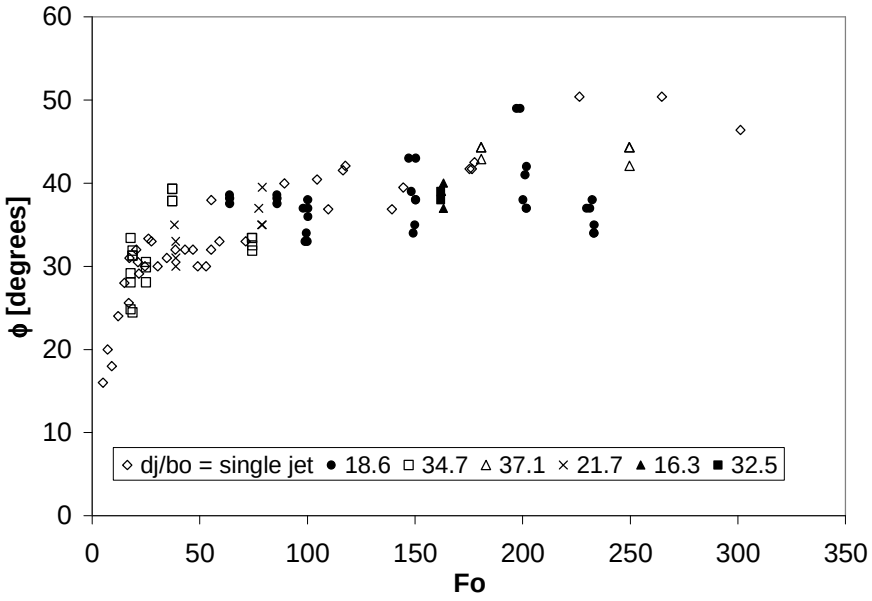

Figure 3-37 Jet angle of expansion, ϕ, as a function of the densimetric Froude number (symbols indicate different values of the different values of the jet spacing to jet diameter ratio, d_j/b_0).

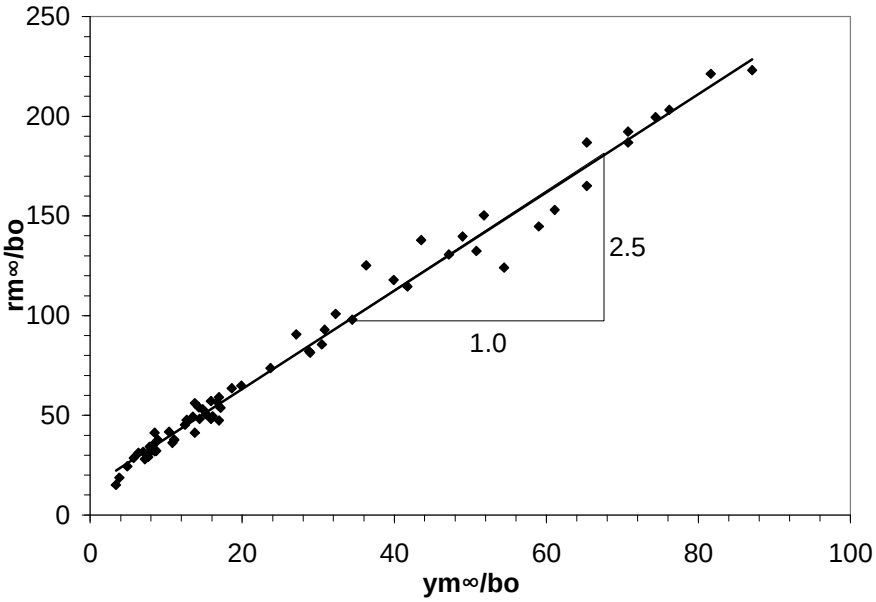

Figure 3-38 Maximum dimensionless scour length versus maximum dimensionless scour width presenting an average ratio of 2.5.

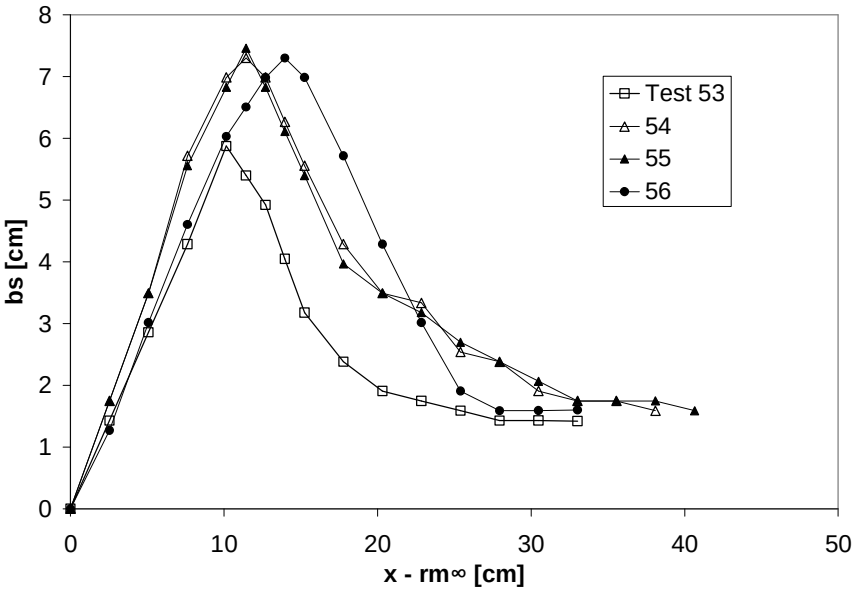

Figure 3-39 Asymptotic longitudinal bed profiles measured downstream from the end of the scour hole, showing the ridge formed in Experiments 53, 54, 55, and 56.

Momentum loss and sediment transport

The flow field of a single wall jet depends on the dimensions and geometry of the nozzle. Plane wall jets present a different behavior than three dimensional wall jets. Among the latter, two categories can be pointed out: bluff jets having a vertical to horizontal nozzle ratio larger than one, and slender jets with a ratio smaller than one. Sforza and Herbst (1970), Rajaratnam and Pani (1974) and Narain (1975) note the existence of three distinct regions along the centerline of the jet. The first one corresponds to the potential core (PC) region, where the flow is characterized by a constant maximum velocity, which is equal to the jet exit velocity at the nozzle The second one corresponds to the characteristic decay (CD) region, where velocity decays as a certain power of the streamwise distance and indicates that mixing from the near boundaries of the jet has reached the center of the flow region, but mixing from the far boundaries has not yet influenced the entire flow field. The velocity decay rate in this region depends on the aspect ratio of the nozzle. Finally, the third zone, where the flow is fully developed, is called the radial decay (RD) region, where mixing from all the jet boundaries has permeated the whole flow field. The maximum velocity decays like that of a radial wall jet and the flow is independent of the orifice geometry. In the case of bluff wall jets, the characteristic region is almost non-existent and the flow passes abruptly from the potential core region to the radial decay region. Circular jets, a specific type of bluff jets, also present this fast velocity decay rate along most of the centerline, mainly due to an unrestrained spanwise spread of momentum. This characteristic turns out to be responsible for a faster reduction in the capacity to move sediment compared to that of a plane wall jet.

When more than one jet is combined, a new variable enters the scene, namely the distance between outlets. Depending on how close the nozzles are located from each other, the flow field might be altered enough to cause a significant increment in the erosive capacity. Knystautas (1964), studying the formation of a two-dimensional turbulent free jet from a series of closely spaced holes, applied Reichardt's hypothesis for the turbulent shear stress to linearize the equation of momentum for the mean square downstream velocity. This enables the superposition of the single jet equation and so the prediction of the velocity field created by an array of multiple free jets. Pani and Dash (1983) also applied Reichardt's hypothesis for a series of turbulent wall jets. They found that neglecting the wall shear stresses in the forward momentum equation results in an error of about 5% in predicting the maximum velocity at a distance of 100 times the nozzle. The error is smaller for sections closer to the outlet. Thus, treating the wall as a frictionless reflector of momentum and superimposing the elementary solution, the following equation for the square of the velocity at the wall ($y = 0$) for an odd number (J) of outlets is obtained:

$$\frac{u^2}{U_0^2} = \frac{0.88\ A}{b_y\ b_z} \left\{ \begin{array}{l} \exp\left[-1.39 \left(\dfrac{z}{b_z} \right)^2 \right] \\ + \displaystyle\sum_{n=1}^{J} \exp\left[-1.39 \left(\dfrac{n\ d_j - z}{b_z} \right)^2 \right] \\ + \displaystyle\sum_{n=1}^{J} \exp\left[-1.39 \left(\dfrac{n d_j + z}{b_z} \right)^2 \right] \end{array} \right\} \tag{3.18}$$

where A denotes the area of the jet nozzle. Similarly, for an even number of jets:

$$\frac{u^2}{U_0^2} = \frac{0.88\ A}{b_y\ b_z} \left\{ \begin{array}{l} \displaystyle\sum_{n=1}^{J} \exp\left[-1.39 \left(\dfrac{(2n-1)\ d_j - 2\ z}{2\ b_z} \right)^2 \right] \\ + \displaystyle\sum_{n=1}^{J} \exp\left[-1.39 \left(\dfrac{(2n-1)\ d_j + 2\ z}{2\ b_z} \right)^2 \right] \end{array} \right\} \tag{3.19}$$

The length scales b_z and b_y can be expressed as:

$$b_y = c_1\ x \tag{3.20}$$

$$b_z = c_2\ x \tag{3.21}$$

where c_1 and c_2 are coefficients given by Pani an Dash (1983), which tend to 0.06 and 0.25, respectively, in the radial decay region. The maximum velocity at the centerline u_m can be obtained by seting z to zero in Equations (3.18) and (3.19). These equations can also be used to estimate how much the velocity field of a certain multiple jet array is

altered with respect to that of a single jet. Fig. 3.40 shows the velocity decay at the centerline for single and multiple circular wall jets (Pani and Dash, 1983). For the sake of comparison, the velocity decay for a plane wall jet (Myers et al., 1963) is also plotted. It can be seen that the higher the number of jets in the array, the more the curves tend to be like that of the plane wall jet. However, no matter how many jets are in the array, beyond a certain distance from the outlet, the decay rate resembles that of the single circular jet. The other important parameter is the separation between nozzles. The closer the jets are to each other, the closer to the nozzle the single velocity fields will start to be affected by the neighbor jets and consequently, the closer the flow will tend to be 2D. Pani and Dash (1983) experimented with a ratio d_j/b_0 equals to 3. For this low ratio the flow decays like that of the plane wall jet, provided that there are enough jets to avoid the 2D flow to spread laterally.

The range of separation in the present experiments ($16.3 < d_j/b_0 < 37.1$) was much larger than that of Pani and Dash ($d_j/b_0 = 3$). This fact is capital to understand why the maximum scour length achieved by a single jet is, on average, not larger than the maximum scour length produced by multiple jets under the same conditions (see Fig. 3.32). If the outlets are separated beyond a certain distance, the flow field of each single jet will be only affected far away from the nozzle and in just a small amount, not enough to increase the bottom shear stress beyond the threshold value. Fig. 3.41 was built using Equation (3.18) for an odd number of 3 jets. It shows how far from the nozzle the maximum velocity at the centerline is increased in a given proportion with respect to the single jet case, as a function of the outlet separation d_j. As expected, the larger the separation, the farther away the influence of the contiguous jets is noticed. It can also be seen that, for a certain separation, higher relative increments of velocity occur farther away from the outlet. This does not necessarily mean that the erosive capacity will be altered beyond its threshold value, because the absolute velocity also decreases away from the nozzle (see Fig. 3.40). Thus, in the present experiments, the scour length produced by multiple jets does not differ from that of a single jet.

Fig. 3.42 shows a plan view of the steady state scour pattern for a single jet case corresponding to Experiment 53. Figs. 3.43, 3.44, and 3.45 show plan views of the steady state scour pattern for multiple jet tests corresponding to Experiments 32, 38, and 58, respectively, where the scour patterns of individual jets merge with those of the neighbor jets. Once the flow is close to the asymptotic state, the surrounding sediment layer does not affect greatly the velocity field as long as the ratio layer thickness to nozzle diameter is kept in the range of the current experiments.

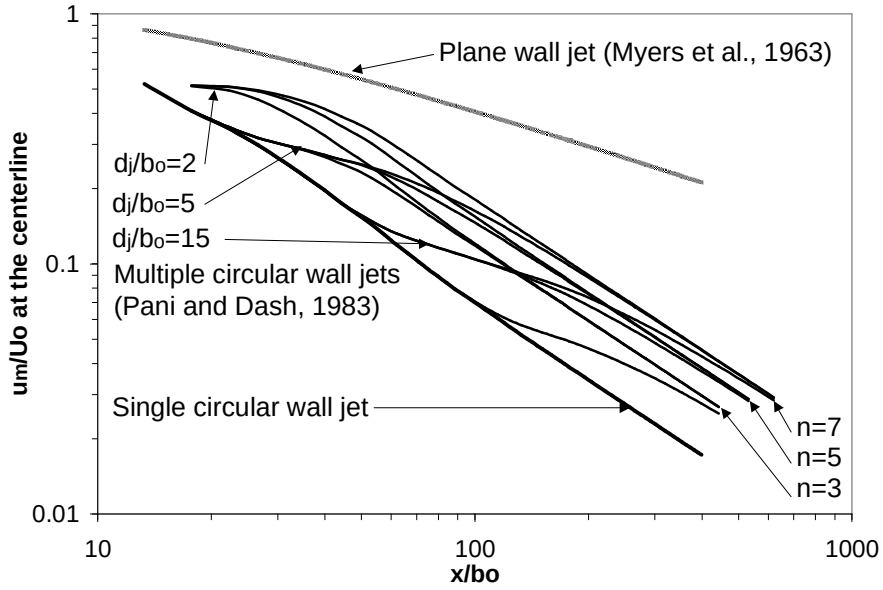

Figure 3-40 Velocity decay of single and multiple circular wall jets and plane wall jet.

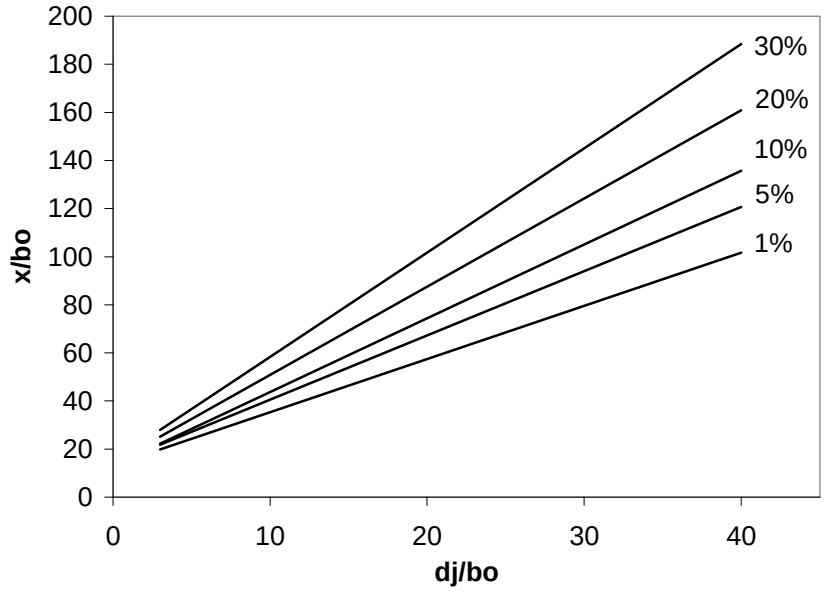

Figure 3-41 Relative increment of maximum velocity at the centerline of a 3-jet array with respect to the single jet case for several outlet separations d_j.

Figure 3-42 Plan view of steady state scour pattern obtained in Experiment 53.

Figure 3-43 Plan view of steady state scour pattern obtained in Experiment 32.

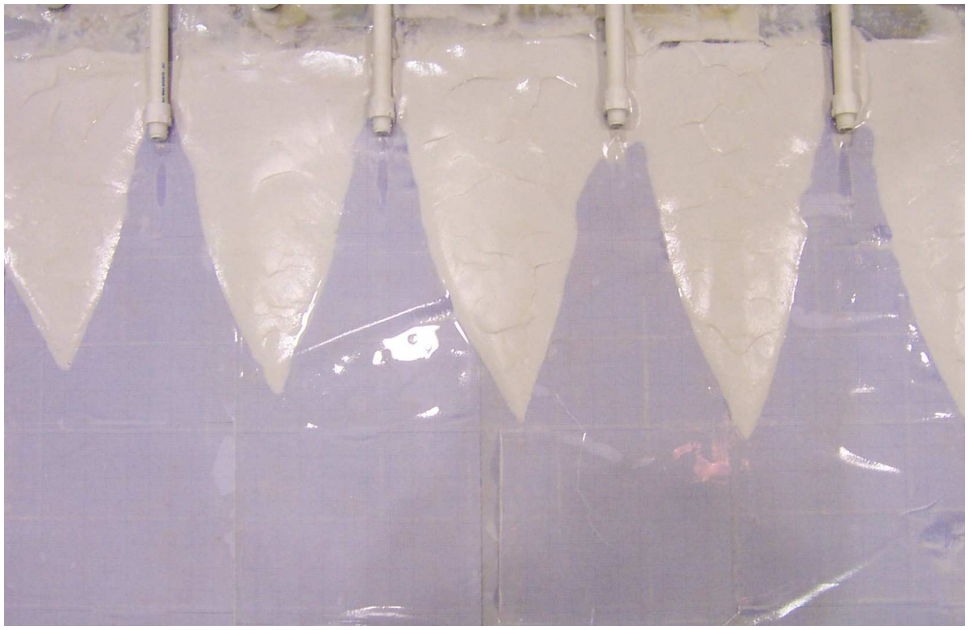

Figure 3-44 Plan view of steady state scour pattern obtained in Experiment 38.

Figure 3-45 Plan view of steady state scour pattern obtained in Experiment 58

Evolution of scour with time

The development of scour in time was studied for seven selected experiments (28, 29, 30, 53, 54, 55, and 56). Experiments with sand (material 1) were entirely recorded using a digital camera. Those with finer sediment (materials 2 and 3) were partially recorded only, because after some minutes turbidity generated by suspended sediment hindered the

vision. Only for these cases the jet was stopped at regular intervals of time and the scour was measured once the suspended material settled.

As Rajaratnam and Berry (1977) noted for circular wall jets applied on a semi-infinite layer of sediment, the erosion length increases with the logarithm of time before the asymptotic state is reached. The scour thus is proportional to the logarithm of time up to a time t^*, beyond which the slope of the scour-time curve starts decreasing and finally becomes zero at the asymptotic or steady state. This same behavior was also observed in the present study, even though the erosion pattern is different. The evolution of the maximum scour length with time is shown in Fig. 3.46 for the mentioned tests.

The length used to evaluate the scour front movement along time was r_m, the instantaneous maximum scour length. In order to collapse the individual profiles into a unique curve, the scour length scale was chosen as $r_{m\infty}$. The time scale was taken as t^*, the time where the scour stops growing proportionally to the logarithmic of time. Fig. 3.47 shows a plot of $r_m/r_{m\infty}$ versus t/t^* for the tests where t^* could be obtained from Fig. 3.46. When t is t^*, r_m is approximately 0.95 $r_{m\infty}$. Conversely, r_m becomes $r_{m\infty}$ when t is approximately 5 times t^* ($t_\infty/t^* \approx 5$). Ade and Rajaratnam (1998) noted that the time it takes for the scour caused by circular wall jets on a semi-infinite sediment layer to reach an asymptotic state should increase with the densimetric Froude number. This was partially confirmed in the few tests where t_∞ was reached. However, they also indicated that it could take days and even weeks to really reach the asymptotic state. In the present tests it was assumed that the asymptotic state corresponded to that measured from the last recorded plan view of the scour hole.

c) Conclusions

The erosion caused by single and multiple circular turbulent submerged wall jets, parallel to a granular layer of sediment of finite thickness, was found to depend on jet velocity and diameter, density of the eroding fluid, and the properties of the sediment to be eroded, in particular the effective or characteristic sediment diameter, related to the critical shear stress. In the asymptotic or equilibrium scour state, the maximum scour length and other representative parameters seem to depend only on the densimetric Froude number and not on the Reynolds number. Equations were proposed for these parameters that best fit the data obtained in this study. Other variables like the sediment thickness to jet diameter ratio, and the distance between jets were found not to affect the final scour for the ranges employed in the experiments. The scour length was found to initially grow with the logarithm of time and then to tend slowly towards an asymptotic value. The dependency of the maximum scour length with the densimetric Froude number and its evolution with time resemble the behavior of the semi-infinite sediment layer erosion case exposed in previous studies.

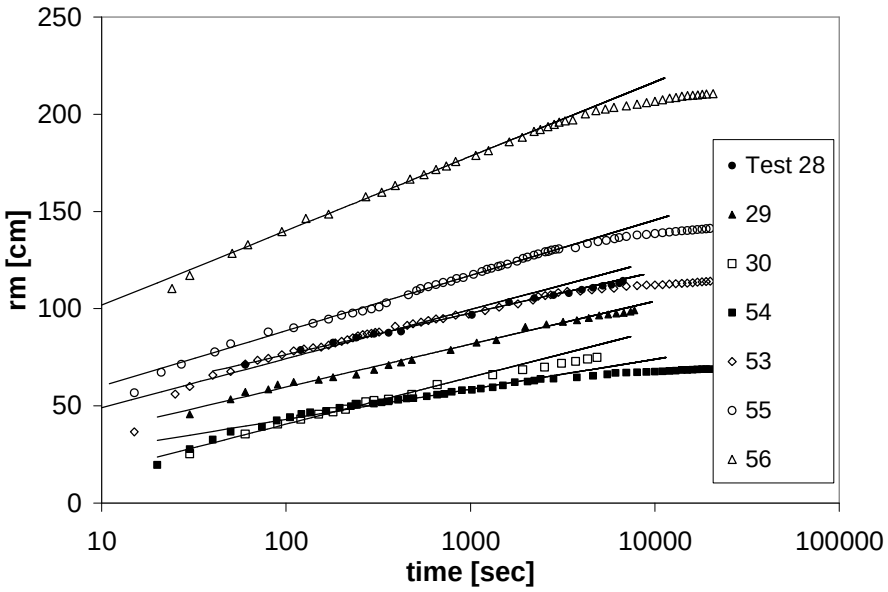

Figure 3-46 Time evolution of maximum scour length for Experiments 28, 29, 30, 53, 54, 55, and 56.

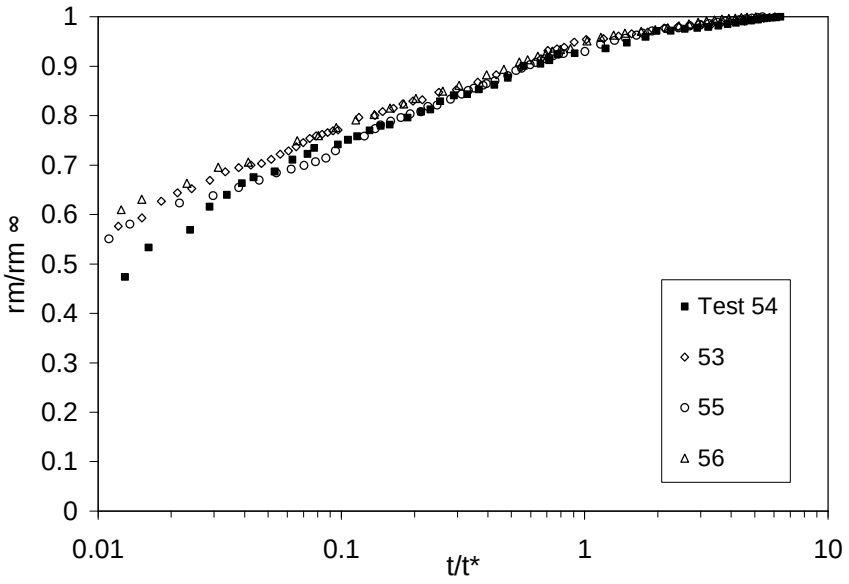

Figure 3-47 Dimensionless time evolution of maximum scour length for Experiments 28, 29, 30, 53, 54, 55, and 56.

4. A DESIGN CRITERION FOR JET ARRAYS

4.1 Introduction

Based on the results of the experimental studies reported in previous sections, a criterion for the design of a jet array system to clean sewer solids deposited on McCook reservoir is proposed here. A general operation strategy for the management of solids in the reservoir using the jet array system is also discussed.

The area in McCook reservoir to be cleaned by the use of jet arrays corresponds to Stage 1, which is located between the Surge Chamber and Stage 2. It is separated from these two areas by weirs. The sewage flow is first conveyed to the Surge Chamber, where according to previous calculations based on physical modeling by USACE (McCook Reservoir Design Documentation Report, USACE Chicago District, 1999), the turbulence will be high enough to carry all but the heaviest particles over the weir to Stage 1. The location of Stage 1 in McCook reservoir can be seen in Fig. 4.1. It has a length of about 660 m and a width ranging from 120 to 240 m.

The main characteristics of the jet array to be calculated are the nozzle diameter, the jets spacing, the water discharge needed and distribution of the jets over the whole area of the reservoir.

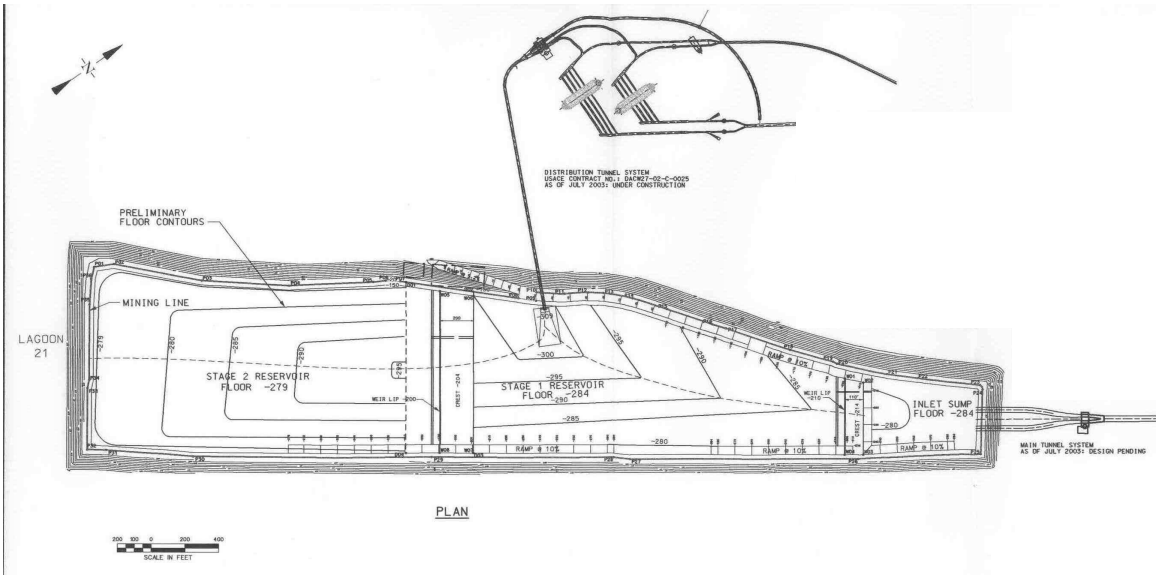

Figure 4-1 Plan view of McCook reservoir. Stage 1 is separated from the Surge Chamber upstream and Stage 2 downstream by weirs.

4.2 Jet design

a) Densimetric Froude number approach

The design proposed here is based on experimental results reported in previous sections, which provided information regarding the behavior and scour characteristics of single and multiple jets acting on a sediment bed of limited thickness.

The first step in the design is to determine the longitudinal extension of the bed area, $r_{m\infty}$, to be cleaned by one individual jet. Obviously, the larger $r_{m\infty}$, the less is the number of jets needed to clean the bed. The extension $r_{m\infty}$ is a function of the nozzle diameter and the densimetric Froude number of the jet. Experimental evidence showed that the larger $r_{m\infty}$ the larger the jet velocity, U_0, needed, and thus the larger the water discharge required to operating the jet. There is a compromise between the largest possible values of $r_{m\infty}$ and reasonable values of the jet discharge.

The calculation procedure is as follows: first, the nozzle diameter, b_0, is set, based on standard commercial values; then, a value of the longitudinal extension, $r_{m\infty}$, is chosen; with the value of the $r_{m\infty}/b_0$ ratio, the required value of the jet Froude number, F_0, is determined from Equation (3.13): $r_{m\infty}/b_0 = 3.51\ F_0^{0.75}$ (see also Fig. 3.32); assuming the effective diameter of the sediment is known, the jet velocity U_0 can be obtained from F_0; with U_0 and b_0, the jet discharge, Q_0, is calculated; if U_0 or Q_0 are too high from a practical point of view, the value of $r_{m\infty}$ is decreased, which increases the number of jets needed to clean the bed. In this process, the value of b_0 could also be revised if necessary.

The next step is to reckon the distance between jets d_j. For this, different criteria can be employed, depending on how much sediment is going to remain in the shadow region between jets that cannot be swept by them. One possible path is to set d_j as a function of $r_{\phi\infty}$, the distance from the nozzle at which the width of the scour hole stops increasing linearly and its boundaries get curved, as shown in Fig. 4.2. Using this criterion, d_j turns out to be equal to $2\ r_{\phi\infty} \tan(\phi/2)$.

The value $r_{\phi\infty}$ and the angle ϕ can be obtained from observations of the dimensions of the scour hole created by the jet array. By entering Figs. 3.36 ($r_{\phi\infty}$ vs F_0) and 3.37 (ϕ vs F_0) with the selected value of F_0, both the ratio $r_{\phi\infty}/b_0$ and ϕ can be determined. This design will leave unclean a triangular region of solids between jets, with an area of about $r_{\phi\infty} d_j/2$. Expressed in terms of $r_{\phi\infty}$ and ϕ, this area is: $r_{\phi\infty}^2 \tan(\phi/2)$. This area could be partially swept away using smaller intermediate jets (see Fig. 4.2).

Consider the case of a jet designed to clean sediment up to 50 meters from its nozzle. The diameter of the jet must be chosen on commercial basis, for example $b_0 = 0.125$ m (5 inches). From Equation 3.13, the densimetric Froude number F_0 corresponding to a ratio $r_{m\infty}/b_0$ of 400 is 553.

$$F_0 = \left(\frac{r_{m\infty} / b_0}{3.51} \right)^{1/0.75} = 553$$

From the densimetric Froude number, the velocity of the jet at the nozzle can be estimated. Based on measurements taken by MWRDGC, the average dry density of the O'Hare reservoir sediment is 1680 kg/m^3, while the wet density is 1030 kg/m^3. The dry

density must be employed in the computation of $\Delta\rho/\rho$. Assuming a characteristic solids diameter of the aggregates of 84 μm, as reported in Section 3.1. The nozzle velocity turns out to be 13.1 m/s, and the discharge 0.161 m^3/s.

$$U_0 = F_0 \sqrt{g\, d_{95} \frac{\Delta\rho}{\rho}} = 13.1 m/s$$

$$U_0 \pi \frac{b_0^2}{4} = 0.161 m^3/s$$

This discharge, or any other found by following a similar process, is the desired discharge for each single jet in the array, however the actual discharge distribution from the manifold to each jet will vary from jet to jet due to variations in the pressure exerted on the jet. The distribution of the flow along the ports of the manifold can be estimated following the procedure described by Roberson et al. (1988). The actual flow distribution from the manifold to the jets depends on the pressure distribution along the manifold. To avoid high velocities, and thus high losses, different criteria could be used. The main variables are the manifold diameter and the number of jets it feeds. Keeping the maximum velocity in the manifold below a certain threshold value implies limiting the number of jets supplied by it. Besides, larger manifold diameters reduce velocities and losses, but for practical reasons the manifold diameter should also be kept under certain dimension. Thus a long line of jets would require more than one supplier manifold.

The jets used in the experiments were circular jets, having an area equal to $\pi b_0^2/4$ and came out short pipes attached to the manifold (see Figure 3.29). It must be pointed that the jet diameter (jet nozzle) b_0 is circular, and in case other nozzle configurations are used the scour pattern can differ from the one found in the present tests.

It must be noted that the equations and figures used for the above calculations refer to the asymptotic or steady state of the jet induced scour. As it was explained in Section 3.2, the time needed to reach steady conditions can be several hours. However, from Fig. 3.26 ($x_m/x_{m\infty}$ vs t/t^* for sewer sediment) it is found that for a time t^* (the time when the scour stops growing proportionally to the logarithmic of time), the scour length is about 95% of the asymptotic value $x_{m\infty}$. From Fig. 3.27 (x_m vs t for sewer sediment) it is concluded that for the sewer solids tested in the experiments of Series E2, this time is approximately 4 minutes. In a prototype scale jet this time should increase to approximately 10 minutes as Dellaripa and Bailard (1986) report. Hence, making the jet work a relatively short period of time, the scour obtained is approximately 95% of the maximum possible extent (for this example about 47 m out of 50 m that would be the maximum scour length). Trying to reach the asymptotic scour would be inefficient and expensive due to the amount of time involved.

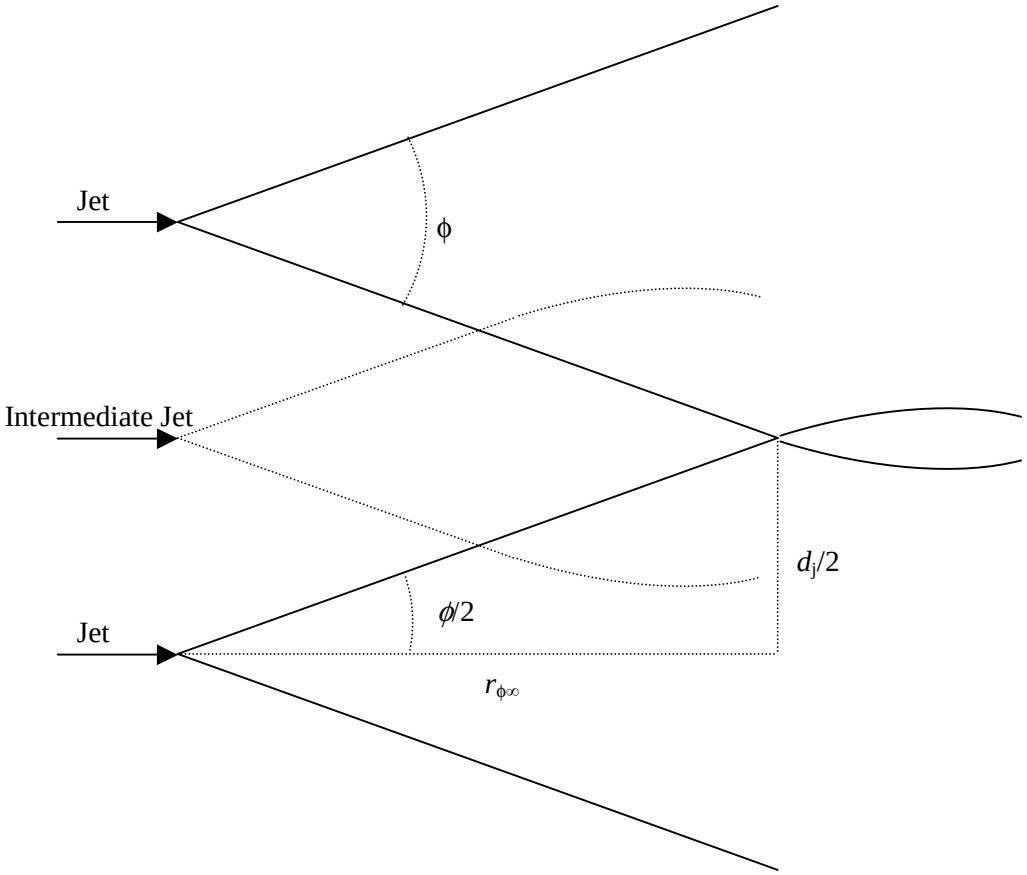

Figure 4-2 Criterion to estimate jet spacing, d_j, in a jet array. Intermediate smaller jets can be placed in between main jets to partially clean the area not scoured by the main jets.

The jet spacing will be estimated following the criterion outlined above. The parameter $r_{\phi\infty}$ is obtained first from Equation 3.17:

$$r_{\phi\infty} = b_0 1.87 F_0^{0.65} \cong 14.2m$$

Then from Figure 3.37 the angle ϕ can be estimated following the tendency for large Froude numbers. For the case of a Froude number equal to 553 the angle ϕ can be estimated as 40°. Thus the jet spacing d_j is computed as follows:

$$d_j = 2\, r_{\phi\infty} \tan(\phi/2) \cong 10\text{m}$$

The maximum scour width y_m should be almost 20 m. Fig. 4.3 illustrates a sketch for a single line array composed by jets having the characteristics above calculated. Van Dorn et al. (1977) showed that the power required to producing a certain threshold scour stress

increases as the fourth power of the maximum scour radius. The power of the jet is proportional to its discharge. This is the reason why trying to clean larger areas of sediment with a single line of jets results in prohibitive discharges. For the sake of comparison in order to sweep a distance of about 100 m with the same jet would require a discharge of 0.404 m^3/s per jet, and to avoid sky-scraping velocities at the nozzle the jet diameter should be increased.

As it was mentioned previously, the use of intermediate jets with a lower discharge to partially clean the triangular areas not scoured by the main jets could be an alternative solution to avoid an excessive accumulation of solids in the areas close to the wall between jets. Another possibility is the use of rotating jets.

b) Critical shear stress approach

In a previous report, Garcia (1999) estimated the scour of a single circular jet using Jenkins equation. This empirical equation relates the bottom shear stress along the main axis of a wall jet for a given Reynolds number. Thus, it is possible to estimate the longitudinal extension of the scour caused by a jet on any sediment as long as the critical shear stress of the sediment is known. One way to express Jenkins equation is:

$$\frac{r_{m\infty}}{b_0} = \left(\frac{\tau_c \, Re_0^{0.4}}{120 \, \rho_m \, U_0^2} \right)^{-0.417}$$

where Re_0 is the Reynolds number at the nozzle, τ_c is the critical shear stress of the sediment, ρ_m is the density of the fluid sediment mixture, U_0 is the jet velocity at the nozzle, b_0 is the nozzle diameter and $r_{m\infty}$ is the scour length.

Assuming a mixture density of 1200 kg/m^3, a critical shear stress for the sewer solids of 0.02 Pa (Pa = Pascal = N/m^2), as estimated from the experiments of Series E2, and the same nozzle velocity selected in the densimetric Froude number approach (13.1 m/s), the scour length predicted by Jenkins equation can then be directly compared with that obtained from the latter approach. Because Jenkins equation is sensitive to the critical shear stress value and given the uncertainties involved in its estimation for the sewer solids in McCook reservoir, a sensitivity analysis was made, using two other values of τ_c: 0.06 Pa (the minimum shear stress value used in the experiments with the annular flume of Series S2, for which resuspension was actually observed); and 0.2 Pa, a value given by Vanoni (1995) for organic mud. Table 4.1 shows the results obtained for $r_{m\infty}$, including those corresponding to the densimetric Froude number method. It is concluded that Jenkins equation overestimates the scour length predicted from the experimental information gathered in the present study for the lowest value of the critical shear stress (0.02 Pa), however it underestimates such scour length for higher values of τ_c. Since the value τ_c = 0.2 Pa seems to be much higher than the values estimated from the present experimental evidence for sewer solids such as those expected to be found in McCook reservoir, and since the scour length estimated with Jenkins equation in that case is only

about 50% of that estimated from the densimetric Froude number method, the result obtained for this value of τ_c is discarded.

With these results, a jet array configuration can be designed to clean the bottom of Stage 1 in McCook reservoir from sewer solids. This is presented in next section.

Table 4-1 Summary of scour length calculation for both densimetric Froude number and shear stress approaches

Method	Characteristic parameter	r_m [m]
Froude number	sediment diameter [μm]	
	84	50.0
Critical shear stress	critical shear stress [Pa]	
	0.02	71.0
	0.06	44.9
	0.20	27.2

4.3 Jet array configurations

There is more than one possible configuration for jet arrays capable of cleaning efficiently and economically a certain area. The configuration showed in Fig. 4.3, composed of a series of parallel jets emanating from the same straight pipe is a simple one. Nonetheless, given the extremely high discharges per jet needed to clean a bottom area of more than about 50 m long in the direction of the jets, it seems that only one line of jets does not give a sufficient cleaning capacity for the whole width of Stage 1, and on the contrary, the cleaning system would have to rely on several lines of jets disposed at specific distances to clean a given area sequentially and by steps. Fig. 4.4.a shows this alternative, where different stages are set to work sequentially at different times to cover the whole bottom area. In the case of Stage 1 in McCook reservoir, having a length of approximately 660 meters, it would also be necessary to set the number of jets working simultaneously depending on the discharge capacity available, thus it is plausible the jets will work on groups of 5 to 10 on the same line to cover the whole length, and after that release the next stage downstream. There would be 6 lines of jets and the total number of jets to install would be 336. Operating 10 jets at a time would require a total discharge of about 1.6 m^3/s. If groups of 10 jets work for about 10 to 15 min (the estimated time required to clean a longitudinal extension close to 50 m), then the total time needed to clean the entire bottom of the reservoir would be of about 8 to 9 hours. This time could be cut in half by doubling the number of jets operated simultaneously, which would require twice as much discharge capacity (about 3.2 m^3/s). The distance between lines of jets should be shorter than the maximum cleaning length $r_{m\infty}$ in order to avoid the same death zones appearing in the first line. If the second line of jet were placed at the extreme end of the scouring pattern, that is at a distance $r_{m\infty}$ from the first line of jets, there would be a another set of unclean death zones between the first and the second lines of jets. This distance can be estimated depending on the parameter $r_{\phi\infty}$. In this case the spacing between jet lines should be $r_{m\infty} - r_{\phi\infty} \approx 36$ m. See Figure 4.4.b.

This configuration designed to wash down the sediment in steps would accumulate the sediment of the first lines downstream before cleaning the whole area. The material removed by the first line of jets will set partially in the area to be washed by the second line, and so on. Thus the last lines will have to scour a thicker layer of sediment. Depending on the initial thickness b_{s0}, it may happen that in the last line or lines the ratio b_{s0}/b_0 turns out to be large enough to alter the scour pattern assumed in the configuration design. This may be used as a criterion to set the frequency of operation. In order no to surpass a certain ratio b_{s0}/b_0 in the order of magnitude tested in the experiments, for example $b_{s0}/b_0 = 10$, the jet system should be turned on. This is a mere qualitative inference, because it is not easy to estimate how far downstream the sediment will be re-deposited once the first lines of jets are washing it away. However it is probable the key point to set up the frequency of operation turns out to be the necessity to avoid an excessive consolidation of the sediments rather than a large ratio b_{s0}/b_0.

Another possible configuration for the jet arrays was given by Van Dorn et al. (1975). They worked with non-parallel jets released at different times, also in a multistage frame (Fig. 4.5). It should be mentioned that the scour angle ϕ in this setup was close to 60° due to a different nozzle configuration. In order for the scour generated by this configuration not to be constrained to narrow strips, it would be necessary to select a nozzle configuration different from the circular one.

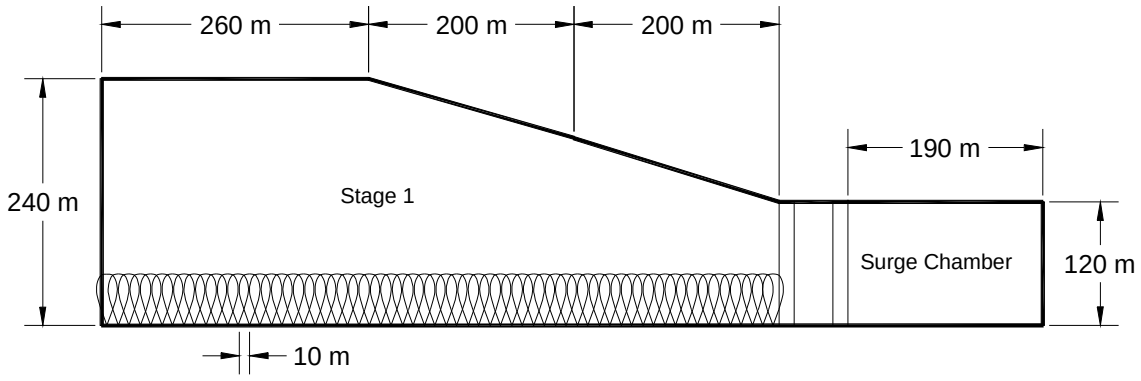

Figure 4-3 Sketch for a single line jet array along Stage 1 of McCook reservoir.

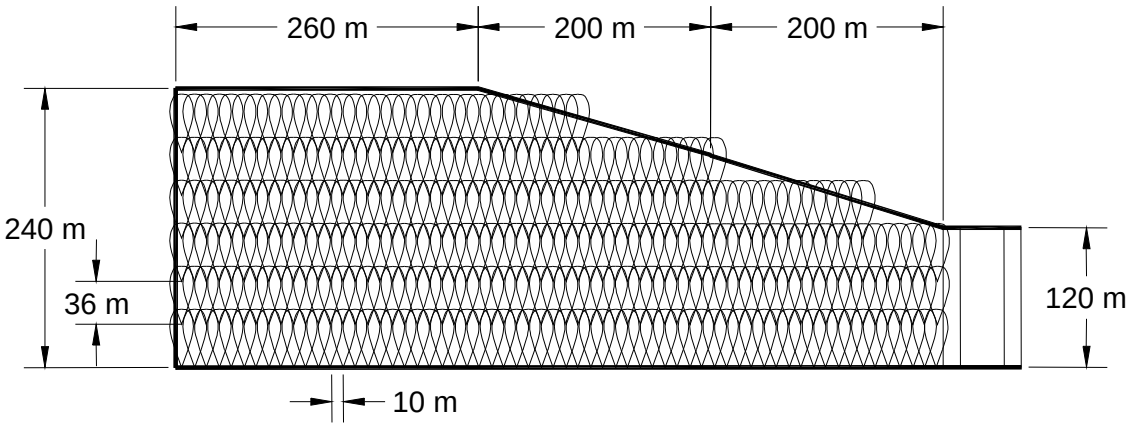

Figure 4-4 a Multistage jet array proposed for Stage 1.

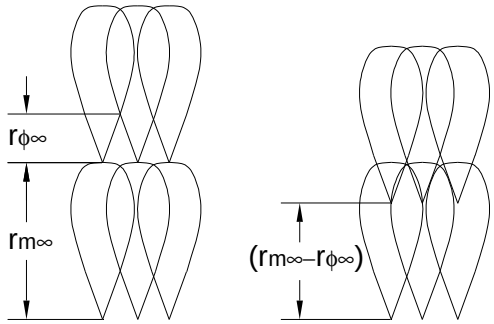

Figure 4-4 b Sketch depicting why the spacing between jet lines should be smaller than the maximum scour length in order to avoid the repetition of death zones.

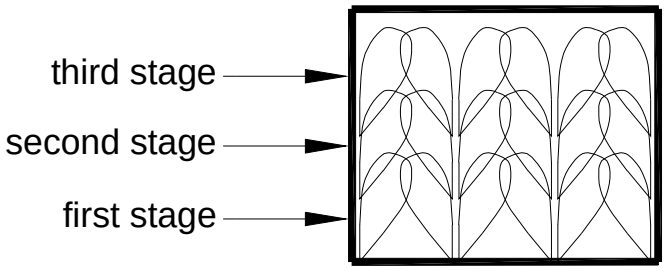

Figure 4-5 Multistage jet array with non-parallel jets facing each other.

4.3.1 Influence of jet height and inclination

So far we have considered jets resting on the reservoir floor. For different reasons, among them minimize corrosion and interference with the movement of the sediment, the jet arrays could be located a certain distance above the reservoir floor resting on support piers or another structure. Bailard and Camperman (1983), and Dellaripa and Bailard (1986), based on the work of Jenkins et al. (1981) showed that the jet scour pattern is also

a function of the jet height from the bottom, *h*, and the jet angle relative to the horizontal, θ (see Figure 2.5). They proposed the following correction to Jenkins formula (Equation 2.3):

$$\frac{r_{m\infty}}{b_0} = \left(\frac{10^4 \tau_c Re_0^{0.4}}{C_0 \rho U_0^2} \right)^{C_1}$$

where

$$C_0 = 10^{-C_2/C_1}$$

$$C_1 = 0.0533 \sin(5.59\theta) - 0.385 + \left(-0.0201 + 0.00593\theta^{0.356}\right)(h/b_0)$$

$$C_2 = 2.442 + 0.0108(h/b_0) - 1.266x10^{-4}(h/b_0)^2 - 0.0118\theta - 9.33x10^{-5}\theta^2$$

According to Dellaripa and Bailard (1986) small jet angles and low heights are most effective in producing scour over a significant distance. Figure 4.6 was done using the modified equation of Jenkins that takes account of *h* and θ in the coefficient C_0, C_1, and C_2. Depending on the angle θ and the ratio h/b_0 the maximum scour length is increased compared to the case where both θ and *h* are zero. The increment depends also on the jet velocity and the Reynolds number at the nozzle, and the critical shear stress of the sediment, τ_c. The jet seems to scour farther when it is placed a certain distance above the floor, however if the height *h* is beyond a certain limit the scour length starts decreasing and eventually becomes shorter than the scour caused by the jet at the floor. Regarding the effect of the angle θ, small angles between 0 and 20 degrees seem to increase the scour, but larger angles turn out to be inefficient. Figure 4.6 corresponds to U_0 = 10 m/s, b_0 = 0.125 m, mixture density ρ = 1200 kg/m^3, and τ_c = 0.1 Pa (to use the critical shear stress of the original experiments by Van Dorn (1977) corresponding to diatomaceous earth). The viscosity ν required to compute the Reynolds number was assumed to be 1E-6m^2/s. The curves were found to be sensitive to the critical shear stress τ_c, thus they should be handled with care.

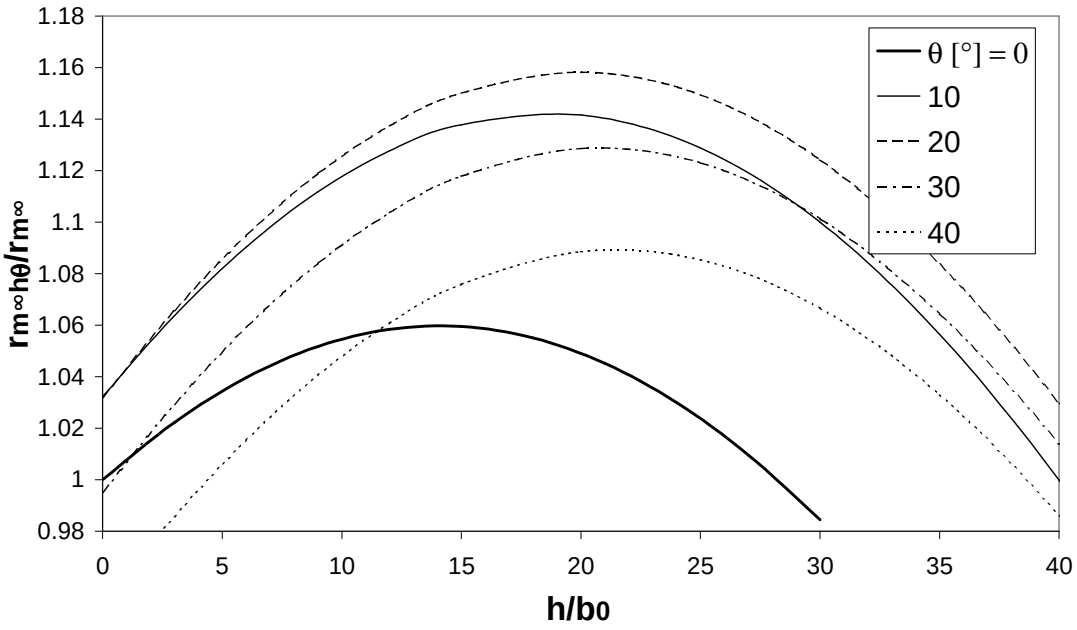

Figure 4-6 Effect of jet height from the bottom, h, and the jet angle relative to the horizontal, θ, on the maximum scour length. In the ordinate axis $r_{m\infty h\theta}$ stands for the maximum scour length when h and θ are different than zero. The parameter $r_{m\infty h\theta}$ is made non-dimensional using the maximum scour length $r_{m\infty}$ for $h = 0$ and $\theta = 0$.

Table 4.2 summarizes the data in Figure 4.6, it presents for different angles θ the range of h/b_0 that can be used without reducing the scour capacity (h/b_0 maximum). Also showed is the optimum value of h/b_0 that maximizes erosion (h/b_0 optimum) as well as the increment in scour length corresponding to the optimum ratio h/b_0 expressed as the ratio $r_{m\infty h\theta}/r_{m\infty}$. For example, assuming the jet angle relative to the horizontal is 10 degrees, the jet nozzle could be placed a height equals to 40 times the jet diameter b_0 and the scour would not be reduced. In case of setting the jet nozzle 20 times b_0 from the floor, there would be an increment of 14 % in the scour length compared to the scour of the same jet parallel to the bottom and resting on the floor. The maximum h/b_0 comes from the intersection between the descending side of the curve and the horizontal line corresponding to $r_{m\infty h\theta}/r_{m\infty} = 1$, while the optimum h/b_0 comes from the maximum value of $r_{m\infty h\theta}/r_{m\infty}$. Larger angles were not considered because as Figure 4.6 shows for angles θ larger than 20 degrees the efficiency of the scour starts to be reduced, this is because a significant amount of the vertical component of jet momentum is being wasted against the floor.

Table 4-2 Influence of height h and angle θ in the scour length.

θ [degrees]	h/b_0 maximum	h/b_0 optimum	$r_{m\infty h\theta}/ r_{m\infty}$
0	28	15	1.06
10	40	20	1.14
20	42	20	1.16

4.4 Operation strategy

Having a preliminary design for the jet array cleaning system for McCook reservoir, it is necessary to make a few comments regarding the operation strategy of the system. Three operational stages are foreseen: when the reservoir is full and the solids are being deposited on the bottom; when the reservoir is being drained; and when the reservoir is almost empty and a layer of solids covers the bottom. It is assumed that a drainage channel exists in the reservoir to help extract water with high solids concentration resulting from the cleaning process.

In the first operational stage, with the reservoir is full and a significant amount of solids have been deposited on the bottom, the jets can be operated in order to create a density current along the bed. The jet velocity should be small enough not to create a strong resuspension of the fine bed material throughout the water column. The idea is to avoid consolidation of the solids on the bottom and to help remove at least the finer fractions of the bed material, which would be transported in the direction of the jets. Probably only the first line of jets would be operated at this stage.

In the second operational stage, when the reservoir is being drained, the jet array system would be used in full, as discussed in the previous section, to clean the bed, operating groups of about 10 to 20 jets sequentially. At this stage the water depth should be around 2 to 3 m (value that scales with the nozzle diameter to water depth ratio used in the experimental study of Series E3 and E4). During this stage water with high solids concentration would be extracted from the drainage channel.

In the third operational stage, when the reservoir is almost empty, the jet array system would be used to sweep the bottom clean, in case it is necessary, by operating the jets with maximum discharge. There were no experiments performed to test the efficiency of this operational stage.

A pilot study should be conducted at prototype scale to explore these ideas and validate the experimental results reported in previous sections.

4.5 Conclusions

The basic parameters for a possible jet array configuration for Stage 1 in McCook reservoir have been proposed. These parameters are jet diameter, jet discharge, and jet spacing. In order for each jet to clean a length of 50 m, a nozzle diameter of 0.125 m (5 inches) should be used with a discharge of about 161 l/s for about 10 minutes. The jet separation was set to 10 meters. A possible array that would clean the whole bottom area of McCook reservoir has been proposed, composed by 6 lines of jets with a total of 336 jets. The spacing between jet lines is 36 m. It should be noted that the design parameters could be altered depending on other restraints such as maximum velocity allowed in the manifold or minimization of energy losses in the manifold, not taken into account in this analysis. An operational strategy has also been proposed, composed of three stages, depending on the water level in the reservoir. With a full reservoir and a significant

deposit of solids on the bottom, the jets would be operated with low velocity to create slow density currents to avoid consolidation of the bed and remove the finer fractions of bed material. With water depth of about 2 to 3 m, during drainage of the reservoir, the jet array system would be operated in full, with groups of 10 to 20 jets being activated sequentially to clean the whole bottom area of the reservoir. Finally, with an empty reservoir, the jets would be operated with maximum discharge to sweep the bottom clean of solids.

For the experiments carried out the influence of the floor slope on the scour during the second operational stage was found to be not important because the momentum responsible of washing down the sediment comes from the jets, and depends on the jet velocity and jet diameter. However the floor slope could have a more significant role in the first operational stage, where density currents are created to avoid consolidation.

5. CONCLUSIONS

The main conclusions obtained from the experimental studies conducted and the analysis of design alternatives for the jet array system described in detail in previous sections are summarized next.

5.1 Conceptualization of the problem

As concluded from the analysis of the jetting system to clean the bottom of McCook reservoir from sewer solids, the near field transport problem depends on a number of dimensionless parameters whose values need to be conserved in both laboratory and field situations. Nonetheless the precise influence of those parameters on the behavior of the cleaning system could only be measured through laboratory experiments.

The expected complex behavior of McCook solids imposed the use of prototype sediments in the experimental study. Given the impossibility of using prototype scale discharges for the jets, this lead to some distortion on the values of the dimensionless parameters governing the cleaning efficiency of the jetting system. To overcome this problem, an approach consisting of combining different experiments regarding flow and sediment transport induced by the jet array systems, involving prototype solids but also granular sediment of different sizes, was followed, in order to study at a laboratory scale the main aspects of the jetting system, eventually validate models of some of the process involved using the experimental data, and then, apply them for the final design of the sediment cleaning system for McCook reservoir

Some pilot studies at prototype scale will be also needed (not included in the scope of the present study) to validate conclusions of this project and gather information for the final design of the jetting system.

Based on this strategy, an experimental research program was conducted, aimed first at characterizing solids from O´Hare reservoir (surrogate for McCook type solids), and then at characterizing flow and erosion processes induced by plane and circular single and multiple jets over a bed of limited thickness such as that expected to form on McCook bottom from the settling of sewer solids.

5.2 Characterization of McCook sediments

The results from the sediment characterization analysis (Experiments of Series S1, S2, and S3) suggest that the type of solids to be deposited within McCook reservoir might be characterized as to be composed mainly by two fractions: a disperse fraction and flocs or aggregates of larger size and higher settling velocity. It is apparent from these results, that the process of formation of aggregates observed in the original O'Hare solid samples studied has time scales that are longer than 12 to 24 hours. Those aggregates do not respond sensibly to variations of shear stress values in the range expected to generate resuspension by the jet array system. It was concluded from the experiments conducted

that cohesion effects are not relevant to the behavior of solids of O'Hare reservoir from the point of view of their management using a jet array system, and the same can be expected for solids to be deposited in McCook reservoir. The experiments conducted yielded characteristic sizes, settling velocity and threshold shear stress values for resuspension of McCook type solids.

5.3 Flow and sediment transport processes induced by jets

5.3.1 Series E1. Experimental study on flow and scour pattern by plane wall jet on a bed of limited thickness.

It was shown experimentally that a wall plane jet can be used to effectively clean a bed created by fine granular sediment resting on a fixed boundary. The erosion induced by plane wall jets impinging on a granular non-cohesive layer of sediment was found to be a function of the densimetric Froude number. The variables involved in this parameter are the jet velocity at the nozzle, the acceleration of gravity, the effective diameter that characterizes the sediment, and the relative density difference between fluid and sediment. The sediment bed is eroded in the form of a scour hole with a depth equal to the bed thickness, whose longitudinal extension increases in time as the scour front advances in the downstream direction. The characteristics of the jet induced flow change significantly once the jet is deflected by the sediment front. Before the jet is deflected, flow velocity profiles match satisfactorily the empirical equation proposed by Verhoff (1963) for a plane wall jet. Downstream, the front the velocity profiles become more uniform resembling the logarithmic profiles found in gravity driven flows. The scour hole was found to grow initially with the logarithm of time and then tend slowly towards an asymptotic value, however, the asymptotic state was not reached in these tests. In any case it was found that the maximum extension of the scoured region increases as the densimetric Froude number of the jet increases.

5.3.2 Series E2. Experimental study on scour pattern by plane wall jet on a bed of CSO solids with limited thickness.

The erosion caused by a plane turbulent wall jet applied onto a bed of sewer sediment of limited thickness appears to be a function of the jet properties: velocity and thickness, the properties of the eroding fluid, and the characteristics of the sediment: critical shear stress and bed thickness. The final scour seems to depend only on the factor $(\lambda-\lambda_c)/\lambda_c$, a variable closely related with the dimensionless excess shear stress, and not on the jet Reynolds number or the bed to nozzle thickness ratio, b_{s0}/b_0. Nevertheless, these last two last variables could play a role in the development of the scour front with time, at least for the range of Reynolds numbers covered in this study. A power law that relates the final scour length or asymptotic scour front position with the parameter $(\lambda-\lambda_c)/\lambda_c$ was fitted to the data gathered. Initially, the scour grows with the logarithm of time, after a certain time t^* the rate of scouring decreases and finally the asymptotic scour state is reached.

The sewer solids used in the experiments presented singular characteristics that make them unclassifiable either as granular or cohesive material. The size of the particles and aggregates, and the flocks observed are typical of cohesive sediments, but the extremely low value of the critical shear stress obtained in the experiments distinguishes them from typical cohesive sediment. This is supported by the experiments of Series S1, S2, and S3.

5.3.3 Series E3 and E4. Experimental study on flow and scour pattern of single and multiple circular jets on bed of limited thickness.

It was shown experimentally that single or multiple circular wall jets can be used to effectively clean a bed created by fine sediment resting on a fixed boundary. The erosion caused by single and multiple circular turbulent submerged wall jets, parallel to a granular layer of sediment of finite thickness, was found to depend on jet velocity and diameter, density of the eroding fluid, and the properties of the sediment to be eroded, in particular the effective or characteristic sediment diameter, related to the critical shear stress. In the asymptotic or equilibrium scour state, the maximum scour length and other representative parameters seem to depend only on the densimetric Froude number and not on the Reynolds number of the jet induced flow. Predictive relationships were proposed for these parameters that best fit the data obtained in this study. Other variables like the sediment thickness to jet diameter ratio, and the distance between jets were found not to affect the final scour for the ranges used in the experiments. The scour length was found to initially grow with the logarithm of time and then to tend slowly towards an asymptotic value. The dependency of the maximum scour length with the densimetric Froude number and its evolution with time resemble the behavior of the semi-infinite sediment layer erosion case exposed in previous studies.

5.4 A design criterion for jet arrays

The basic parameters for a possible jet array configuration for Stage 1 in McCook reservoir were proposed in Section 4. These parameters correspond to jet diameter, discharge, and spacing. In order for each individual jet of an array to clean a distance of about 50 m, a nozzle diameter of 0.125 m (5 inches) should be used with a discharge of about 161 l/s for about 10 minutes. The jet separation was set to 10 meters. A possible array that would clean the whole bottom area of McCook reservoir was proposed, composed by 6 lines of jets with a total of 336 jets. An operational strategy has also been proposed, composed of three stages, depending on the water level in the reservoir. With a full reservoir and a significant deposit of solids on the bottom, the jets would be operated with low velocity to create slow density currents to avoid consolidation of the bed and remove the finer fractions of bed material. With water depths of about 2 to 3 m, during drainage of the reservoir, the jet array system would be operated in full, with groups of 10 to 20 jets being activated sequentially to clean the whole bottom area of the reservoir. Finally, with an empty reservoir, the jets would be operated with maximum discharge to sweep the bottom clean of solids.

It is recommended that a pilot study should be conducted at prototype scale to explore the ideas and validate the experimental results reported in previous sections.

REFERENCES

ABT, S. R. & RUFF J. R. (1982). "Estimating culvert scour in cohesive material." *Journal of the Hydraulics Division*, ASCE, 108(1), 25-34.

ADE, F. & RAJARATNAM, N. (1998). "Generalized study of erosion by circular horizontal turbulent jets." *Journal of Hydraulic Research*, 36(4), 613-635.

ADERIBIGBE, O. & RAJARATNAM, N. (1998). "Effect of sediment gradation on erosion by plane turbulent wall jets." *Journal of Hydraulic Engineering*, ASCE, 124(10), 1034-1042.

ALI, K. H. M. & LIM, S. Y. (1986). "Local scour caused by submerged wall jets." *Proc. Instn Civ. Engrs*, Part 2, 81, 607-645.

AZERAD, P. & GUILLEN, F. (2001). "Mathematical justification of the hydrostatic approximation in the primitive equations of geophysical fluid dynamics." *J. Math. Anal.*, SIAM, 33(4), 847-859.

BAILARD, J. A. & CAMPERMAN, J. M. (1983). "A design for a test bed scour array for Mare Island Naval Shipyard." *Technical Report R-899*. Naval civil Engineering Laboratory, Port Hueneme, Calif.

CHATTERJEE, S. S. & GHOSH, S. N. (1980). "Submerged horizontal jet over erodible bed." *Journal of the Hydraulics Division*, ASCE, 106(11), 1765-1782.

CHATTERJEE, S. S., GHOSH, S. N. & CHATTERJEE, M. (1994). "Local scour due to submerged horizontal jet." *Journal of Hydraulic Engineering*, ASCE, 120(8), 973-992.

CHIEW, Y. M. & LIM, S. Y. (1996). "Local scour by a deeply submerged horizontal circular jet." *Journal of Hydraulic Engineering*, Technical Note No. 7152. ASCE, 122(9), 529-532.

DEY, S. & WESTRICH, B. (2003). "Hydraulics of submerged jet subject to change in cohesive bed geometry." *Journal of Hydraulic Engineering*, ASCE, 129(1), 44-53.

DELLARIPA, F. & BAILARD, J. A. (1986). "Studies of scour patterns produced by rotating jets in a flow field." *Technical Note N-1753*. Naval civil Engineering Laboratory, Port Hueneme, Calif.

GARCIA, M. H. (1999) "Feasibility of using water jets for sedimentation management in McCook reservoir, Chicago, Illinois." Ven Te Chow Hydrosystems Laboratory, University of Illinois at Urbana-Champaign, Urbana, USA.

GARCIA, M. H., NIÑO, Y., ABAD, J., CANTERO, M., LEON, A., MANGINI, S. & SEQUEIROS. O. E. (2003). "Sedimentation management in combined sewer overflow storage reservoirs using water jets." *Progress Report,* Ven Te Chow Hydrosystems Laboratory, University of Illinois at Urbana-Champaign, Urbana, USA.

GLAUERT, M. B. (1956). "The wall jet." *J. Fluid Mechanics*, 1(5), 625-643.

HAMM, B. A., WEST, W. L. & TATTERSON, G. B. (1989). "Sludge suspension in waste storage tanks." *AIChE Journal*, 35(8), 1391-1394.

HOFFMANS, G. J. C. (1998). "Jet scour in equilibrium phase." *Journal of Hydraulic Engineering*, ASCE, 124(4), 430-437.

HOGG, A. J., HUPPERT, H. E. & DADE, W. B. (1997). "Erosion by planar turbulent wall jets." *J. Fluid Mech.*, 338, 317-340.

JENKINS, S. A, INMAN, D. L. & VAN DORN, W. G. (1981). "The evaluation of sediment management procedures." *Phase IV-VI. Final Report*. SIO Reference Series No. 81-22. Scripps Institution of Oceanography, La Jolla, Calif.

KNYSTAUTAS, R. (1964). "The turbulent jet from a series of holes in line." *The Aeronautical Quarterly*, 15, 1-28.

KUTI, E. O. & YEN, C. (1976). "Scouring of cohesive soils." *Journal of Hydraulic Research,* 14(3), 195-206.

LAUNDER, B. E. & RODI, W. (1983). "The turbulent wall jet –measurements and modeling." *Ann. Rev. Fluid Mech.,* 15, 429-459.

LAW, A. W. & HERLINA (2002). "An experimental study on turbulent circular wall jets." *Journal of Hydraulic Engineering*, ASCE, 128(2), 161-174.

LITTLE, W. C. & MAYER, P. G. (1976). "Stability of channel beds by armoring." *Journal of the Hydraulics Division*, ASCE, 102(11), 1647-1661.

MATHIEU, J. & TAILLAND, A. (1963). "Etude d'un jet plan dirige tangentiellement a une paroi." *C. R. Acad. Sc.* Paris, 256, 2768-2771.

MATHIEU, J. & TAILLAND, A. (1965). "Jet parietal." *C. R. Acad. Sc.* Paris, 261, 2282-2285.

MAZUREK, K. A., RAJARATNAM, N. & SEGO, D. C. (2001). "Scour of cohesive soil by submerged circular turbulent impinging jets." *Journal of Hydraulic Engineering,* 127(7), 598-606.

MAZUREK, K. A., RAJARATNAM, N. & SEGO, D. C. (2003). "Scour of a cohesive soil by submerged plane turbulent wall jets." *J. Hydraul. Res.,* 41(2), 195-206.

MYERS, G. E., SCHAUER, J. J. & EUSTIS, R. H. (1963). "Plane turbulent wall jet flow development and friction factor." *Journal of Basic Engineering*, Trans. A.S.M.E., 47-54.

NARAIN, J. P. (1975). "Three dimensional turbulent wall jets." *Canadian Journal of Chemical Engineering*, 53, 245-251.

NEWMAN, B. G., PATEL, R. P., SAVAGE, S. B. & TJIO, H. K. (1972). "Three-dimensional wall jet originating from a circular orifice." *The Aeronautical Quarterly,* 23, 188-200.

PANI, B. S. & DASH, R. N. (1983). "Three-dimensional wall jets from multiple outlets." *Proc. Instn Civ. Engrs*, Technical Note 376, Part 2, 75, 735-749.

PANI, B. S. & DUGAD, S. B. (2002). "Turbulent jets: application of point source concept." *Research perspectives in hydraulics and water resources engg.*, Ed. Rama Prasad and Vedula S., World Scientific Pub. Co. Singapore, pp 1-37.

RAJARATNAM, N. (1967). "Plane turbulent wall jets on rough boundaries." *Water Power*, England.

RAJARATNAM, N. (1976). *Turbulent Jets*. Elsevier, Amsterdam, The Netherlands.

RAJARATNAM, N. (1981). "Erosion by plane turbulent jets." *Journal of Hydraulic Research*, 19(4), 339-358.

RAJARATNAM, N. & BERRY, B. (1977). "Erosion by circular turbulent wall jets." *Journal of Hydraulic Research*, 15(3), 277-289.

RAJARATNAM, N. & PANI, B. S. (1974). "Three-dimensional turbulent wall jets." *Journal of the Hydraulics Division*, ASCE, 100(1), 69-83.

RAUDKIVI, A. J. (1990). *Loose boundary hydraulics*. 3rd Ed., Pergamon Press, Oxford, England.

ROBERSON, J. A., CASSIDY, J. J. & CHAUDHRY, M. H. (1988*). Hydraulic Engineering*, Houghton Mifflin Company, Boston.

SCHLICHTING, H. (1955). *Boundary layer theory*. McGraw-Hill, New York.

SCHWARZ, W.H. & COSART, W.P. (1961). "The two-dimensional turbulent wall-jet." *J. Fluid Mech.* **10**, 481-495.

SFORZA, P. M. & HERBST, G. (1970). “A study of three-dimensional, incompressible, turbulent wall jets.” *AIAA Journal*, 8(2), 276-282.

SIGALLA, A. (1958). “Measurements of Skin Friction in a Plane Turbulent Wall Jet.” *J. R. Aeronaut. Soc.*, **62**, 873-877.

STEIN, O. R., JULIEN, P. Y. & ALONSO, C. V. (1993). “Mechanics of jet scour downstream of a headcut.” *Journal of Hydraulic Research*, 31(6), 723-738.

TAILLAND, A., SUNYACH, M. & MATHIEU, J. (1967). “Jet parietal.” *C. R. Acad. Sc.* Paris, 264, 562-565.

VAN DORN, W. G., INMAN, D. L. & HARRIS, R. W. (1975). “The evaluation of sediment management procedures.” *Phase I. Final Report*. SIO Reference Series No. 75-32. Scripps Institution of Oceanography, La Jolla, Calif.

VAN DORN, W. G., INMAN, D. L., HARRIS, R. W. & McELMURY, S. S. (1977). “The evaluation of sediment management procedures.” *Phase II. Final Report*. SIO Reference Series No. 77-10. Scripps Institution of Oceanography, La Jolla, Calif.

VAN DORN, W. G., INMAN, D. L. & McELMURY, S. S. (1978). “The evaluation of sediment management procedures.” *Phase III. Final Report*. SIO Reference Series No. 78-18. Scripps Institution of Oceanography, La Jolla, Calif.

VANONI, V. (1975) (ed.) *Sedimentation Engineering: Manual 54*, American Society of Civil Engineers, New York, 1975.

VERHOFF, A. (1963). “The two-dimensional turbulent wall jet with and without and external stream.” *Report No. 626*, Princeton University, Princeton, USA.

WYGNANSKI, I., KATZ, Y. & HOREV, E. (1992). “On the applicability of various scaling laws to the turbulent wall jet.” *J. Fluid Mech.*, 234, 669-690.